



THE UNIVERSITY OF
WAIKATO
Te Whare Wānanga o Waikato

Research Commons

<http://researchcommons.waikato.ac.nz/>

Research Commons at the University of Waikato

Copyright Statement:

The digital copy of this thesis is protected by the Copyright Act 1994 (New Zealand).

The thesis may be consulted by you, provided you comply with the provisions of the Act and the following conditions of use:

- Any use you make of these documents or images must be for research or private study purposes only, and you may not make them available to any other person.
- Authors control the copyright of their thesis. You will recognise the author's right to be identified as the author of the thesis, and due acknowledgement will be made to the author where appropriate.
- You will obtain the author's permission before publishing any material from the thesis.

Synthesis of Perfluoroaryl Heterocycles To Provide Synthons For Crystal Engineering Using π - π Stacking Interactions

A thesis

submitted in partial fulfillment
of the requirements for the degree

of

Master of Science in Chemistry

at

The University of Waikato

by

Hanan Ibrahim Althagbi



THE UNIVERSITY OF
WAIKATO
Te Whare Wānanga o Waikato

2013

Abstract:

Approximately 42 new arene-perfluoroarene compounds were synthesised by the reaction of pentafluorophenyl derivatives (C_6F_5R ; $R = CN, Br, Cl, I, CHO, CF_3, H$) with imidazole, benzimidazole, pyrazole, indazole and their derivatives such as 2-methylimidazole, 4-methylimidazole, 2-phenylimidazole and 2-methylbenzimidazole. Attempts to synthesize 1-(2,3,5,6-tetrafluoropyridyl)pyrazole and 1-(2,3,5,6-tetrafluoropyridyl)indazole were unsuccessful. However, these reactions were achieved using different solvents, varying amounts of solvents and varying temperatures. Various chemical analytical techniques, such as NMR spectroscopy, mass spectrometry, infrared spectroscopy, single-crystal X-diffraction and micro-elemental analysis, were used to characterise the compounds. The crystallization of these compounds was performed by the slow evaporation of their solutions in different solvents at ambient temperature. Single crystal structures were obtained for 1-(2,3,5,6-tetrafluoropyridyl)-2-methylbenzimidazole, 1-(4-bromo-2,3,5,6-tetrafluorobenzyl)-3-benzyl-4-methylimidazolium bromide and 1-(2,3,5,6-tetrafluoropyridyl)-3-benzyl-4-methylimidazolium bromide and this result has shown that π - π stacking interactions have an essential role in the packing of these compounds.

Acknowledgements:

The deepest appreciation to my God, without his willing, this work would not have been possible, and I would like to thank my family, my father, my mother, my husband and my son for their support.

I also thank the King Abdullah Scholarship Program and the ministry of education in Saudi Arabia for the financial support.

I would particularly like to thank my honourable adviser Dr. Graham Saunders for his valuable assistance, Who encouraged and helped me to improve my skills, knowledge, confidence, responsibility and ambitious, acknowledgment for Pat Gread for training me to use analytical instruments and Wendy Jackson for her persistent help.

Finally, I would thank my Waikato University and chemistry department which provided the most appropriate environment to work and research, University of Auckland for X-ray crystallographic analysis and University of Otago for elemental analysis to some compounds in this project.

Contents

| | |
|--|-----|
| Abstract: | ii |
| Acknowledgements: | iii |
| List of Table: | x |
| 1. Chapter One: | 1 |
| 1.1. Introduction:..... | 1 |
| 1.2. Arene-Perfluoroarene Interactions:..... | 2 |
| 1.3. Crystal Engineering: | 10 |
| 1.4. Supramolecular Chemistry:..... | 15 |
| 1.5. Biological Activity:..... | 23 |
| 1.6. Pharmaceutical Activity:..... | 25 |
| 2. Chapter Two:..... | 29 |
| 2.1. Introduction:..... | 29 |
| 2.2. Materials: | 30 |
| 2.2.1. Pentafluorobenzene:..... | 30 |
| 2.2.2. Imidazole: | 31 |
| 2.2.3. Pyrazole: | 32 |
| 2.2. Preparation: | 39 |
| 2.3. Characterization: | 41 |
| 3. Chapter Three:..... | 63 |
| 3.1. Introduction:..... | 63 |
| 3.2. Materials: | 63 |
| 3.2.1. Pentafluorobenzene:..... | 63 |
| 3.2.2. Benzimidazole: | 64 |
| 3.2.3. Indazole:..... | 65 |
| 3.3. Synthesis: | 68 |
| 3.4. Characterization: | 68 |
| 4. Chapter Four: | 80 |
| 4.1. Conclusion: | 80 |
| 5. Chapter Five:..... | 82 |
| 5.1. General Synthesis: | 82 |

| | |
|---|----|
| 5.2. Imidazole: | 83 |
| 5.2.1. 1-(2,3,6-Trifluorobenzonitrile)imidazole (1): | 83 |
| 5.2.2. The Expected Compound 1-(3,4,6-Trifluoropyridyl)imidazole (2): | 84 |
| 5.2.3. The Expected Compound 1-(2,3-Difluorobenzonitrile)imidazole (3): | 84 |
| 5.2.4. The Expected Compound 1-(3,4,6-Trifluorobenzonitrile)imidazole (4): .. | 85 |
| 5.2.5. The Expected Compound 1-(4,6-Difluoropyridyl)imidazole (5):..... | 85 |
| 5.2.6. The Expected Compound 1-(3,6-Difluorobenzonitrile)imidazole (6): | 85 |
| 5.2.7. 1-(Heptafluorotolyl)imidazole (7): | 86 |
| 5.2.8. 1-(5-Bromo-3,4,6-trifluorobenzotrifluoride)imidazole (8a) and 1-(6-Bromo-3,4,5-trifluorobenzotrifluoride)imidazole (8b): | 86 |
| 5.2.9. 1-(2,3,5,6-Tetrafluorobenzonitrile)-2-methylimidazole (9): | 87 |
| 5.2.10. 1-(2,3,5,6-Tetrafluoropyridyl)-2-methylimidazole (10): | 87 |
| 5.2.11. 1-(Heptafluorotolyl)-2-methylimidazole (11):..... | 87 |
| 5.2.12. 1-(4-Bromo-2,3,5,6-tetrafluorobenzyl)-2-methylimidazole (12): | 88 |
| 5.2.13. 1-(2,3,5,6-Tetrafluorobenzonitrile)-4-methylimidazole (13):..... | 89 |
| 5.2.14. 1-(2,3,5,6-Tetrafluoropyridyl)-4-methylimidazole (14): | 89 |
| 5.2.15. 1-(Heptafluorotolyl)-4-methylimidazole (15):..... | 89 |
| 5.2.16. 1-(4-Bromo-2,3,5,6-tetrafluorobenzyl)-4-methylimidazole (16):..... | 90 |
| 5.2.17. 1-(2,3,5,6-Tetrafluorobenzyl)-4-methylimidazole (17): | 90 |
| 5.2.18. 1-(4-Iodo-2,3,5,6-tetrafluorobenzyl)-4-methylimidazole (18):..... | 91 |
| 5.2.19. 1-(2,3,5,6-Tetrafluorobenzonitrile)-2-phenylimidazole (19): | 92 |
| 5.2.20. 1-(2,3,5,6-Tetrafluorobenzaldehyde)-2-phenylimidazole (20): | 92 |
| 5.2.21. 1-(2,3,5,6-Tetrafluoropyridyl)-2-phenylimidazole (21):..... | 93 |
| 5.3. Pyrazole: | 93 |
| 5.3.1. 1-(2,3,5,6-Tetrafluorobenzonitrile)pyrazole (22):..... | 94 |
| 5.3.2. 1-(2,3,5,6-Tetrafluorobenzonitrile)-3,5-dimethylpyrazole (23):..... | 94 |
| 5.3.3. 1-(2,3,5,6-Tetrafluoropyridyl)-3,5-dimethylpyrazole (24): | 95 |
| 5.3.4. Attempt to synthesize 1-(2,3,5,6-Tetrafluoropyridyl)pyrazole (25): | 95 |
| 5.4. Imidazolium Salts: | 96 |
| 5.4.1. 1-(4-Bromo-2,3,5,6-tetrafluorobenzyl)-3-benzyl-4-methylimidazolium bromide (26): | 96 |
| 5.4.2. 1-(2,3,5,6-Tetrafluorobenzonitrile)-3-benzyl-4-methylimidazolium bromide (27): | 98 |
| 5.4.3. 1-(2,3,6-Trifluorobenzonitrile)-3-benzyl-imidazolium bromide (28): | 98 |
| 5.4.4. 1-(2,3,5,6-Tetrafluoropyridyl)-3-benzyl-2-methylimidazolium bromide (29):..... | 99 |

| | |
|---|-----|
| 5.4.5. 1-(4-Bromo-2,3,5,6-tetrafluorobenzyl)-3-benzyl-2-methylimidazolium bromide (30): | 99 |
| 5.4.6. 1-(Heptafluorotolyl)-3-benzylimidazolium bromide (31): | 100 |
| 5.4.7. 1-(Heptafluorotolyl)-3-benzyl-4-methylimidazolium bromide (32):..... | 100 |
| 5.4.8. 1-(2,3,5,6-Tetrafluoropyridyl)-3,4-dimethylimidazolium iodide (33):.... | 100 |
| 5.4.9. 1-(2,3,5,6-Tetrafluoropyridyl)-3-benzyl-4-methylimidazolium bromide (34):..... | 101 |
| 5.5. Benzimidazole: | 103 |
| 5.5.1. 1-(2,3,6-Trifluorophthalonitrile)benzimidazole (35): | 103 |
| 5.5.2. 1-(2,3,5,6-Tetrafluorobenzaldehyde)benzimidazole (36): | 104 |
| 5.5.3. 1-(6-Chloro-2,3,5-trifluoropyridyl)benzimidazole (37):..... | 104 |
| 5.5.4. 1-(2,3,5,6-Tetrafluoropyridyl)benzimidazole (38):..... | 105 |
| 5.5.5. 1-(Heptafluorotolyl)benzimidazole (39): | 105 |
| 5.5.6. 1-(Heptafluorotolyl)-2-methylbenzimidazole (40): | 106 |
| 5.5.7. 1-(2,3,5,6-Tetrafluorobenzonitrile)-2-methylbenzimidazole (41): | 106 |
| 5.5.8. 1-(2,3,5,6-Tetrafluoropyridyl)-2-methylbenzimidazole (42):..... | 107 |
| 5.6. Indazole:..... | 110 |
| 5.6.1. Attempt to synthesize 1-(2,3,5,6-Tetrafluoropyridyl)indazole (43):..... | 110 |
| 5.7. Benzimidazolium Salt: | 110 |
| 5.7.1. 1-(2,3,5,6-Tetrafluoropyridyl)-3-benzyl-benzimidazolium bromide (44): | 110 |
| References:..... | 111 |
| Appendix | 119 |

List of Figures:

| | |
|--|----|
| Figure 1: The different geometries of polyfluoroaryl-aryl group interactions ^[8] | 2 |
| Figure 2: The different orientations of face to face geometry ^[6] | 4 |
| Figure 3: Alternating stacking of octafluoronaphthalene and acenaphthene ^[16] | 5 |
| Figure 4: Inter-planar separation in the packing of arene-perfluoroarene synthons ^[17] | 6 |
| Figure 5: 1-(2,3,4,5,6-pentafluorobenzyl)-3-benzylimidazolium bromide ^[17] | 6 |
| Figure 6: Face to face packing of 1-(2,3,4,5,6-pentafluorobenzyl)-3-benzylimidazolium bromide ^[17] | 6 |
| Figure 7: The general synthesis reaction of polyfluoroaryl and imidazole compounds with their derivatives ^[18] | 7 |
| Figure 8: 1-(2,3,5,6-tetrafluoropyridyl)-3-benzylimidazolium bromide ^[5] | 9 |
| Figure 9: Two directional face-to-face packing geometry ^[5] | 9 |
| Figure 10: The various geometries of a π system, a) edge to face geometry, b) offset face to face geometry, c) face to face geometry ^[22] | 10 |
| Figure 11: The effect of the polarized substituents on the attraction force of the face to face geometry ^[23] | 1 |
| Figure 12: Aryl groups containing different number and position of nitrogen atoms ^[21] | 3 |
| Figure 13: Effect the orientation on the electrostatic interactions ^[25] | 3 |
| Figure 14: On the left side hand the different sizes of the different molecules have been represented by different colours such as a1 to a8, b1 to b8 and c1 to c5, whereas on the right hand side the delocalization of π -electrons has been shown by the electron density pictures of the largest molecules ^[26] | 4 |
| Figure 15: Substituted benzene–benzene complexes in (a) parallel-displaced over a vertex and (b) parallel-displaced edgewise orientations. X = H, F, CN, and OH ^[27] | 5 |
| Figure 16: Substituted meta and para-substituted <i>N</i> -benzyl-2-(2-fluorophenyl)-pyridinium bromides ^[31] | 7 |
| Figure 17: Experimental aromatic stacking interaction energies ($\phi\phi G$) correlate with the Hammett substituent constant for X (σX). Interactions with phenyl (b) and pentafluorophenyl (O) are shown ^[34] | 9 |
| Figure 18: Studying the effect of solvent on the aromatic stacking interactions using metal complexes, $\Delta\delta = \delta$ (H3 in 59) - δ (H3 in 60) ^[25] | 10 |
| Figure 19: Dependence of the free energy of complexation of the cyclophane pyrene complex, $-\Delta G$ (kJ mol ⁻¹), with solvent polarity, $ET(30)$ (kJ mol ⁻¹) ^[25] | 11 |
| Figure 20: In this crystal structure a combination of stacking interactions is involved ^[36] | 12 |

| | |
|--|----|
| Figure 21: a) Beta (β) packing, b) gamma (γ) packing, c) sandwich herringbone and d) sandwich geometries..... | 14 |
| Figure 22: The planar and crystal structures of the molecular tweezer with two corannulene subunits ($C_{60}H_{24}$) ^[53] | 18 |
| Figure 23: In the solid state, the geometry of stilbene derivative is determined by the stacking interactions of phenyl–pentafluorophenyl (a) which lead to formation of the stereo-chemical cyclobutane photodimer (b) ^[25] | 19 |
| Figure 24: (a) Diyne polymerisation to give (<i>E</i>)-polybutadiyne. (b) Butadiyne units arrange to form the (<i>Z</i>) polymer ^[25] | 20 |
| Figure 25: Head-to-tail structure of 1-(2,3,4,5,6-pentafluorophenyl)-4-phenylbutadiyne ^[25] | 20 |
| Figure 26: The terminal edge-to-face aromatic interaction in complex A has been determined by using a chemical double mutant cycle. The X-ray crystal structure of a model compound which contains the same intermolecular interaction is shown in the inset ^[25] | 22 |
| Figure 27: The arene-perfluoroarene interactions in α 2D protein ^[62] | 23 |
| Figure 28: I is an incorporated self-assembly model of benzyl-PD, II represents the incorporated self-assembly model of benzyl-PD in both a twisted fashion with red colour and horizontally bound to the cavitand with orange colour ^[69] | 25 |
| Figure 29: The electrostatic interactions between Tyr155 and the pentafluorophenyl group in 1,3,4-thiadiazole-2-thione-based inhibitor ^[63] | 27 |
| Figure 30: Chemical structure of pentafluorobenzene with six-membered ring. From [upload.wikimedia.org] and [asd.molfield.org]..... | 30 |
| Figure 31: Chemical structure of imidazole with five-membered ring ^[77] | 31 |
| Figure 32: The chemical structure of pyrazole ^[93] | 32 |
| Figure 33: The labels that have been used to represent the NMR data of imidazole, pyrazole compounds and imidazolium salts ($R = Br, I, F, R^1, R^2 = H, CH_3, R_1, R_2, R_3 = H, F$)...... | 41 |
| Figure 34: The HSQC spectrum of 1-(4-bromo-2,3,5,6-tetrafluorobenzyl)-2-methylimidazole 12..... | 44 |
| Figure 35: The HMBC spectrum of 1-(4-bromo-2,3,5,6-tetrafluorobenzyl)-2-methylimidazole 12..... | 45 |
| Figure 36: The HSQC spectrum of 1-(4-iodo-2,3,5,6-tetrafluorobenzyl)-4-methylimidazole 18..... | 46 |
| Figure 37: The HMBC spectrum of 1-(4-iodo-2,3,5,6-tetrafluorobenzyl)-4-methylimidazole 18..... | 47 |
| Figure 38: The formation of the expected compound 1-(3,4,6-trifluoropyridyle)imidazole 2 over months starting from green to blue. | 48 |
| Figure 39: The formation of the expected compound 1-(2,3-difluorobenzonitrile)imidazole 3 over months starting from green to blue. | 49 |
| Figure 40: The formation of the expected compound 1-(3,4,6-trifluorobenzonitrile)imidazole 4 over months starting from green to blue..... | 50 |
| Figure 41: The formation of the expected compound 1-(4,6-difluoropyridyle)imidazole 5 over months starting from green to blue..... | 51 |

| | |
|--|----|
| Figure 42: The formation of the expected compound 1-(3,6-difluorobenzonitrile)imidazole 6 over months starting from green to blue. | 52 |
| Figure 43: Structure of 1-(4-bromo-2,3,5,6-tetrafluorobenzyle)-3-benzyl-4-methylimidazolium bromide 26. | 55 |
| Figure 44: The structure of 1-(2,3,5,6-tetrafluoropyridyl)-3-benzyl-4-methylimidazolium bromide 34. | 55 |
| Figure 45: The monoclinic crystal system of 1-(4-bromo-2,3,5,6-tetrafluorobenzyle)-3-benzyl-4-methylimidazolium bromide 26. | 59 |
| Figure 46: The monoclinic crystal system of 1-(2,3,5,6-tetrafluoropyridyl)-3-benzyl-4-methylimidazolium bromide 34. | 59 |
| Figure 47: The π - π stacking of 1-(4-bromo-2,3,5,6-tetrafluorobenzyle)-3-benzyl-4-methylimidazolium bromide 26. | 60 |
| Figure 48: The π - π stacking of 1-(2,3,5,6-tetrafluoropyridyl)-3-benzyl-4-methylimidazolium bromide 34. | 60 |
| Figure 49: The crystal packing of 1-(4-bromo-2,3,5,6-tetrafluorobenzyle)-3-benzyl-4-methylimidazolium bromide 26 viewed along the b axis. | 61 |
| Figure 50: A & B The crystal packing of 1-(2,3,5,6-tetrafluoropyridyl)-3-benzyl-4-methylimidazolium bromide viewed along different axes. | 62 |
| Figure 51: The chemical structure of benzimidazole ^[104] | 64 |
| Figure 52: The chemical structure of indazole compound ^[113] | 65 |
| Figure 53: The labels that have been used to represent the NMR data of benzimidazole compounds and their salts. (R_1 = F, CF ₃ , CN, CHO, R_2 = F, CN, R= F, Cl and R^1 = H, CH ₃). | 68 |
| Figure 54: The HSQC spectrum of 1-(2,3,5,6- tetrafluoropyridyl)-2-methylbenzimidazole 42. | 71 |
| Figure 55: The HMBC spectrum of 1-(2,3,5,6- tetrafluoropyridyl)-2-methylbenzimidazole 42. | 72 |
| Figure 56: Decomposing of 1-(2,3,5,6-tetrafluoropyridyl)-3-benzylbenzimidazolium bromide 44 over months from yellow to blue. | 73 |
| Figure 57: The crystal structure of 1-(2,3,5,6- tetrafluoropyridyl)-2-methylbenzimidazole 42. | 75 |
| Figure 58: The orthorhombic crystal system of 1-(2,3,5,6-tetrafluoropyridyl)-2-methylbenzimidazole 42. | 78 |
| Figure 59: The crystal structure of 1-(2,3,5,6-tetrafluoropyridyl)-2-methylbenzimidazole 42. | 78 |
| Figure 60: The crystal packing of 1-(2,3,5,6-tetrafluoropyridyl)-2-methylbenzimidazole 42 viewed along the C-C ₅ F ₄ N bond. | 79 |
| Figure 61: The general reaction of polyfluoroaryl and imidazole with their derivatives and examples of imidazolium salts (with the labels that have been used to represent the NMR data) (R = Br, I, F. R^1 , R^2 = H, CH ₃ . R_1 , R_2 , R_3 = H, F). .. | 83 |
| Figure 62: The general reaction of polyfluoroaryl and pyrazole and their derivatives (with the labels that have been used to represent the NMR data, R^1 , R^2 = H, CH ₃). | 93 |

| | |
|---|-----|
| Figure 63: The general reaction of polyfluoroarene and benzimidazole derivatives (with the labels that have been used to represent the NMR data), ($R_1 = F, CF_3, CN, CHO$), $R_2 = F, CN$, $R = F, Cl$ and $R^1 = H, CH_3$ | 103 |
| Figure 64: The ^{13}C NMR spectrum of 1-(4-bromo-2,3,5,6-tetrafluorobenzyl)-2-methylimidazole (12). | 119 |
| Figure 65: The ^{13}C NMR spectrum of 1-(4-iodo-2,3,5,6-tetrafluorobenzyl)-4-methylimidazole (18). | 120 |
| Figure 66: The ^{13}C NMR spectrum of 1-(2,3,5,6-tetrafluoropyridyl)benzimidazole (38). | 121 |
| Figure 67: The ^{13}C NMR spectrum of 1-(2,3,5,6-tetrafluoropyridyl)-2-methylbenzimidazole (42). | 122 |

List of Table:

| | |
|--|-----|
| Table 1: Nucleophilic substitution of pentafluorobenzene (I) with imidazole ^[18] . .. | 8 |
| Table 2: Values measured in $CDCl_3$ at 293 K, and errors are 0.7-1.1 $kJ\ mol^{-1}$ ^[25] . .. | 8 |
| Table 3: Substituents with high and low electron density that were added to edge-to-face rings ^[25] | 22 |
| Table 4: Chemical reactions of PFB-R with imidazole, pyrazole and their derivatives, and the chemical reactions of these compounds to form imidazolium salts. | 37 |
| Table 5: Selected bond lengths (\AA) and bond and torsion angles ($^\circ$) for salts 26 and 34, except those related to C17, Br2 and N3. | 58 |
| Table 6: Selected bond lengths (\AA) and bond and torsion angles ($^\circ$) for salts 26 and 34 that related to C17, Br2 and N3. | 58 |
| Table 7: Chemical reactions of PFB-R with benzimidazole, indazole and their derivatives, and the chemical reactions of these compounds to form benzimidazolium salts. | 68 |
| Table 8: Selected bond lengths (\AA) and bond and torsion angles ($^\circ$) for compounds 42A and 42B. | 77 |
| Table 9: Estimated standard deviations are given in parentheses. Data were collected at 100(2) K with graphite monochromated copper radiation ($\lambda = 1.54184\ \text{\AA}$). | 97 |
| Table 10: Estimated standard deviations are given in parentheses. Data were collected at 89(2) K with graphite monochromated radiation ($\lambda = 0.71073\ \text{\AA}$). .. | 102 |
| Table 11: Estimated standard deviations are given in parentheses. Data were collected at 89(2) K with graphite monochromated radiation ($\lambda = 0.71073\ \text{\AA}$). .. | 109 |

List of General Abbreviations:

| | |
|-------|--|
| Å | Angstrom |
| Calc. | Calculated |
| cent | centroid |
| Comp. | Compound |
| d | doublet(NMR) |
| DMSO | dimethylsulfoxide |
| HMBC | Heteronuclear Multiple Bond Correlation |
| hrs | hours |
| HSQC | Heteronuclear Single-Quantum Correlation |
| IR | infrared spectroscopy |
| J | coupling constant (NMR) |
| m | multiplet (NMR) |
| MS | Mass Spectrum |
| m.p. | melting point |
| m/z | mass to charge ratio |
| NMR | nuclear magnetic resonance |
| No. | Number |
| o | ortho |
| p | para |
| RT | room temperature |
| ppm | part per million |
| s | singlet (NMR) |
| t | triplet (NMR) |
| TOF | Time of Flight |
| THF | Tetrahydrofuran |
| XRD | X-ray diffraction |

1. Chapter One:

1.1. Introduction:

$\pi - \pi$ stacking interactions between arenes and perfluoroarenes has potential in crystal engineering ^[1], and has received attention as a result of this. The interactions are a mixture of electrostatic interactions and Van der Waals ^[2], between slipped parallel stacks of $\text{Ar}^{\text{H}}-\text{Ar}^{\text{F}}$ ^[3]. These interactions have been known over four decades ^[4], but only in the past few years, they have been used as a main tool of crystal engineering ^[5], synthesis and control of molecular structure to achieve functional properties. Due to their ability of arene-perfluoroarene synthons to incorporate easily into molecules ^[6], this lead to enhance their crucial role in various fields such as biology ^[3], pharmaceutical industry, supra-molecular chemistry ^[7] and crystal engineering ^[7]. This thesis will investigate molecules that contain both polyfluoroaryl and aryl groups. These are based on nitrogen containing heterocycles, in particular imidazole and benzimidazole compounds.

1.2. Arene-Perfluoroarene Interactions:

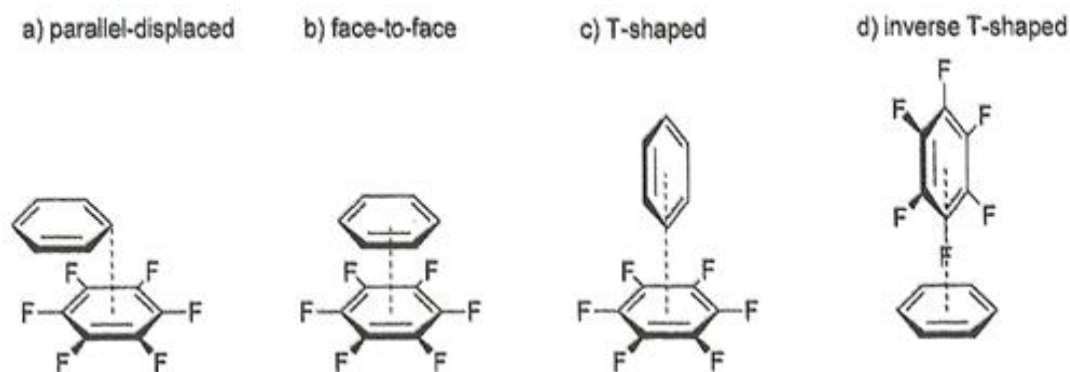


Figure 1: The different geometries of polyfluoroaryl-aryl group interactions ^[8].

It has been found that for the perfluoroarene–arene synthons the contact C–H...F–C is the factor that dominates the stability of these synthons. Hexafluorobenzene (mp 5.0° C) and benzene (mp 5.4° C) have been used by Patrick and Prosser to form the first complex (mp 23.7° C) using this type of interaction. As a model of perfluoroarene–arene synthons ^[9], C₆H₅–C₆F₅ synthon has been studied using CCSD(*T*) ("coupled cluster single and doubles with perturbative triples") method, and it has been found that The T-shaped geometries have the lowest stability ($\Delta E = -1.74$ and -0.88 kcalmol⁻¹), whereas, the parallel displaced geometry has the highest stability ($\Delta E = -5.38$ kcalmol⁻¹), followed by the face-to-face geometry ($\Delta E = -5.07$ kcalmol⁻¹) (Fig. 1), and the drop of the stability is because of the reduction of dispersion forces and undesired type of electrostatic interactions. To study the effect of substituent on this synthon (C₆H₅X–C₆F₆), it has found also that the face-to-face motif is less favorable than the parallel displaced motifs. Other complexes have been synthesized, such as methyl-substituted arene (p-xylene, mesitylene, durene and hexamethylbenzene) with hexafluorobenzene, and the crystallographic data of these compounds has shown a combination of stacking with edge to face $\pi - \pi$ stacking interactions.

Studies of hexafluorobenzene-arene complexes by using spectroscopy and refractometry have been shown that there are VdW and electrostatic interactions and other charge transfer interactions, consider $\pi - \pi$ stacking interactions. It has also been shown that the face to face geometry of these interactions between the compounds that pack on the top of each other can have variable orientations ^[8], in which, it can be columnar geometry with angle of 90° θ or slipped geometry with angle of 45° θ , with longer distance in the first geometry than the second (Fig. 2) ^[6].

This project will aim to synthesis new arene-perfluoroarene compounds. Imidazole, benzimidazole, pyrazole, indazole and their derivatives are the starting materials in this project, and these will be introduced individually in each chapter. The other starting material is a derivative or analogue of hexafluorobenzene (HFB). HFB has a planar aromatic ring, like benzene, with a symmetry of D_{6h} , a dissociation energy of ≥ 0.5 eV, an electron affinity of $\geq 1.8 + 0.3$ eV of the front endothermic negative ion charge transfer reaction and 3.45 eV of E. A. ^[10]. It was first prepared as a molecular complex with benzene in 1960 ^[9]. This was followed by similar complexes of its derivatives such as octafluoronaphthalene (OFN) with trans-stilbene or trans-azobenzene, pentafluorophenyl group with chiral amino alcohol ^[11], phenyl-perfluorophenyl complex ^[12], pentafluorobenzoate in $Cu(py)_2(pfb)_2$ and $Cu(py)_2(pfb)_2(H_2O)$ ^[13], and it has been found that all these complexes are sharing common properties. First of all the arene and perfluoroarene aromatic rings are perseverant in the 1:1 complex. Secondly, the complexes have higher melting points than the starting materials. Thirdly, the infinite stacking of their components leads to crystal structures with different geometries ^[14]. In this project, the derivatives of HFB that have been used as a

starting materials to form arene-pentafluoroarene complexes are tetrafluorophthalonitrile, pentafluorobenzaldehyde, 3-chloro-2,4,5,6-tetrafluoropyridine, 2-pentafluorobenzonitrile, Pentafluorobenzaldehyde, tetrafluoropyridine, 2,3,4,5,6-pentafluorobenzonitrile, penatfluoropyridine, bromopentafluorobenzene, 4-bromo-2,3,5,6-tetrafluorobenzotrifluoride, pentafluorobenzene, Iodo-pentafluorobenzene, 2,3,4,5-tetrafluorobenzonitrile, 2,3,5,6-tetrafluoropyridine, 2,3,5,6-tetrafluorobenzonitrile, 2,4,5-trifluorobenzonitrile, 2,3,4-trifluorobenzonitrile, 2,3,5-trifluoropyridine and octafluorotoluene. HFB and its derivatives are biologically active, hexafluorobenzene solvate of hexameline shows anticancer activity [15], and different instruments have been used to study these compounds. For example, in CH₃CN, NMR and CD spectroscopy have been used to study the effect of pentafluorobenzene on the secondary structure of peptoids, oligomers of N-substituted glycines [8].

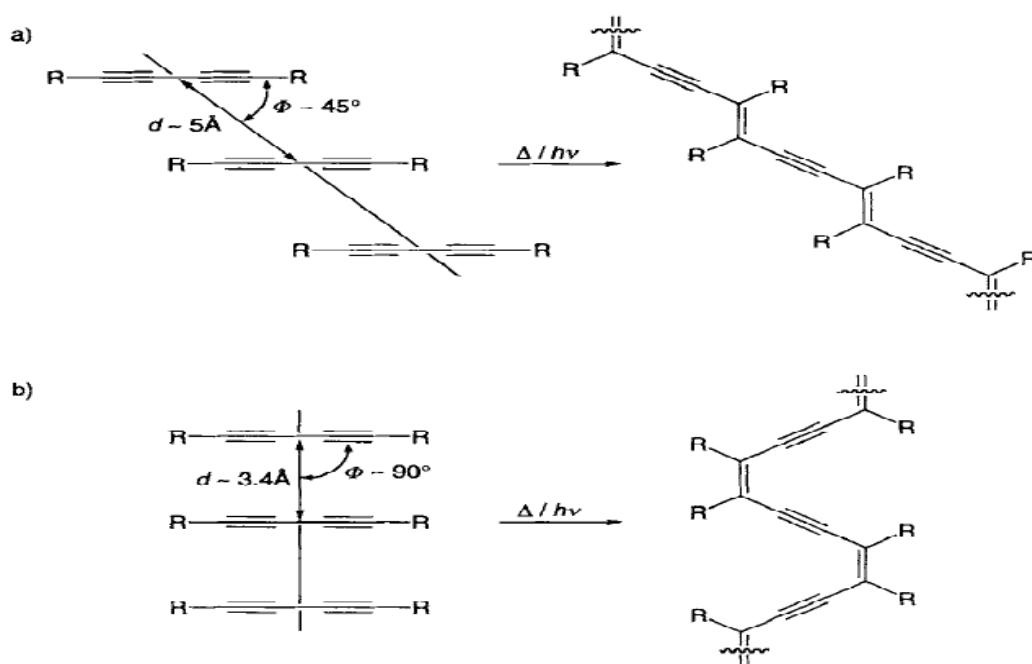


Figure 2: The different orientations of face to face geometry [6].

To study these interactions, the octafluoronaphthalene–acenaphthene complex has been prepared and crystalized by Collings. The crystal structure of this complex, has an infinite column of alternating OFN and acenaphthene with a small distance (d) between the aryl and perfluoroaryl rings and slip angles (θ), angles (ϕ) and stack shifts (s) as shown below (Fig. 3) ^[16].

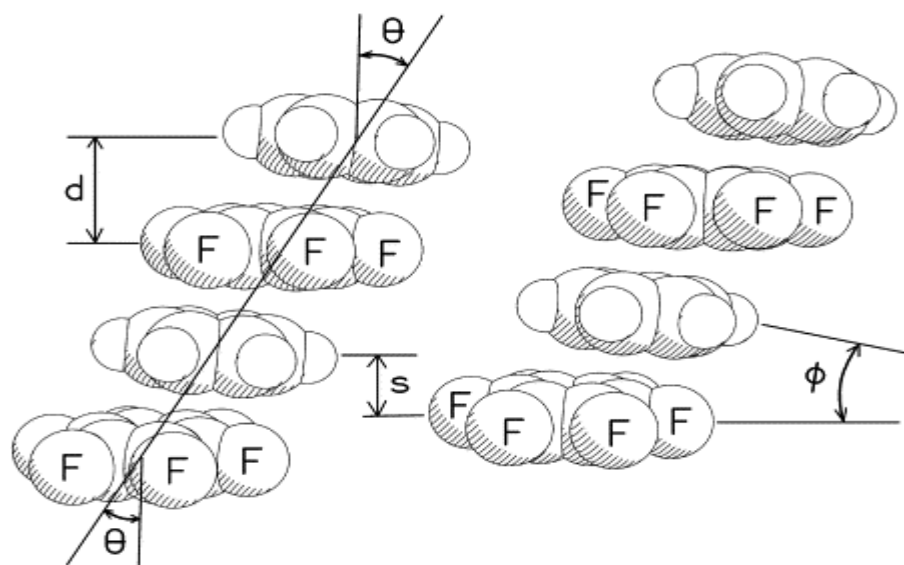


Figure 3: Alternating stacking of octafluoronaphthalene and acenaphthene ^[16].

And it has been shown that favorable interaction is possible with inter-planar separation over than 4 \AA , and this has been confirmed during studying 1-(2,3,4,5,6-pentafluorobenzyl)-3-benzylimidazolium bromide, which has an inter-planar separation of 4.3 \AA ^[17] (Fig. 4, 5, & 6).

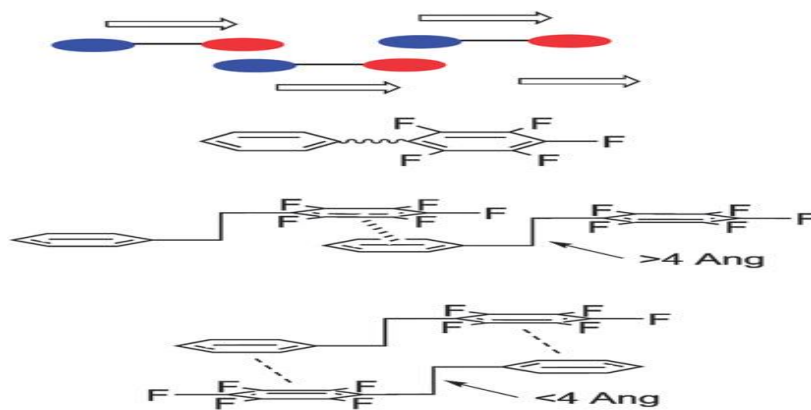


Figure 4: Inter-planar separation in the packing of arene-perfluoroarene synthons ^[17].

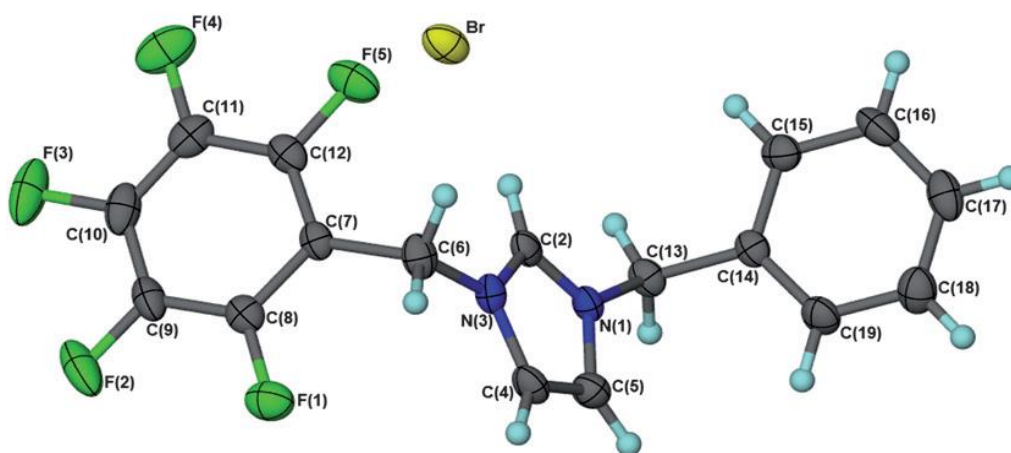


Figure 5: 1-(2,3,4,5,6-pentafluorobenzyl)-3-benzylimidazolium bromide ^[17].

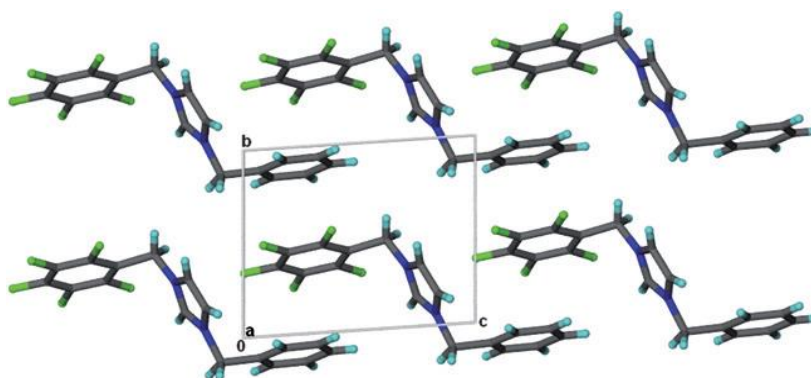


Figure 6: Face to face packing of 1-(2,3,4,5,6-pentafluorobenzyl)-3-benzylimidazolium bromide ^[17].

However, there are similar complexes and salts to arene-perfluoroarene complexes and imidazolium salts in this project have been synthesized by an easy route and good yields such as the complexes that have been reported by Fujii et al, which are (4'-nitrotetrafluorophenyl) imidazole, 1-(2'-nitrotetrafluorophenyl) imidazole, 1-(4'-formyltetrafluorophenyl) imidazole, 1-(4'-formyltetrafluorophenyl) imidazole ethyl hemiacetal, 4'-ethoxycarbonyltetrafluorophenyl) imidazole, 1-(4'-bromotetrafluorophenyl) imidazole, 1-(4'-chlorotetrafluorophenyl) imidazole, 1-(2'-chlorotetrafluorophenyl) imidazole, (2',4'-dibromotrifluorophenyl)imidazole, (2'-bromo-3',5',6'-trifluorophenyl)imidazole, and it has shown that the reactivity of PFB has been achieved at room temperature with NO₂ and CN as substituent groups, whereas, it has not been achieved with Me or MeO groups even with strong base at high temperature (over 99 C°)^[18] as shown below in (Fig. 7) and (Table. 1).

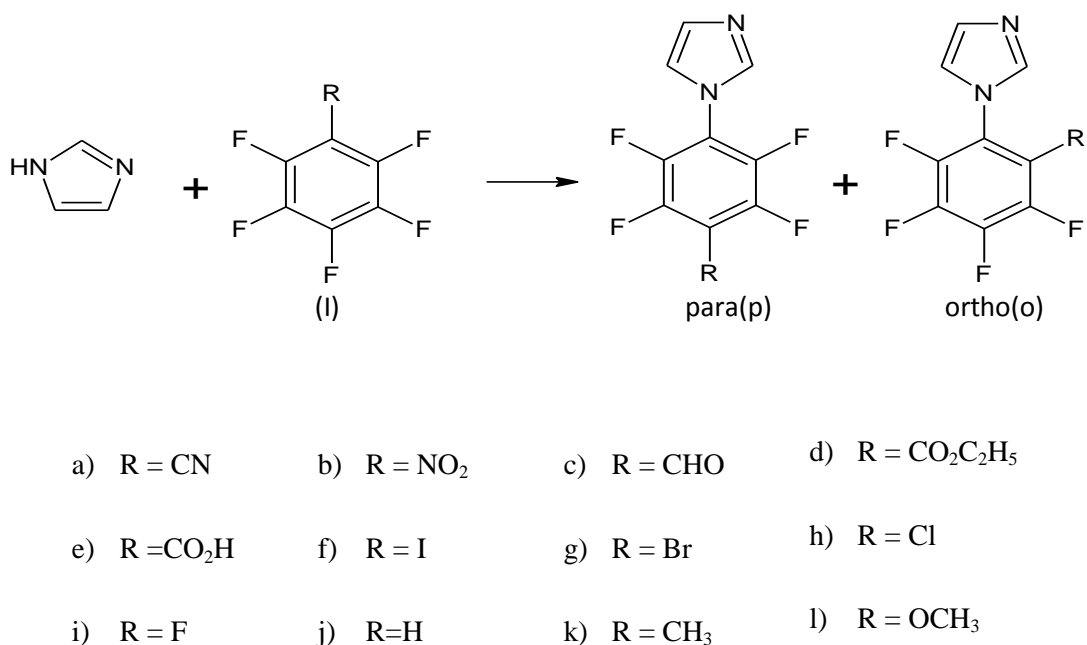


Figure 7: The general synthesis reaction of polyfluoroaryl and imidazole compounds with their derivatives^[18].

| I | | solvent | Reaction conditions ¹ | | | Product yields (%) | |
|----|---|---------|----------------------------------|--------------------|--------------|--------------------|------|
| | | | Base | Temp.°C | Time. hrs | p | o |
| Ia | C ₆ H ₅ CN | THF | | r. t. ² | 3 | 83.8 | |
| Ib | C ₆ H ₅ NO ₂ | THF | | r. t. | 4 | 51.8 | 13.9 |
| Ic | C ₆ H ₅ CHO | THF | | r. t. | 20 | 83.5 | |
| Id | C ₆ H ₅ CO ₂ C ₂ H ₅ | THF | | 65 | 10 | 81.5 | |
| Ie | C ₆ H ₅ CO ₂ H | THF | | 65 | 10 | | |
| If | C ₆ H ₅ I | DMSO | | 80 | 43 | 70.4 | |
| Ig | C ₆ H ₅ Br | DMSO | | 80 | 96 | 40.3 | |
| Ih | C ₆ H ₅ Cl | DMSO | | 100 | 40 | 65.9 | 2.8 |
| Ih | C ₆ H ₅ Cl | DMSO | KOH ³ | 80 | 4 | 38.4 | 4.1 |
| Ih | C ₆ H ₅ Cl | THF | KOH ³ | 60 | 66 | 26.8 | 2.4 |
| Ih | C ₆ H ₅ Cl | tBuOH | KOH ³ | 80 | 20 | 54.4 | 4.3 |
| Ii | C ₆ H ₅ | DMSO | KOH ³ | 80 | 24 | | |
| Ij | C ₆ H ₅ H | DMSO | KOH ³ | 55 | 3 | 73.6 | |
| Ik | C ₆ H ₅ CH ₃ | DMSO | | 100 | 24 | | |
| Il | C ₆ H ₅ OCH ₃ | DMSO | | 100 | 24 | | |

¹ Imidazole 10 mol; Pentafluorobenzene (I) 20 mol; solvent 30 ml.

² Ambient temperature (13~16 °C).

Table 1: Nucleophilic substitution of pentafluorobenzene (I) with imidazole ^[18].

The similar salts to this project, that have been prepared are 1-(2,3,5,6-tetrafluoropyridyl)-3-benzylimidazolium bromide (Fig. 9), which has been done by Saunders. G; with $\pi - \pi$ stacking interactions to control the structure, which provided an infinite two directional face-to-face packing geometry as in this project (Fig. 8) ^[5].

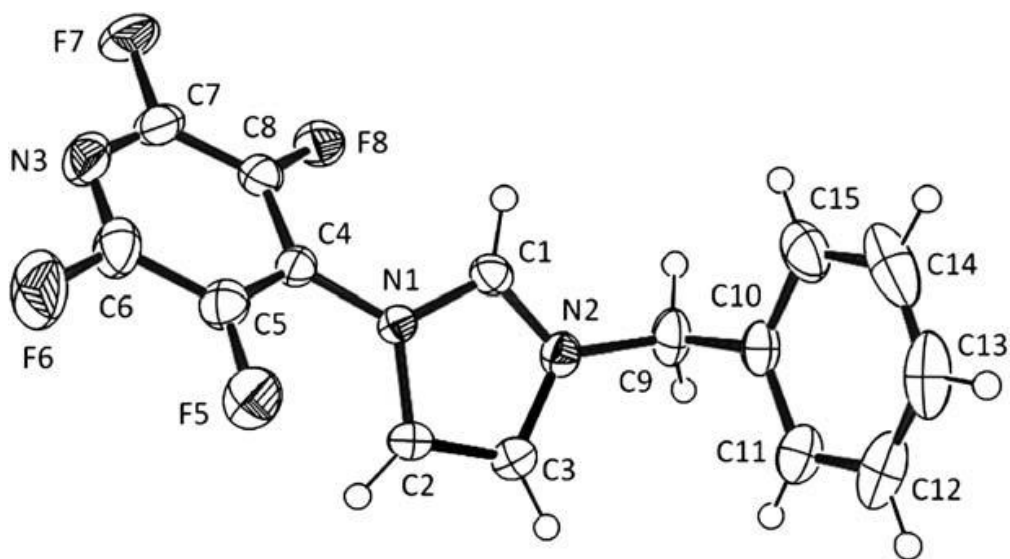


Figure 8: 1-(2,3,5,6-tetrafluoropyridyl)-3-benzylimidazolium bromide ^[5].

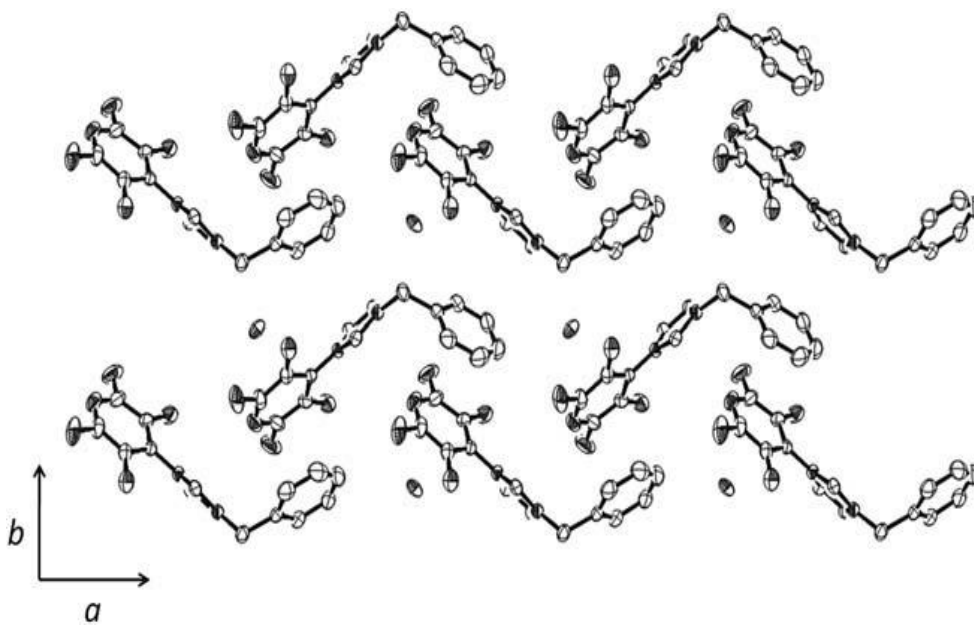


Figure 9: Two directional face-to-face packing geometry ^[5].

1.3. Crystal Engineering:

Crystal engineering is the study of structures and the control of packing of molecules or ions (synthons) to enhance the materials' structures and achieve functional properties ^[19].

In $\pi - \pi$ stacking interactions the nuclei of carbon atoms each have a positive charge (+1) surrounded by two negative charges (-1/2) with δ distance between these opposite charges (Fig. 10). The possible motifs that can be formed in this system have been explained by Hunter and Sanders, and they are the repulsion face-to-face geometry, attractive offset face-to-face geometry and attractive edge-to-face geometry ^[20]. The face to face geometry can be attractive if the polarization of the two aromatic rings is different. This can be achieved by using atoms with electronegativities different to carbon and hydrogen (Fig. 11) ^[21].

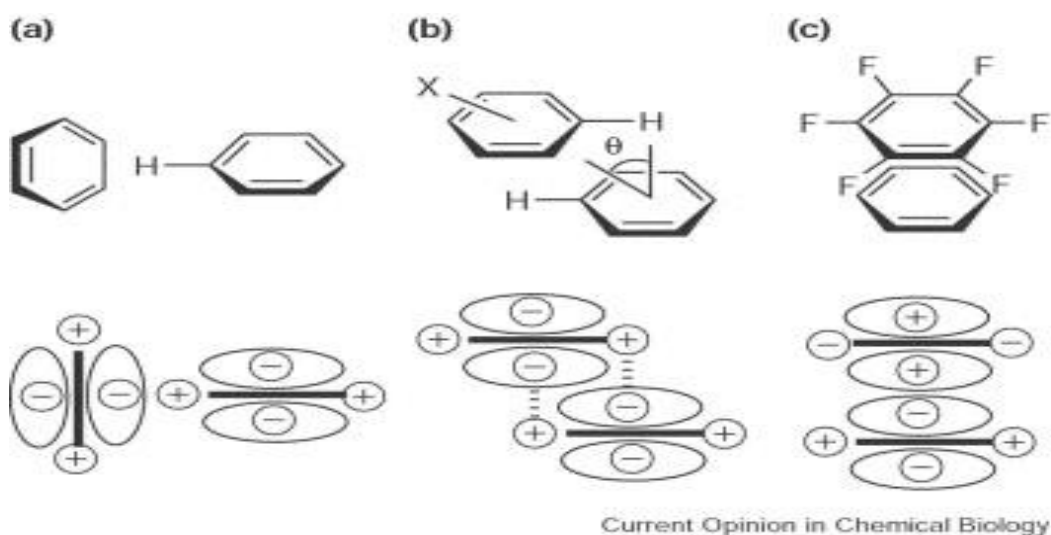


Figure 10: The various geometries of a π system, a) edge to face geometry, b) offset face to face geometry, c) face to face geometry ^[22].

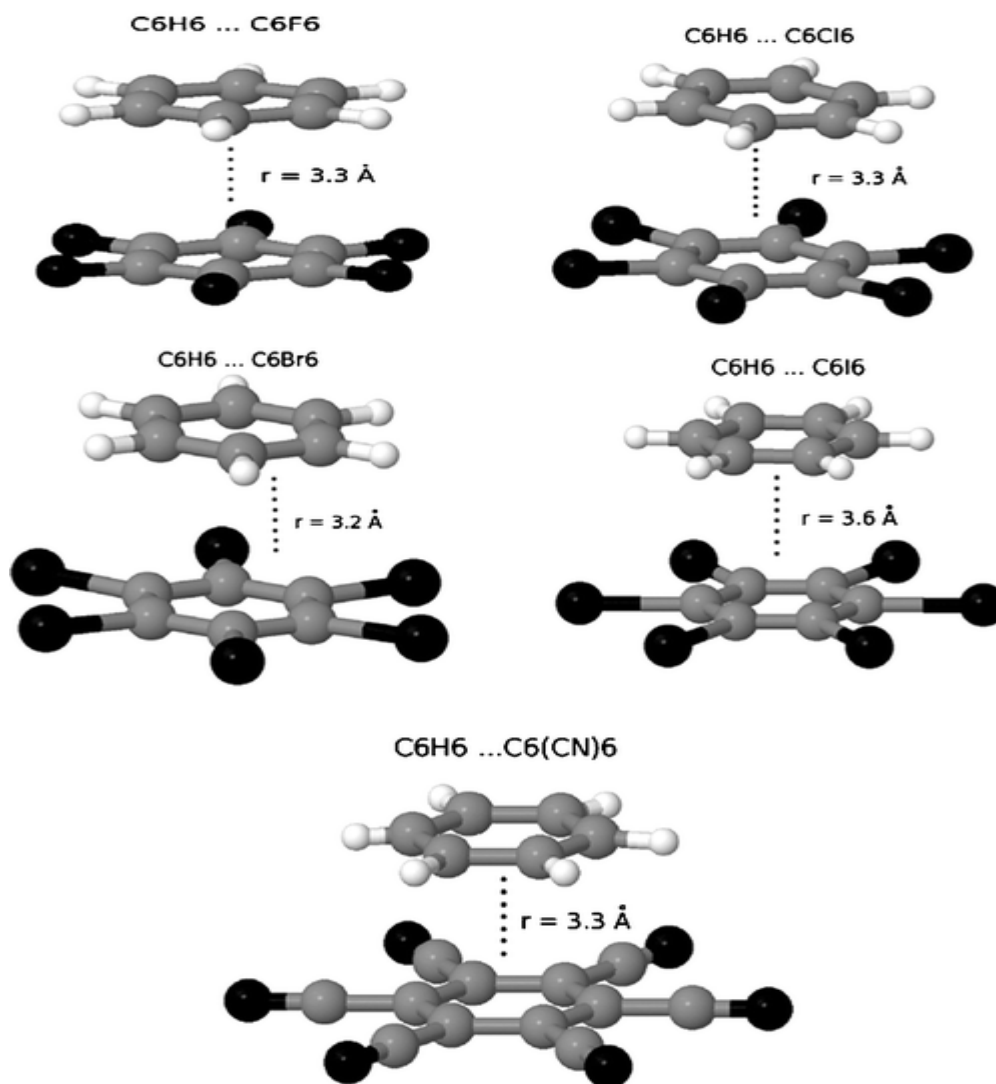
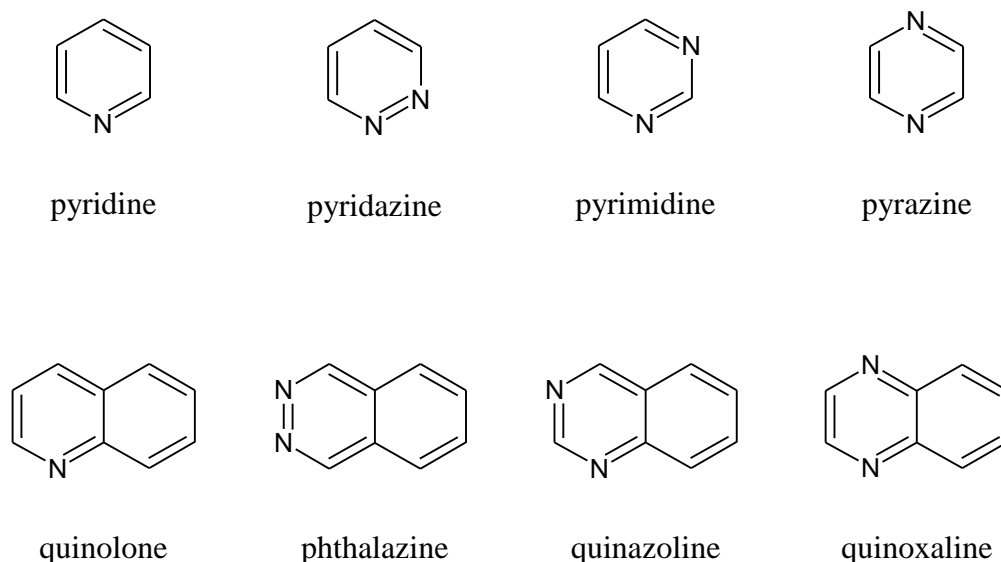
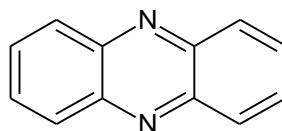


Figure 11: The effect of the polarized substituents on the attraction force of the face to face geometry^[23].

By modifying the polarization favorable $\pi - \pi$ stacking interactions can be achieved. This can be done based on the position and number of the polar substituents, and this has been investigated through studying the packing of different aromatic rings that have variable numbers and positions of nitrogen atoms in aryl groups, such as pyridine, pyridazine, pyrimidine, pyrazine,

quinolone, phthalazine, quinazoline, quinoxaline and phenazine (Fig. 12). Studies have confirmed that adjusting the polarization affects the packing and allows for the best orientation to have the desired face to face $\pi - \pi$ stacking interactions [21]. This type of interactions can be interpreted using an electron donor-acceptor model, which has been confirmed by Chang et al reference, who synthesized new compounds and found crystal packing with favourable offset face to face geometry as a result of the different polarization between aromatic rings. These compounds are 2,5-di(pyrimidin-2-yl)thieno[3,2-b]thiophene, 2,5-di(pyrimidine-5-yl)thieno[3,2-b]thiophene, 2,5-di(pyridine-5-yl)thieno[3,2-b]thiophene, 2,5-bis(4-(trifluoromethyl)phenyl)thieno[3,2-b]thiophene and 2-thieno[3,2-b]thiophene-2-yl-benzothiazole [24]. So $\pi - \pi$ stacking interactions can be attractive or repulsive. The incorporation of heteroatoms can overcome the repulsion in this type of interaction, and the orientation also is able to provide attraction forces [20] (Fig. 13).





phenazine

Figure12: Aryl groups containing different number and position of nitrogen atoms^[21].

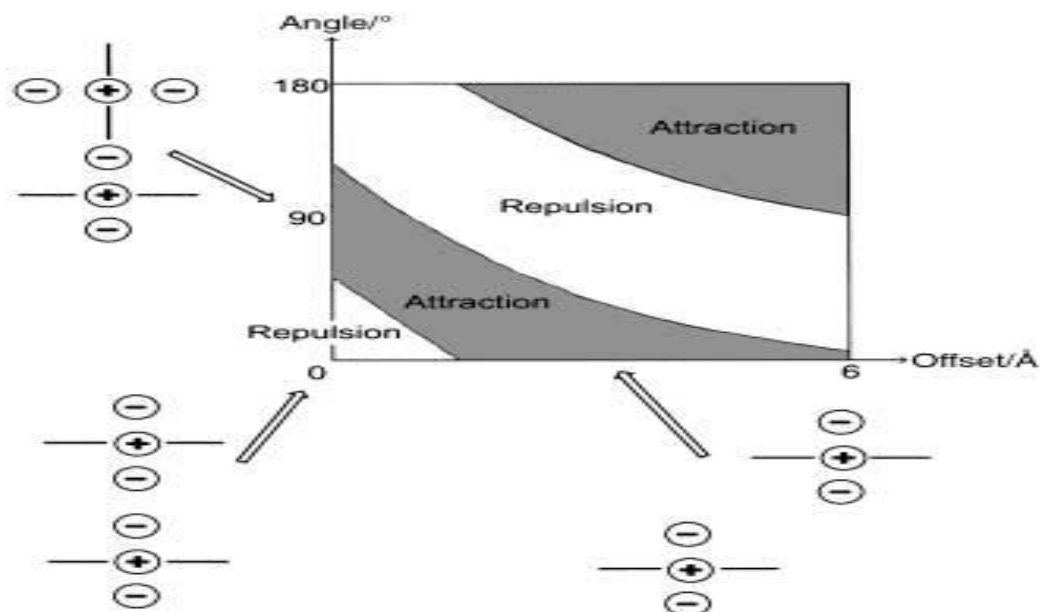


Figure 13: Effect the orientation on the electrostatic interactions^[25].

There are other factors that can affect the geometry of these interactions. A study has been carried out by Zhang to investigate the effect of size and shape of face-to-face dimers on the $\pi - \pi$ stacking interactions, which consist of six condensed arenes of regular hexagonal (RH), eight ladder-shaped (LS) and eight wavy-linear all-trans conjugated alkene (Fig. 14)^[26].

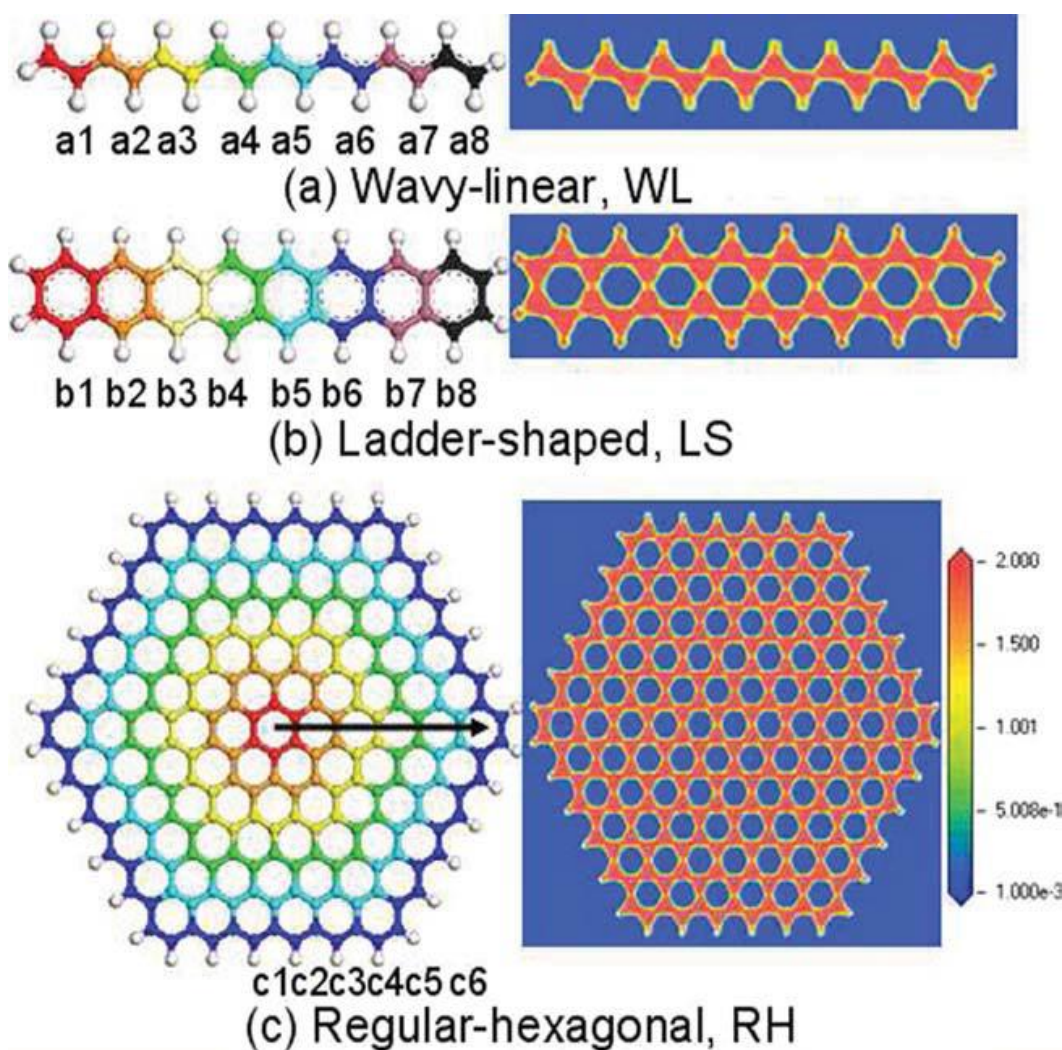


Figure 14: On the left side hand the different sizes of the different molecules have been represented by different colours such as a1 to a8, b1 to b8 and c1 to c5, whereas on the right hand side the delocalization of π -electrons has been shown by the electron density pictures of the largest molecules ^[26].

He deduced that if the monomers have a decreased symmetry and an increase in their size, or vice versa, then the energy of these interactions will be affected by rotation. In the dimers with the same shape, only the shape of these monomers has the ability to control the distance of centroid-centroid $\pi - \pi$ stacking interactions. He found there is a directly proportional relationship between the strength of $\pi - \pi$ stacking interactions and the electron density, and reported that the face-to-face geometry ^[26].

In the 1980s, Ferguson and Diederich found that the main factor to control the stability of complexes is the electrostatic forces in the absence of charge transfer effect. They studied 2,6-disubstituted naphthalene derivatives interacting with cyclophanes in d_4 -methanol, using various substituents with low and high electron density, such as CH_2OH , NH_2 , CH_3 , CO_2H , NO_2 and CN . In 1987 edge to face geometry based on substituents that have different electron density was shown in the class of thymine receptors that had been synthesised by Hamilton and his colleagues ^[25]. Partially extended helical theory has been used by Chesnut and Mosely to measure charge transfer complexes geometrically, which were similar to the crystal structures determined by XRD, and a slight increase in the stability can be achieved through the charge transfer bonds in these complexes ^[25].

Another factor that has been investigated is the effect of substituents on the parallel-displaced geometry, which has been carried out by Arnstein and Sherrill. They found that the position of the (PES) potential energy surface could be positive or negative (Fig. 15). They also found that the horizontal fluorine substituent leads to decrease the energy of $\pi - \pi$ stacking interactions, whereas, hydroxyl substituent leads to enhance the dispersion interactions ^[27].

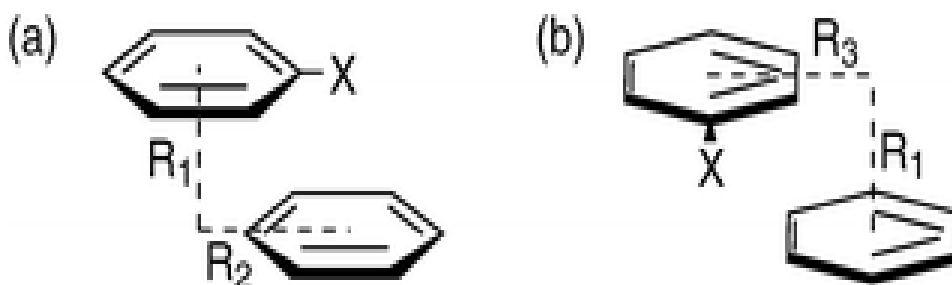


Figure 15: Substituted benzene–benzene complexes in (a) parallel-displaced over a vertex and (b) parallel-displaced edgewise orientations. X = H, F, CN, and OH ^[27]

In this project compounds containing both polyfluoroaryl and aryl groups and their potential for crystal engineering are investigated. Koizumi et al, have confirmed that the selectivity of inter-and intra-molecular A-D-A $\pi - \pi$ stacking interactions between phenylene and two pyridinium rings can be affected by the type of substituents ^[28]. In 2012 the effect of various substituents in different position was studied using the structure of racemic 2- and 4-substitued benzyl leucine diethyl amides. It has been found that, 4-NO₂, 3-Me, 3-OMe, 3-NO₂, 3F, 3-Br and 3-Cl enhance the stability of $\pi - \pi$ stacking interactions and lead to self-assembly, whereas, 4-CN, 4-OMe, 4-Me, 4-Cl and 4-Br failed to self-assemble and enhance the stability of $\pi - \pi$ stacking interactions. This difference arises because of some factors such as exchange repulsion, dispersion, induction and electrostatic forces, and two of them, which are electrostatic dispersion forces, have been reported to strongly affect the energy and direction of the interactions between the benzene dimers in T-shaped and slipped parallel geometries ^[29]. Regarding the effect of anti-parallel and parallel mono-substituted benzene dimes on the energy of $\pi - \pi$ stacking interactions, it has found that mono-substituted benzene dimers in parallel-displaced form leads to less stability than the antiparallel-displaced form of benzonitrile-phenyl, fluorobenzene-phenol and nitrobenzene-phenol ^[30].

A study by Rashkin and Waters based on the Hunter and Sanders model has shown unusual substituents effect during their studying of meta and para-substituted *N*-benzyl-2-(2-fluorophenyl)-pyridinium bromides. T-shaped geometry can be seen between the B and C aromatic rings through using the methylene group as a bridge. Water solubility can be provided through the pyridinium ring A, which led to the diastereomer of Ha and Hb. The energy using

different substituents (e.g. X=H, 4-CH₃, 3-CH₃, 3,5-(CH₃)₂, 4-CF₃, 3-CF₃, 3,5-(CF₃)₂, 4-NO₂, 3-NO₂, 3,5-(NO₂)₂) has been measured (Fig. 16).

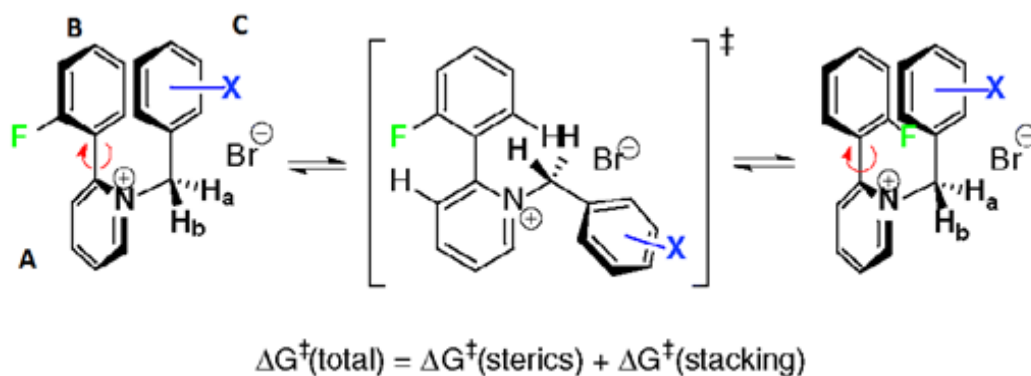


Figure 16: Substituted meta and para-substituted *N*-benzyl-2-(2-fluorophenyl)-pyridinium bromides ^[31].

Based on the collected data they reported that the magnitude of interaction can be affected by the orientation of two attached aromatic rings, which can be affected by the electron density in para-substituted *N*-benzyl-2-(2-fluorophenyl)-pyridinium bromides using 4-NO₃ as substituent, whereas using 3-NO₃ substituent lead to higher rotation as a result of the attractive force between oxygen and hydrogen atoms, and this difference impact positively on other stacking interaction that involved DNA bases as substituted rings ^[32]. Similar consequences have shown the importance of electrostatic and substituent effects on $\pi - \pi$ stacking interactions, and this has been confirmed by Cockroft et al, through characterization of new synthetic supramolecular zipper complexes using NMR with chloroform as a solvent ^[33].

Cockroft et al, have confirmed the effect of electrostatic forces in controlling the non-covalent interactions between aromatic rings through supramolecular chemistry. They have measured this type of interaction using four complexes with double mutant cycles to quantify them. ¹H NMR spectroscopy in CDCl₃ was used for characterization. Various substituents have been used to show their different effects in the interactions of pentafluorophenyl and phenyl such as (NMe₂, H, OMe, Cl, NO₂), through comparison of their measured energies (Table. 2) with the Hammett constants (Fig. 17). They have found that substituents with low electron density lead to highly attractive forces in pentafluorophenyl. As a result these substituents lead to a positive surface, which makes it more attractive for substituents with high electron density. In contrast, the surface of aromatic phenyl ring has negative charge which makes it attractive for substituents with low electron density ^[34].

| Substituents X | pentafluorophenyl | phenyl |
|------------------------|--------------------------|---------------|
| NMe₂ | -3.2 | +1.5 |
| H | -3.0 | +0.3 |
| OMe | -2.2 | +0.9 |
| Cl | -1.2 | 0.0 |
| NO₂ | -0.2 | -1.0 |

Table 2: Values measured in CDCl₃ at 293 K, and errors are 0.7-1.1 kJ mol⁻¹ ^[25].

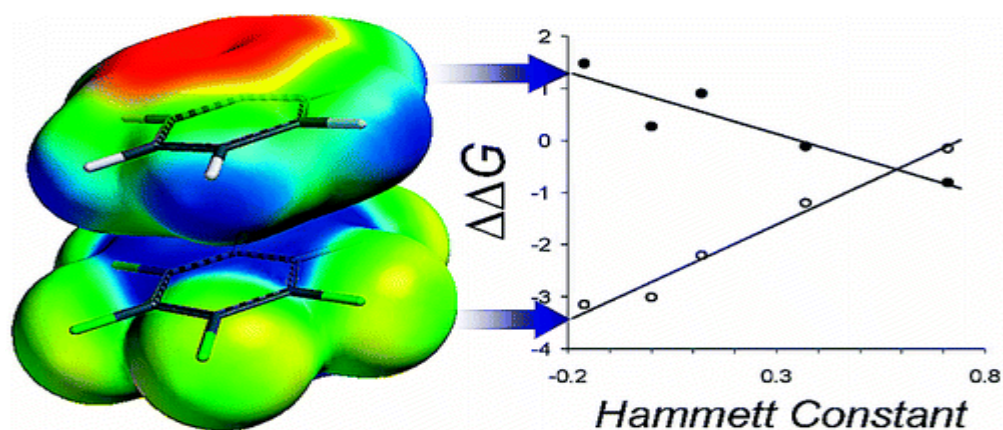


Figure 17: Experimental aromatic stacking interaction energies ($\Delta\Delta G$) correlate with the Hammett substituent constant for X (σ_X). Interactions with phenyl (●) and pentafluorophenyl (○) are shown ^[34].

Metal tris(bipyridine) complexes have been used to determine the effect of solvent on aromatic interactions by Beaut et al. These were quantified by ^1H NMR spectroscopy of bipyridine with the involvement of pendant alkyl and aromatic esters. A proportional relationship has been found between the chemical shifts and the polarity of the solvent, with the presence of polar solvent in the upfield chemical shifts. In DMSO a further reduction of this solvent lead to a minimum reduction of the strength of aromatic interactions followed by an increase. Water and CDCl_3 give similar results, which show that attractive forces of aromatic interactions are controlled by the electrostatic forces and non-polar solvent (Fig. 18).

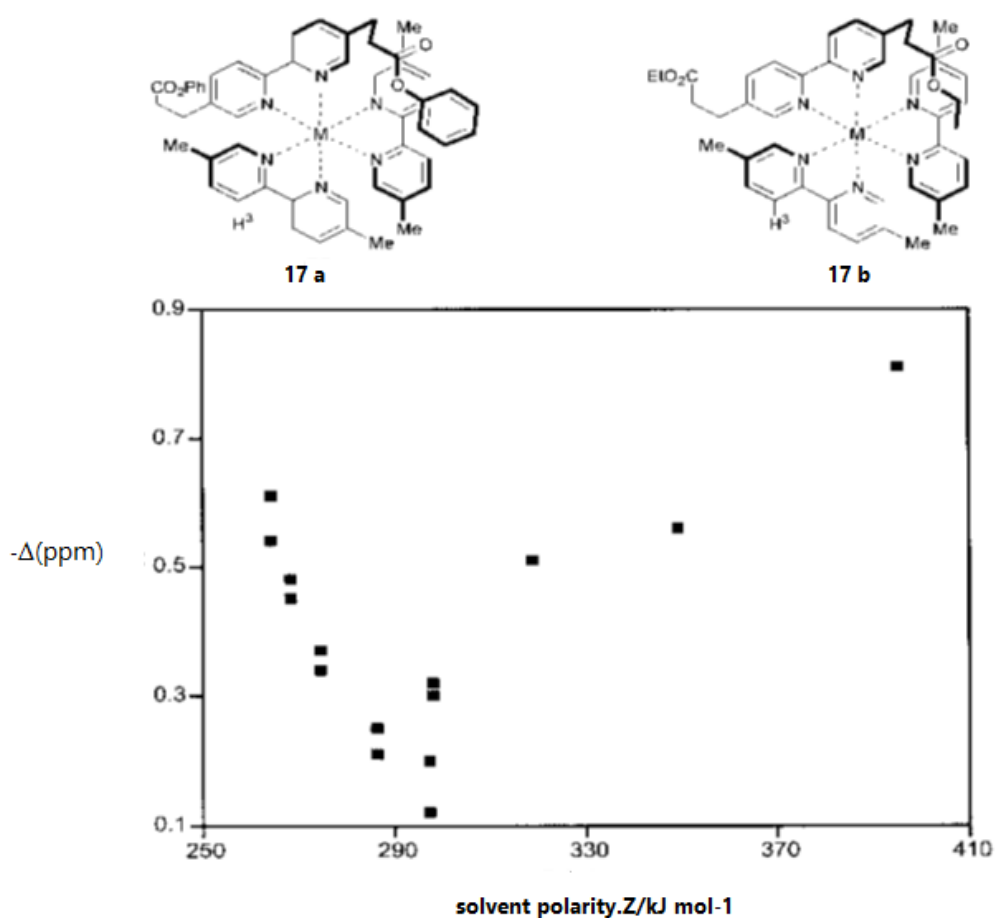


Figure 18: Studying the effect of solvent on the aromatic stacking interactions using metal complexes, $\Delta\delta = \delta(\text{H3 in } 59) - \delta(\text{H3 in } 60)$ ^[25].

Smithrud and Diederich have confirmed that aromatic interactions can be affected by solvent. Pyrene complexes with cyclophane in over 15 solvents of different polarities have been used to determine the constant and to describe these different polarities, an empirical parameter has been used. The relationship between the polarity and the stability of these interactions was represented by a line as shown below (Fig. 19) ^[25].

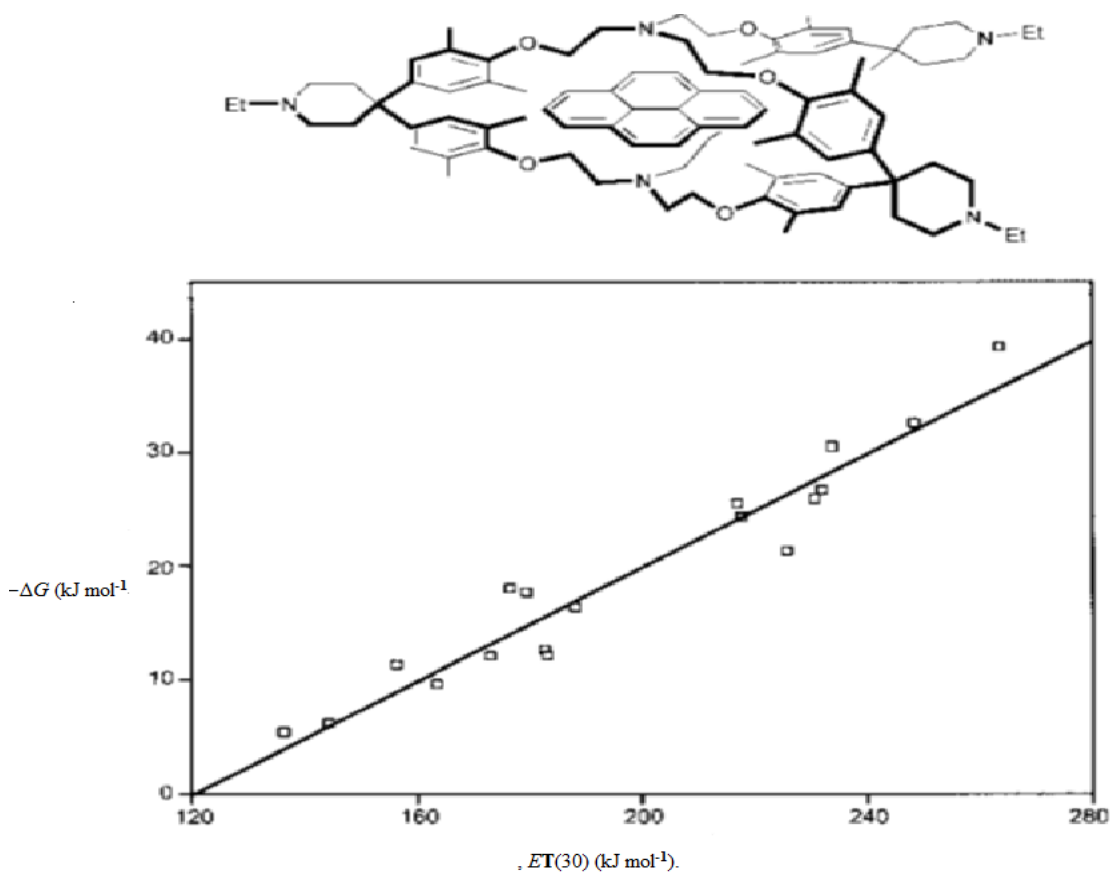


Figure 19: Dependence of the free energy of complexation of the cyclophane pyrene complex, $-\Delta G \text{ (kJ mol}^{-1}\text{)}$, with solvent polarity, $ET(30) \text{ (kJ mol}^{-1}\text{)}$ [25].

The importance of this non-covalent interaction refers to its importance in the design, control and enhancement of the crystal structure to obtain functional properties. For example, modify the behaviour of liquid phase through p-p interactions has been achieved by Wech et al, based on arene-perfluoroarene interactions. A perfluoroarene has been added to the moieties of triphenylene, that are involved in four compounds, which enhance the stability of liquid crystalline mesophase with an increase in the temperature [32]. These interactions have also used to form the crystal structure of hexafluorobenzene trans-stilbene, which has shown a stacking combination with different orientations and same direction (Fig. 20) [36]. However, variation in crystal packing can be obtained by

$\pi - \pi$ stacking interactions such as sandwich herringbone, sandwich, gamma (γ) and beta (β) packing geometries ^[21] (Fig. 21).

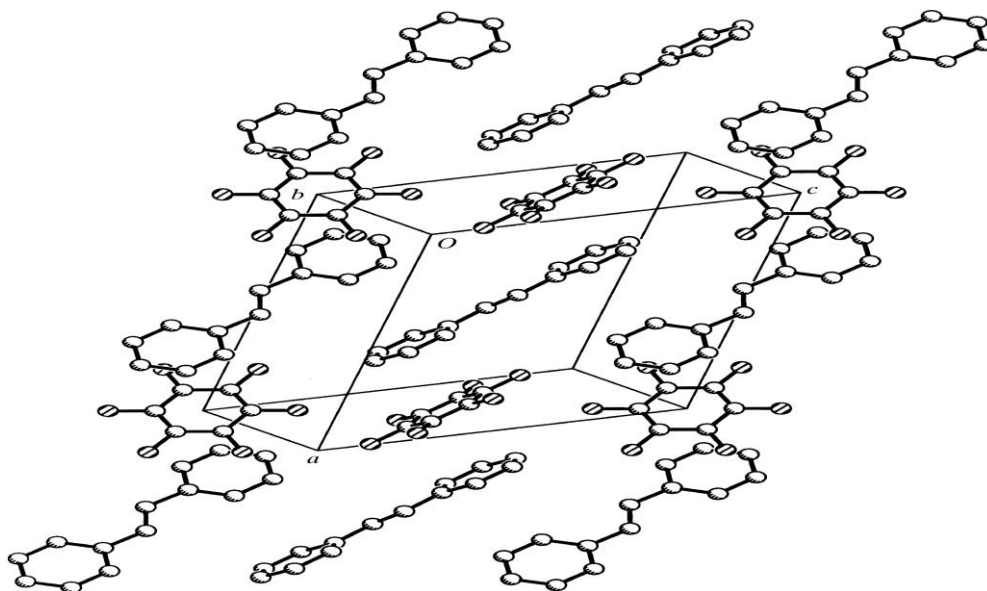
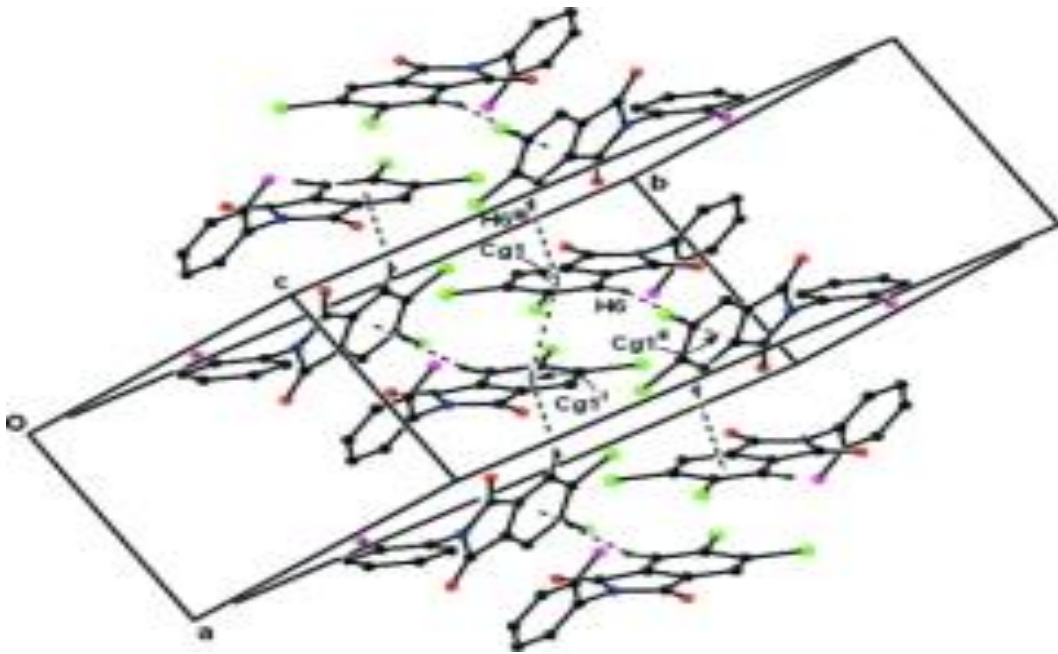
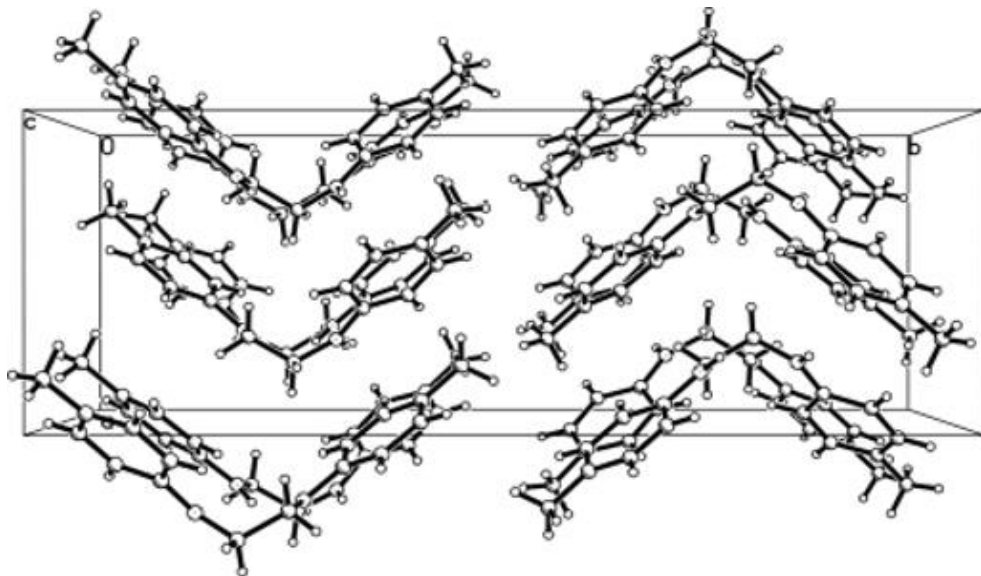


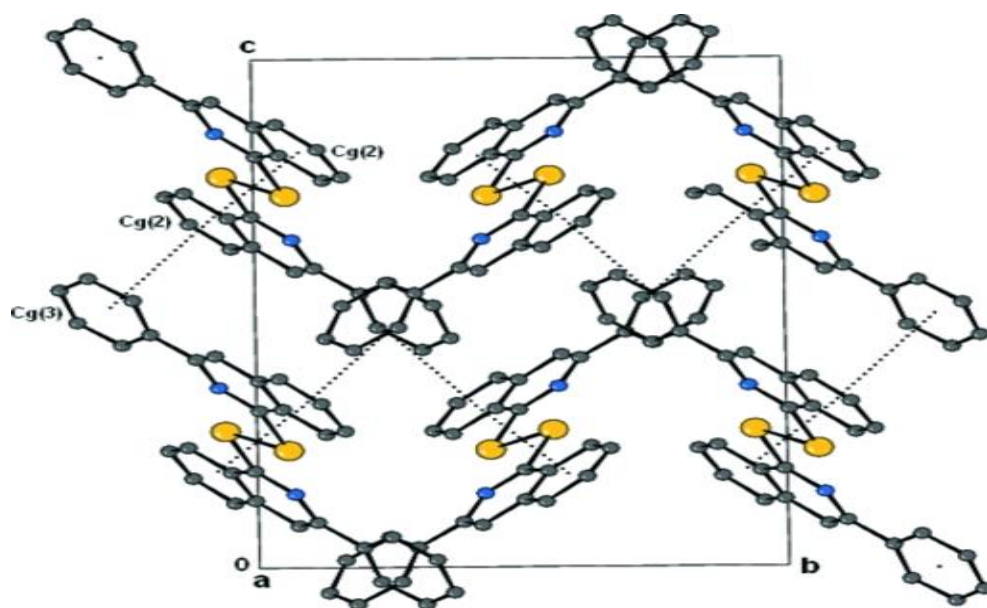
Figure 20: In this crystal structure a combination of stacking interactions is involved ^[36].



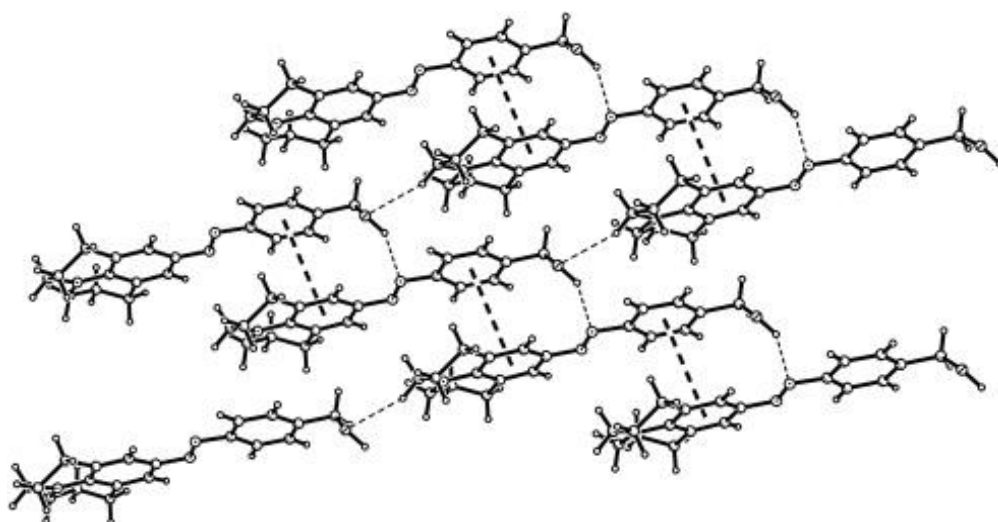
a) 5,6-Dichloro-2-(2-fluorophenyl)isoindoline-1,3-dione (beta (β) packing) from [openi.nlm.nih.gov].



b) N,N'-Di-p-tolythylenediamine (gamma (γ) packing) From [openi.nlm.nih.gov].



c) Benzo-fused-1,3,2-dithiazolylium salt (sandwich herringbone). From [openi.nlm.nih.gov].



d) Molecules connected by O-H...N and C-H...O inter-molecular hydrogen bonds (sandwich) ^[37]

Figure 21: a) Beta (β) packing, b) gamma (γ) packing, c) sandwich herringbone and d) sandwich geometries.

1.4. Supramolecular Chemistry:

In supramolecular chemistry, it has been found that $\text{Ar}^{\text{H}}\text{-Ar}^{\text{F}}$ synthons, which are based on $\pi - \pi$ stacking interactions, are important in controlling the packing of crystals. For example, a specific stacking of phenyl-perfluorophenyl has shown an increase in reactivity^[6]. $\pi - \pi$ Stacking interactions have an essential role in forming lots of supramolecular synthons that have importance in various fields. For example, supramolecular synthons of naphthalimide rings of one dimer with four adjacent dimers have been formed by $\pi - \pi$ stacking interactions^[38].

Also a combination of this stacking has been used between 1,8-naphthalimide moieties to form four new paddlewheel $\text{Cu}_2(\text{OCR})_4(\text{L})_2$ compounds with unusual magnetic properties and highly organized structures, and with possibility of unusual physical properties^[39]. Zhao et al, have investigated the role of these non-covalent interactions in forming an infinite stacking of supramolecular synthons and have evaluated the different types of stacking between various aromatic rings by studying four types of polymeric crystals which have been found in silver nitrate as a solvent. These are $[\text{R-C}\equiv\text{C-Ag}]_n$ ($\text{R}=\text{3-pyridyl, 2-pyrazinyl}$) and $[\text{Ag}_2(\text{C}\equiv\text{C-R-C}\equiv\text{C})]_n$ ($\text{R}=\text{m-C}_6\text{H}_4, \text{2,3-C}_4\text{H}_2\text{S}$), and it has been deduced that the assembly of supramolecular synthons is controlled by $\pi - \pi$ stacking interactions, which are preferential in multidimensional metal-organic frameworks^[40].

This has been confirmed by Bai et al, who studied three-dimensional helical chains, which are $\text{Ce}(\text{bpdc})_2\cdot\text{H}_2\text{O}$ and $\text{Zn}(\text{6-bpc})_2\cdot\text{H}_2\text{O}$, where 6-Hbpc is 2,2'-bipyridine-6-carboxylic acid, and then reported that the directionality and extension of these two supramolecular synthons are controlled by hydrogen

bonding and $\pi - \pi$ stacking interactions ^[37]. It has been shown that, the high stability of these supramolecular synthons can be obtained through these non-covalent interactions, and this has been reported by Santons et al during their study the cooperativity between $\pi - \pi$ stacking interactions and H-bonding, between 2-[9-(1,3-dithiol-2-ylidene) anthracen-10(9H)-ylidene]-1,3-dithiole and C₆₀ based on the donor-acceptor model. It has been found that $\pi - \pi$ stacking interactions dominate the structure of these supramolecular synthons, whereas H-bonding has less contribution for these synthons ^[42].

New supramolecular synthons have been synthesised by $\pi - \pi$ stacking interactions with various dimensions. First of all, one dimensional synthons such as [Cu(phen)(C₁₀H₁₆O₄)].3H₂O, where phen=1,10phenanthroline ^[43], 2-(2-pyridylamine)pyridinium chloride phosphorous acid ^[44], [Mn₁₂O₁₂(O₂CC₆H₄C₄H₃S)₁₆(H₂O)₃].14CH₂CH₂ ^[45], [Zn(NIPH)(py)₃]_n, [Mn(NIPH(-py)₃]_n, {CO(NIPH)(py)₃}.(H₂O)}_n and {[Cd(NIPH)(im)₂.(H₂O)].(H₂O)}_n ^[46].

Secondly, two dimensional synthons such as [Zn(mpdc)C₁₂(phen)₂] (mpdc=2,6-dimethylpyridine-3,5-dicarboxylate ^[47], [Ag₃(tmp)₄][ClO₄]₃.C₃H₆O, [Ag₂(tmp)₂][C₂F₅CO₂]₂, where tmp=2,3,5,6-tetrakis (methylsulfanyl) pyridine ^[48], 2-(2-pyridylamino) pyridinium nitrate monohydrate ^[44].

Finally, three-dimensional synthons such as {[Zn(bpdc)(H₂O)₃].3H₂O}_n (H₂bpdc=2,2'-Bipyridyl-3,3'-dicarboxylic acid) ^[49], {[Ag(4,4'-bpy).H₂O](4-ab).2H₂O}, {[Ag₂(bpe)₂.(tph)].2H₂O}, Ag(tbpe)]0.5(4-hb).3H₂O} and [Ag₂(L)₂.(tph)] (L=4,4'-bpy or tbpe) ^[50], {[Cu₃(terephthalate)₂(dipyrido[3,2-

d:2',3'-f]quinoxaline)₂(OH)₂]}_n, { [Cd₂(5,6-diamino-1,10-phenanthroline)₂(terephthalate)₂(H₂O)₂].2H₂O} _n ^[49].

$\pi - \pi$ stacking interactions have also been used to obtain functional properties. A study by Ali-Boucetta et al. showed that $\pi - \pi$ stacking interactions in multiwalled carbon nano-tube-doxorubicin supramolecular synthons improved the efficiency of carboxic activity as a cancer therapeutic ^[51].

Another study confirmed that enhanced stability of an amorphous blue light emitter which is 2PPPF, with improved film capacity and a broad emission peak resulted from the strong $\pi - \pi$ stacking interactions between its pyrene rings ^[52]. and with an increase in the number of these interactions in the supramolecular polymer nanocomposites enhanced mechanical and healing properties can be achieved. In 2007 a major approach in supramolecular chemistry to obtain stable complexes through molecular receptors, using only by $\pi - \pi$ stacking interactions, which have been used to synthesize a molecular tweezer with two corannulene subunits (C₆₀H₂₄) (Fig. 22) with good yield, and the strength of these $\pi - \pi$ stacking interactions comes only from the absence of any other effects such as polarity or asymmetric atoms ^[53].

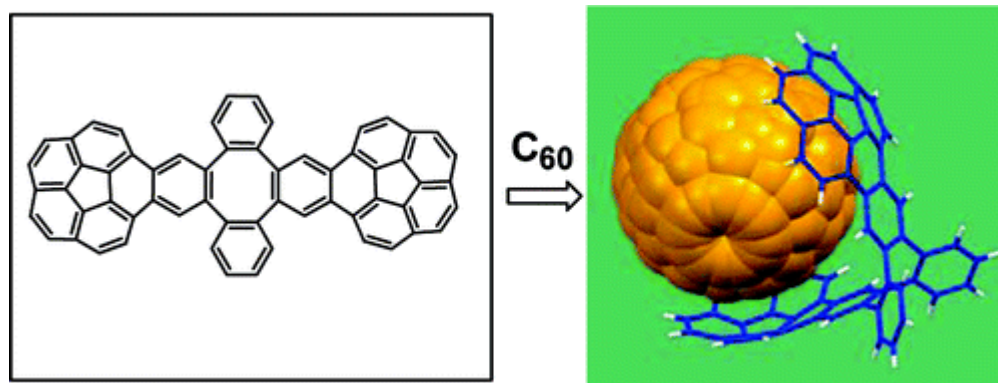


Figure 22: The planar and crystal structures of the molecular tweezer with two corannulene subunits ($C_{60}H_{24}$)^[53].

Other supramolecular complexes that have been stabilized by these interactions are 2,6-pyridylcarboxylic acid bis-4-pyridylamide, bis (hexafluoro acetylacetonate) manganese^[54], 1,3,5-benzonitricarboxylic acid and meta- or para- hydroxyl pyridines^[55], side-by-side polyimidazole tripod coils^[56], $[Cu(butca)0.5(bipy)(H_2O)]n \cdot 2nH_2O$, $[Zn(H_2butca)(phen)(H_2O)]n \cdot nH_2O$ and $[Cd(H_2chhca)0.5(phen)(H_2O)]n \cdot 2nH_2O$, (H4butca=1,2,3,4-butane tetracarboxylic acid, H6chhca=1,2,3,4,5,6-cyclohexanehexacarboxylic acid)^[57]. Other self-assembly supramolecular synthons are bis(μ -7-iodo-8-hydroxyquinoline-5-sulfonato- κ -3N,O:O`)^[58] bis[triaquanickel(II)]tetrahydrate^[58], dinuclear $M_2C_{14}(C_{13}H_9N_3)_2$ ^[59], double-Stranded oligobisnorbornene^[60] and $[Ln(gly)_2(H_2O)_2(phen)_2](ClO_4)_3(phen)_4 \cdot nH_2O$ [n=0, Ln=Nd]^[61].

Further Applications of Aromatic Stacking Interactions:

The photodimerisation of olefins in the solid state has been accomplished through using these interactions by Coates et al. The crystals of (E)-pentafluorostilbene have been formed from the alternated stacking of phenyl and pentafluorophenyl rings, and as a result of this a single isomer of the cyclobutane photodimer was formed. Also, these stacking interactions have been used to obtain the monomeric units for polymerisation by Dougherty. The polymerisation of the diyne lead to formation (E)-polybutadiyne (Fig. 23), the (Z)-polymer can be obtained through the arrangement of butadiyne units (Fig. 24), and the crystals of stacked phenyl-pentafluorophenyl with the mixed phenyl-pentafluorophenyl diyne have been formed and analysed by XDR. The crystallographic data has shown a head to tail arrangement (Fig. 25).

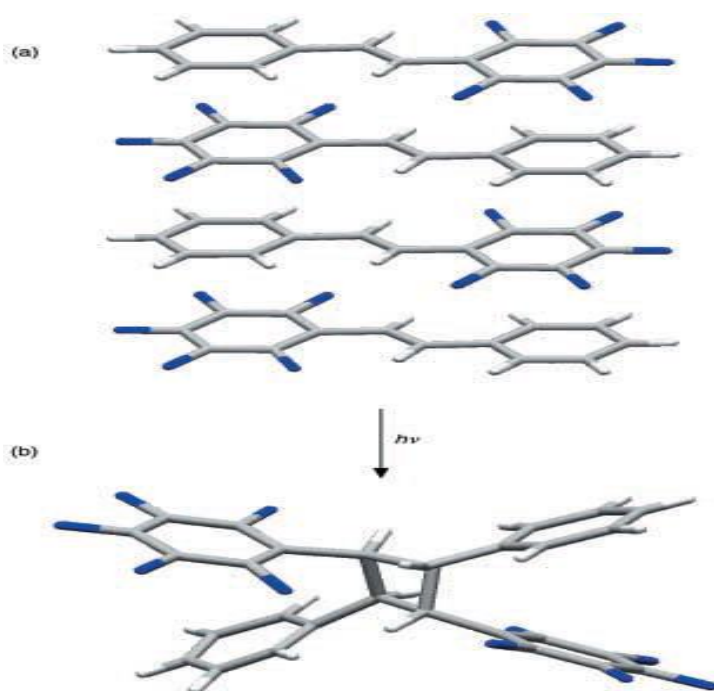


Figure 23: In the solid state, the geometry of stilbene derivative is determined by the stacking interactions of phenyl–pentafluorophenyl (a) which lead to formation of the stereo-chemical cyclobutane photodimer (b) ^[25].

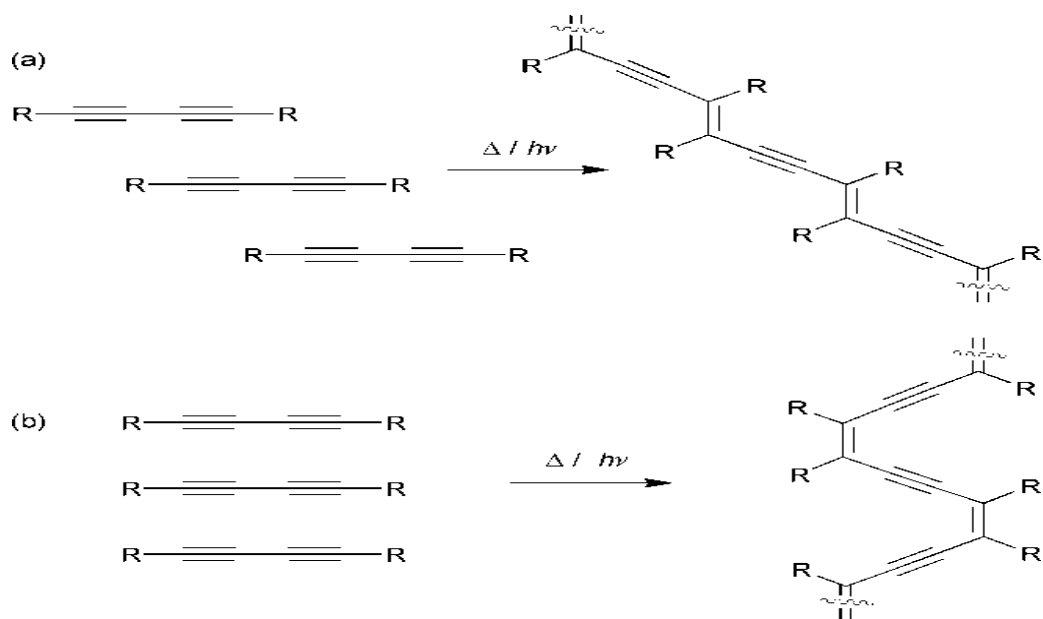


Figure 24: (a) Diyne polymerisation to give (*E*)-polybutadiyne. (b) Butadiyne units arrange to form the (*Z*) polymer ^[25].

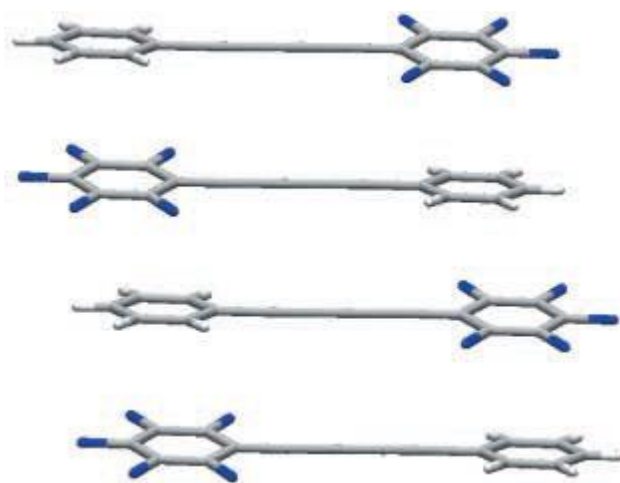


Figure 25: Head-to-tail structure of 1-(2,3,4,5,6-pentafluorophenyl)-4-phenylbutadiyne ^[25].

Functional properties of the molecules in the solid state can be achieved by this stacking interaction. Crystallographic data that have been collected from the engineered crystals of semi-conducting charge transfer complexes such as the derivatives of tetracyanoquinone and tetrathiofulvalene have shown that controlling all the functional properties can be done by controlling the stacking interactions between aromatic rings.

Edge to face geometry has been measured by Hunter et al; a pair of mutant cycles have been built by H-bonded molecular zippers.¹H NMR using CDCl₃ has been used to determine the constants of these complexes, the measured energy of the T-shaped geometry of unfunctionalized aromatic rings was -1.4 ± 0.8 kJ mol⁻¹. In this study a model structure has been studied by XRD, and the geometry of the interaction at the terminus of the zipper. The effect of the substituents has been studied through the addition of these different substituents to the two aromatic rings that form the T-shaped geometry with both substituents that have low and high electron density, and the values that have been obtained from this (Table. 3) were in agreement Hammet parameters for X and Y (Fig. 26) and this has been represented in the following equation ^[25].

$$\Delta\Delta G (\pi-\pi) = 5.2 \sigma_X\sigma_Y - 1.9 \sigma_X - 1.4 \sigma_Y - 1.5$$

| Substituents Y | Substituent X | | |
|------------------|-----------------|------|------------------|
| | NO ₂ | H | NMe ₂ |
| NO ₂ | +1.2 | -0.2 | -1.4 |
| H | -3.4 | -1.4 | -1.1 |
| NMe ₂ | -4.6 | -1.8 | -0.9 |

Table 3: Substituents with high and low electron density that were added to edge-to-face rings ^[25].

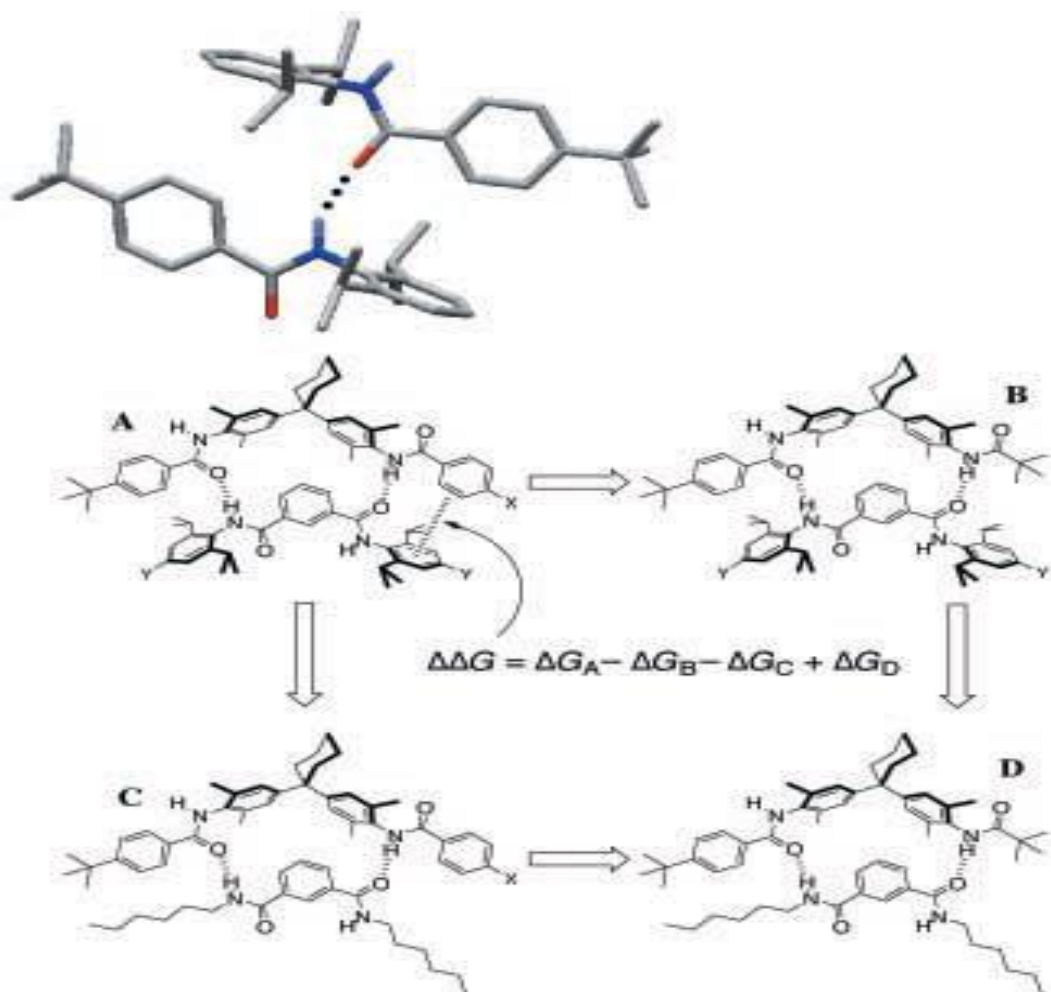


Figure 26: The terminal edge-to-face aromatic interaction in complex A has been determined by using a chemical double mutant cycle. The X-ray crystal structure of a model compound which contains the same intermolecular interaction is shown in the inset ^[25].

1.5. Biological Activity:

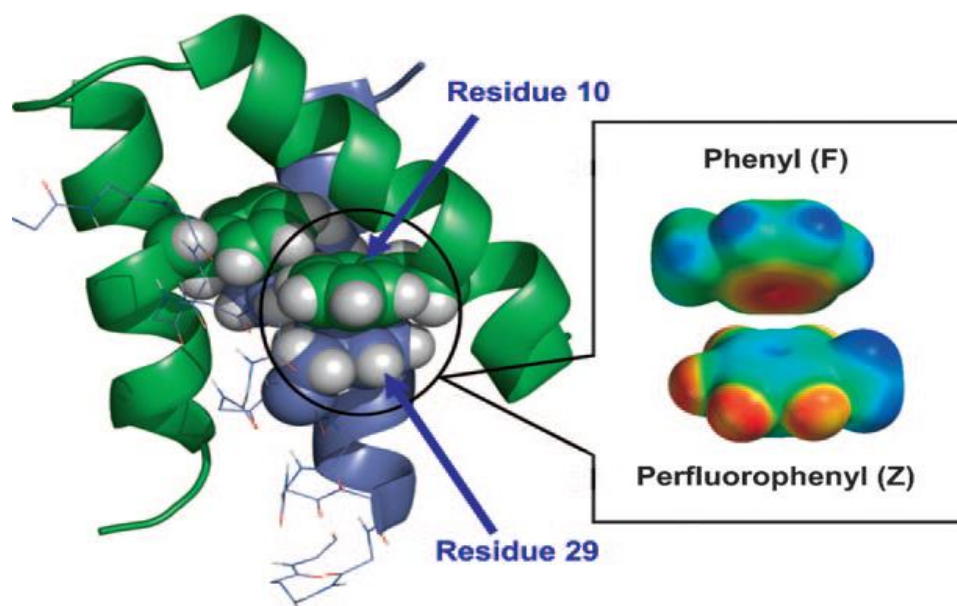


Figure 27: The arene-perfluoroarene interactions in α 2D protein ^[62].

Zheng and Gao used α 2D protein to investigate the role of the strong quadruple interaction of the phenyl-perfluorophenyl complex in controlling the direction of protein-protein interactions in the liquid phase and found that the stability of this protein increased by $-1.0 \text{ kcal mol}^{-1}$ due to the electrostatic attractive forces in this complex ^[62] (Fig. 27). Furthermore, these reactions can be found in the active sites on the interface of proteins. Thus it can be used to enhance the catalysis, selectivity, folding, and stability of proteins and DNA and the self-assembly of H-bonding in the biological systems ^[63]. Yuki et al. made a comparison between the original molecular dynamics simulation method with another molecular dynamics simulation using a modified sander module with different amino acids such as the Trp-cage structure of protein. This showed the importance of $\pi - \pi$ stacking interactions in decreasing by half the distance between the root mean square deviations in the main and secondary chains. To conclude, $\pi - \pi$ stacking

interactions play a key role in the stability of proteins and lead to an increase the precision of the data that have been collected by MD simulations ^[64].

Another study by Mao et al. has confirmed that the stability of pigment-protein complexes arises because of the $\pi - \pi$ stacking interactions between their carotenoids, which also play an important role in folding peridinin-chlorophyll11-protein complexes based on their separation and orientation ^[65]. This type of interaction has also been found in the active site of an aminoglycoside phosphotransferase enzyme (APH(3['])-111a) ^[66] and the DNA, where $\pi - \pi$ stacking interactions cannot be ignored in view of their strength during studies of their stability.

In 2009 a comparison between $\pi - \pi$ and cation $\pi - \pi$ stacking interactions based on the strength of $\pi - \pi$ stacking interactions between nucleobase and amino acid using the data of the potential energy that has been scanned from the surface of dimers in the crystal structure of DNA-protein complexes showed a slight difference of $\Delta E_{\text{correlation}}$ between the protonated histidine and the neutral histidine, although there was a remarkable stability in cation $\pi - \pi$ stacking interactions in the protonated histidine as a result of the huge increase in ΔE_{HF} (Hantree-Fock energy) compared to $\pi - \pi$ stacking interactions in the neutral histidine ^[67].

An additional effect of $\pi - \pi$ stacking interactions on the DNA has been shown by Mignon et al, who confirmed that the parallel stacking of the $\pi - \pi$ stacking interactions affects positively on the efficiency of H-bonding between stacked DNA/RNA bases ^[35], which also were used by Saha et al. to form the quadruples of PNA and DNA ^[68]. The role of $\pi - \pi$ stacking interactions increases the

selectivity of the self-assembly process in the hydrogen-bonded molecular capsules has been shown by Tiefenbacher and Rebek (Fig. 28) ^[69].

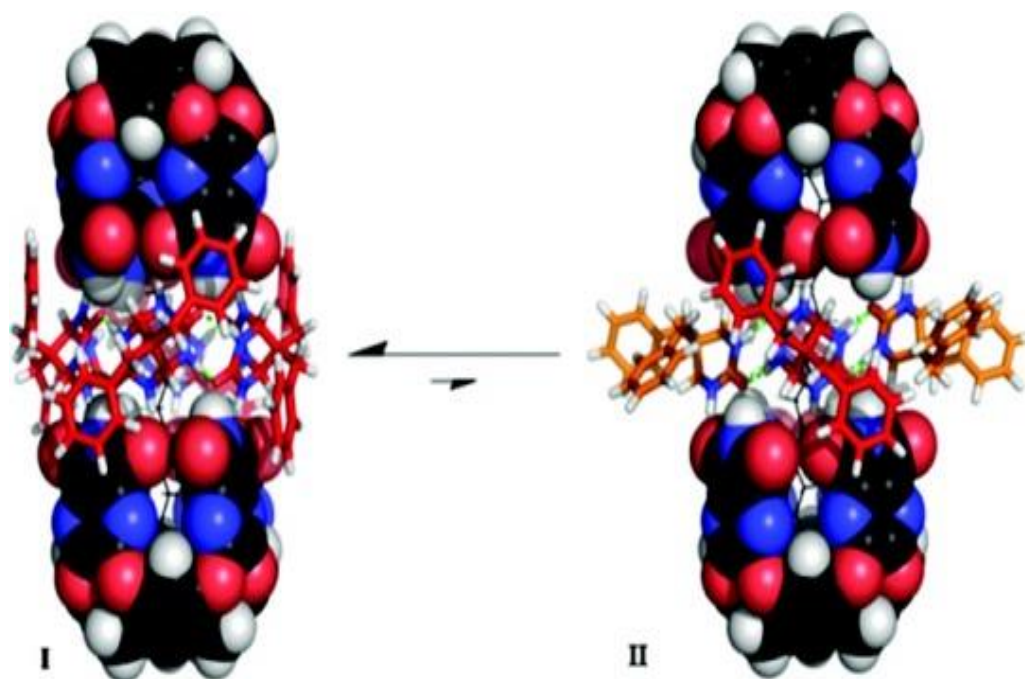


Figure 28: I is an incorporated self-assembly model of benzyl-PD, II represents the incorporated self-assembly model of benzyl-PD in both a twisted fashion with red colour and horizontally bound to the cavitand with orange colour ^[69].

1.6. Pharmaceutical Activity:

In the pharmaceutical industry the interactions between polyfluoroarene-arene synthons have been used widely to design new drugs and enhance the selectivity. New drugs can be designed as a result of $\pi - \pi$ stacking interactions. For example, a survey by Boehr al et, has shown that, a specific inhibitors of aminoglycoside kinases can be achieved by a good knowledge of the nature of this type of interaction between Tyr42 and adenine rings of ADP ^[66]. These interactions have also been involved in the drug metabolism of the enzyme such

as cytochrome P450 (CYP), and forming the complex of this drug is conditional on $\pi - \pi$ stacking interactions, which aim to bind the drug to CYP to form the complex ^[64]. These interactions and the formation of new inhibitors of the human enzyme such as CYP2E1 have been investigated by Martikainen et al., who reported that $\pi - \pi$ stacking interactions in the active site have an important role in affinity folding ^[70].

In 2004 the complexation of these interactions has been used to reduce the toxicity of the high concentration of Amitriptyline, which is tricyclic antidepressant, through low π -electron density with dinitrobenzenesulfonyl groups ^[71]. Nawaz et al have confirmed that cation- π and $\pi - \pi$ stacking interactions allow the selective inhibition of the enhanced butyrylcholinesterase inhibitors to treat Alzheimer's disease, and this can be achieved using cation- π and $\pi - \pi$ stacking interactions, which have been found in the active site and lead to improve the stability of BCHE complexes ^[72]. Moreover, it has been shown that the function of protein kinase inhibitors can be enhanced by increasing the energies of $\pi - \pi$ stacking interactions in the active site between the ligand and the aromatic rings ^[73], and by increasing the strength of this type of interaction the selectivity and low toxicity can be obtained. For example, strong $\pi - \pi$ stacking interactions between cyclodextrin with adamantine, and between cyclodextrin with adamantine, and between graphene oxide and porphyrin ^[74]. Furthermore, this type of interaction has the ability to interact with caffeine and with various sorts of anti-cancer drugs and DNA.

Christianson et al. found that the number of fluorine atoms can contribute to the strength of electrostatic interactions in arene-perfluoroarene synthons which make it more effective than other interaction forces such as quadruple-quadruple

interactions. For example, the high binding affinity of 1,3,4-thiadiazole-2-thione-based inhibitor of the metalloproteinase stromelysin was achieved through electrostatic interactions between Tyr155 and the pentafluorophenyl group in this inhibitor (Fig. 29) ^[63].

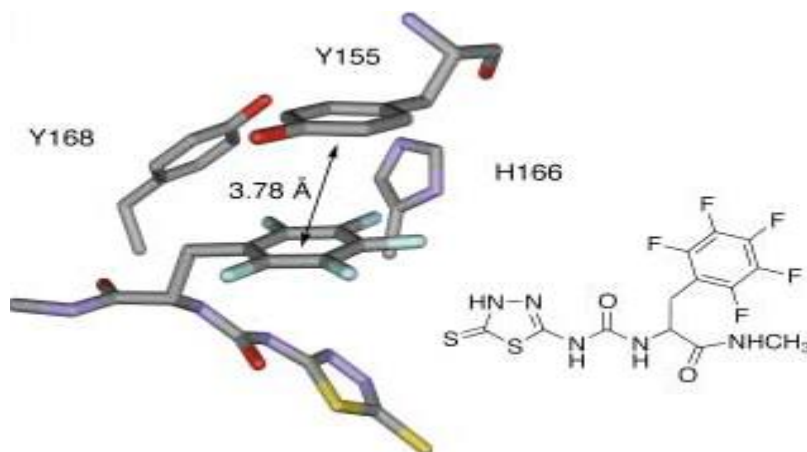


Figure 29: The electrostatic interactions between Tyr155 and the pentafluorophenyl group in 1,3,4-thiadiazole-2-thione-based inhibitor ^[63].

In this project the new compounds were synthesized using different solvents such as THF, DMSO and CH_2Cl_2 , and left at room temperature for different times, then rotary evaporation was used to remove the solvents. The products have been dissolved in different solvents such as CDCl_3 and $\text{d}_6\text{-DMSO}$ to be analyzed by NMR, and same solvent to be analyzed by MS, which is methanol. Then the product was dissolved in CH_2Cl_2 and filtered to calculate the product's yield.

Analytical techniques that have been used in this project are nuclear magnetic resonance, mass spectrometry, infra-red spectroscopy, and single-crystal X-ray Diffraction (XRD). In NMR, all the H nuclei in the different environments were

revealed by ^1H NMR (e.g., 10 H atoms in aromatic rings and one methyl group), but F nuclei were revealed by ^{19}F NMR (e.g., 4 F atoms in aromatic rings and CF_3 group) and C nuclei by ^{13}C NMR (e.g., 9 C atoms in aromatic rings and one CO group).

Functional groups can be introduced by revealing the chemical bonds in the compounds using infrared spectroscopy (e.g. one of CN, one of CO and none of the OH group). Mass spectrometry has been used to determine the molecular mass (e.g. 259; $\text{C}_{16}\text{H}_{21}\text{NO}_2$), and X-ray Diffraction (XRD) can only be used if the very pure crystals have been formed to give the data that lead to determine the structure of those crystals [75].

In this project, ^1H , ^{19}F and ^{12}C NMR spectra were performed using a 400 MHz spectrometer, using different NMR solvents such as CDCl_3 and d_6 -DMSO. Both one and two dimensional NMR spectroscopy have been used, 1D was used to detect the chemical shifts and scalar coupling with only a single frequency axis, whereas, 2D was used to detect the relationship between the spins of two axis. The chemical shifts of 1D NMR spectroscopy have been collected for all the prepared compounds, but 2D NMR spectroscopy have been determined only for those that gave clear ^{13}C NMR spectrum. For example, HMQC and HSQC have been used for 1-(4'-bromo, 2, 3, 5, 6-tetrafluorobenzene)-2-methylimidazole and 1-(2, 3, 5, 6-tetrafluoropyridyl)-2-methylbenzimidazole [76].

The molecular weights for all products were determined using (micro-TOF) mass spectrometry. Mass spectral data has been collected mostly in the mass range from 50 to 800 m/z, with positive ion polarity, using MeOH for distillation. In Infra-red Spectroscopy, identical spectra were obtained from the data that have been recorded in the region from 4000 to 400 cm^{-1} , using KBr pellets.

2. Chapter Two:

2.1. Introduction:

All compounds in this project (in chapter 2 and 3) have been prepared under similar conditions to those compounds that have been synthesized by Fuji et al, (that have been mentioned in chapter 1), which include using solvents such as THF and DMSO under room temperature (from 13° to 16° C), to end up with yields from 26 to 83 % with compounds that have imidazole attached in the para position compared to the meta position which have yields from 2 to 13 %. In this chapter imidazole and prazole and some derivatives have been treated with PFB-R then stirred in THF, DMSO or both for different periods of time under temperature between RT and 142°C. The solvent was removed by rotary vacuum evaporatoion to give the products, which were analyzed by NMR and IR spectroscopy, and mass spectrometry, and then crystallized to be analyzed by XRD. The imidazolium salts of these compounds have been prepared in the same way as compounds **1** to **25** in this chapter using CH₂Cl₂ as a solvent.

2.2. Materials:

2.2.1. Pentafluorobenzene:

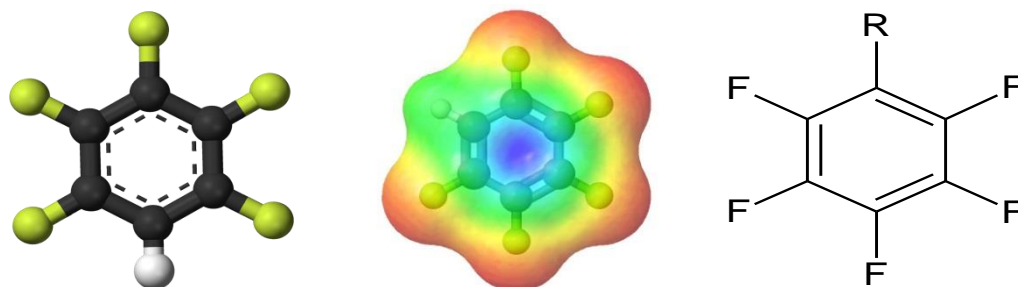


Figure 30: Chemical structure of pentafluorobenzene with six-membered ring. From [upload.wikimedia.org] and [asd.molfield.org]

The chemical structure of pentafluorobenzene has been shown above (Fig. 30), and this compound and some of its derivatives have been used starting materials to be treated with imidazole and its derivatives to form compounds containing both aryl and polyfluoroaryl groups. These derivatives are 2,3,4,5-tetrafluorobenzonitrile, 2,3,5,6-tetrafluoropyridine, 2,3,4-trifluorobenzonitrile, 2,3,5,6-tetrafluorobenzonitrile, octafluorotoluene, 2,4,5-trifluorobenzonitrile, 2,3,5-trifluoropyridine, 4-bromo-2,3,5,6-tetrafluorobenzotrifluoride, pentafluorobenzonitrile, pentafluoropyridine, octafluorotoluene, bromopentafluorobenzene and pentafluorobenzaldehyde (the importance of these compounds has been mentioned in chapter one).

2.2.2. Imidazole:

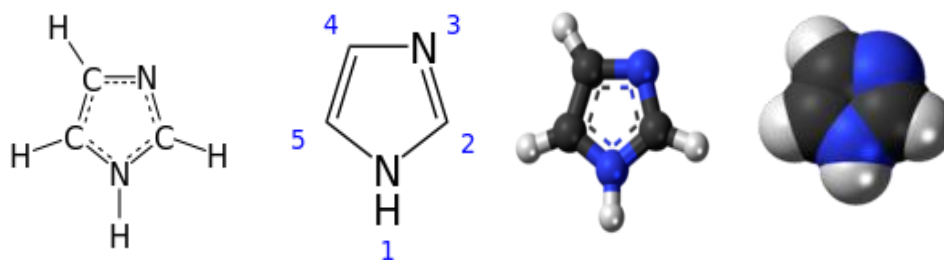


Figure 31: Chemical structure of imidazole with five-membered ring ^[77]

$C_3H_4N_2$ is the chemical formula of the organic imidazole compound. The chemical structure is shown above (Fig. 31), and the first synthesis of this compound was in 1858 by Heinrich Debus ^[78]. Imidazole and some of its derivatives have been used as starting materials in this project to react with HFB and its derivatives to form compounds containing both aryl and polyfluoroaryl groups, because in Fuji et al, they have reacted easily with the derivatives of HFB. Also, they have an essential role in biological and pharmaceutical industry, dyestuffs, agrochemicals, and polymer products. For example, cis-1-[[4- (1-Imidazolylmethyl) cyclohexyl] methyl] imidazole-succinic acid complex has shown inhibitor activity as nonsteroidal aromatase ^[79], and antifungal imidazole derivative has been investigated as an inhibitor of cytochromes P450 by Zhang et al such as 1-(3,5-diaryl-4,5-dihydro-1H-pyrazole-4-yl)-1H-imidazole derivatives ^{[80] [81]}. They have been used also as antimicrobial agents such as 2,4,5-trisubstitued imidazole derivatives ^{[82] [83]}, Histidine Decarboxylase inhibitors ^[84], anticancer agents such as anti-HIV-1-phenylamino-1H-imidazole derivatives ^[85], antioxidants and selective inhibitors of nNOS ^[86], antiproliferative agents against melanoma cell lines such as pyrimidin-4-yl-1H-imidazole derivatives ^[87], aromatase inhibitors such as novel indole-imidazole

derivatives ^[88], tubulin inhibitor such as 4-aryl-5-(3,4,5-trimethoxyphenyl)-2-alkylthio-1H-imidazole derivatives ^[89], antibacterial as 2-substitued-4,5-diphenyl-alkyl imidazole derivatives and inhibitor of CYC enzyme ^[90] ^[91]. However, in this project, the derivatives of imidazole that have been interacted with PFB and their derivatives are 2-, 4-methylimidazole and 2-phenylimidazole compounds. it has been shown that methyl group as a substituent lead to increase the strength of imidazole, and it has been found that methyl group in the two position of imidazole compound provided higher strength of imidazole ring than the methyl group in the four position ^[92].

2.2.3. Pyrazole:

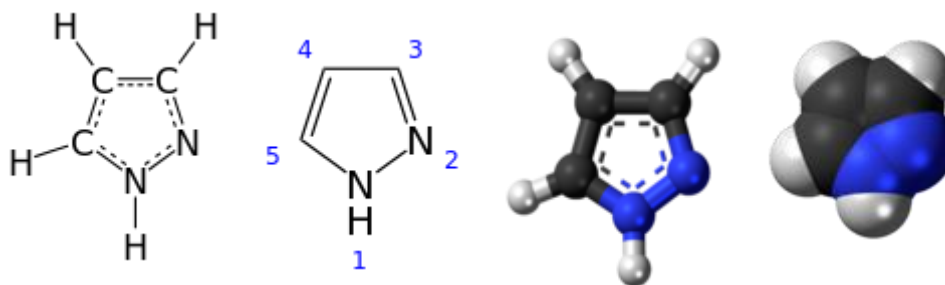


Figure 32: The chemical structure of pyrazole ^[93]

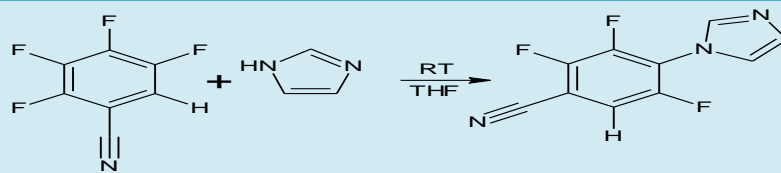
Pyrazole ($C_3H_4N_2$) has same chemical formula as imidazole, but with different positions of nitrogen atoms as shown in the chemical structure above (Fig.32) and it with its derivatives have also similar biological activity to imidazole and its derivatives. For example, N,N-tetrakis-[(1,5-dimethylpyrazol-3-yl)methyl]-para-

phenylenediamine, N,N-bis[(3,5-dimethylpyrazol-1-yl)methyl]aniline and N,N-tetrakis[(3,5-dimethylpyrazol-1-yl)methyl]-para-phenylenediamine have shown anticancer and cytotoxicity activity against Hep and P815 cell lines ^[94], have been used as amine oxidase inhibitors, such as 1-acetyl-3,5-diphenyl-4,5-dihydro-(1H)-pyrazole derivatives ^[95], antimicrobial agents, such as 4-hetarylpyrazole and four[2,3-C]pyrazole derivatives ^[96] and 3-methyl-4-phenyl-5-(p-substituedphenyl)-1-(p-sulphamylphenyl)pyrazoles ^[97], and have shown antiviral activity, such as 5-(4-benzyloxy)phenyl-3-(4-bromophenyl)-1-thiocarbonylmethyl-4,5-dihydro-1H-pyrazole ^[98], antitubercular activity such as 3-(4-chlorophenyl)-4-substitued pyrazole derivatives ^[99], antifungal activity, such as 4-(4-bromo-3-aryl-5-(6,6-dimethyl-4-oxo-4,5,6,7-tetrahydro-1H-indol-2-yl)-1H-pyrazol-1-yl)-N-(phenylcarbamothioyl)benzenesulfonamide against *Candida albicans* ^[100], and are antimalarial agents, such as 3-phenyl-1-(4-methylphenyl)-1H-pyrazole-4-carboxylic acid (147-ftp), analgesic agents such as 1,2,4-triazole and benzoxazoles ^[101], telomerase inhibitors, such as novel aryl-2H-pyrazole derivatives ^[102], and antibacterial agents such as 1,3-diaryl pyrazole derivatives bearing rhodanine-3-fatty acid moieties ^[103].

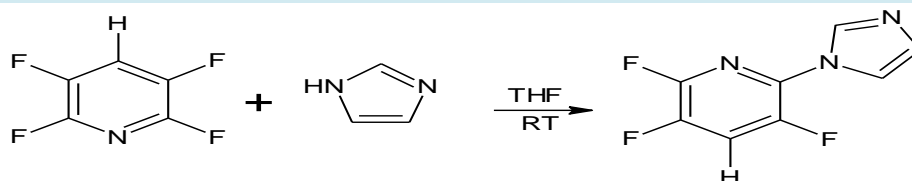
Comp
or salt

Chemical reactions

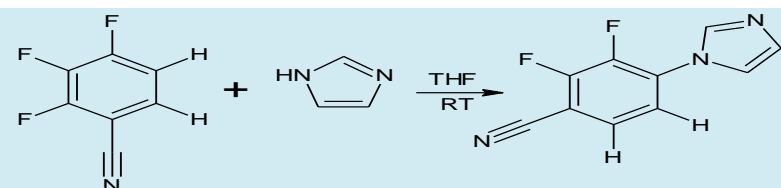
1



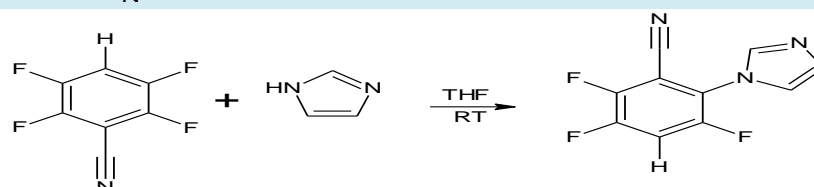
2



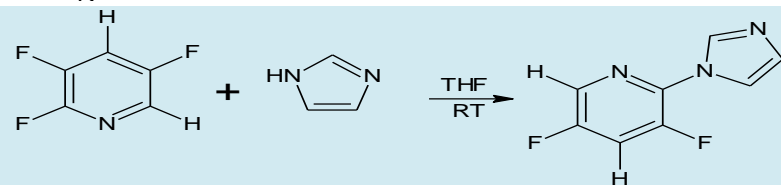
3



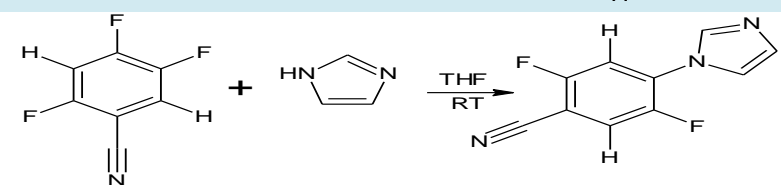
4



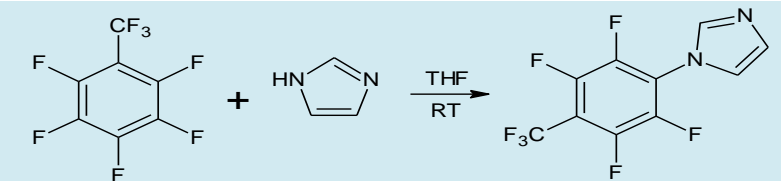
5



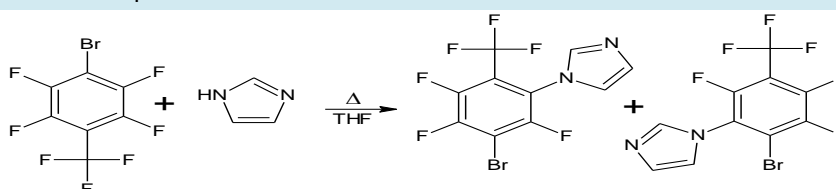
6



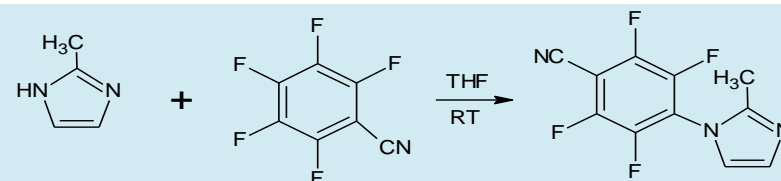
7

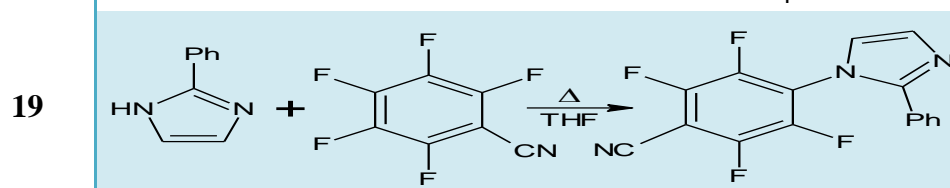
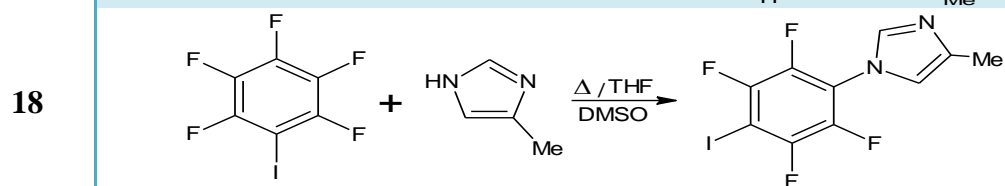
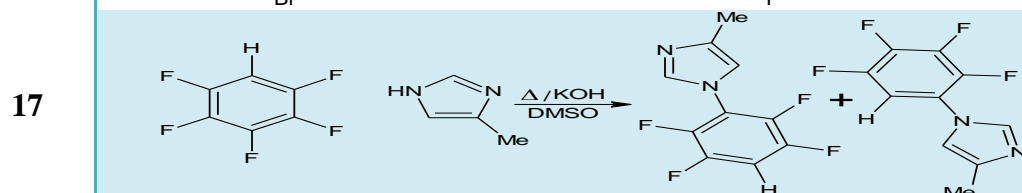
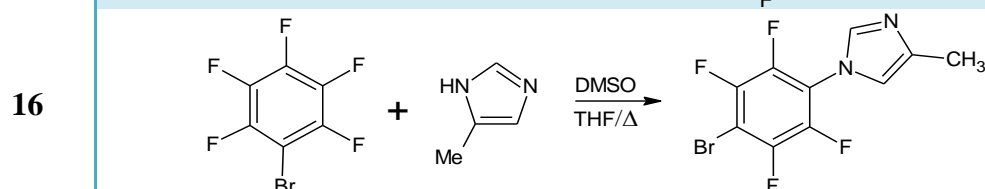
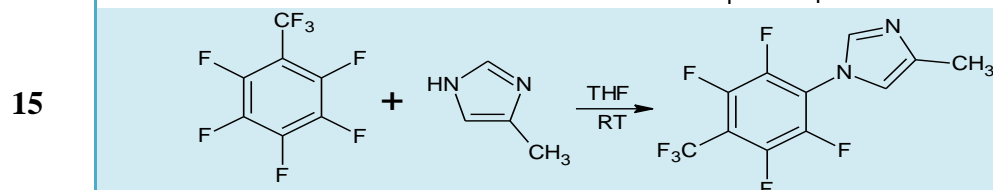
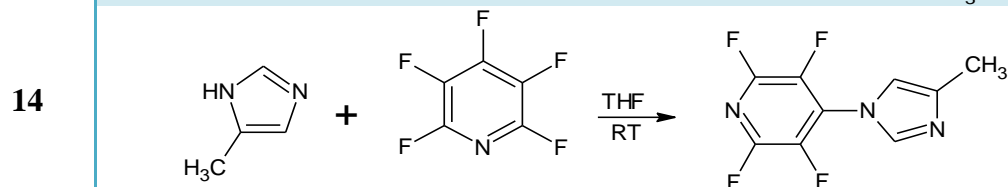
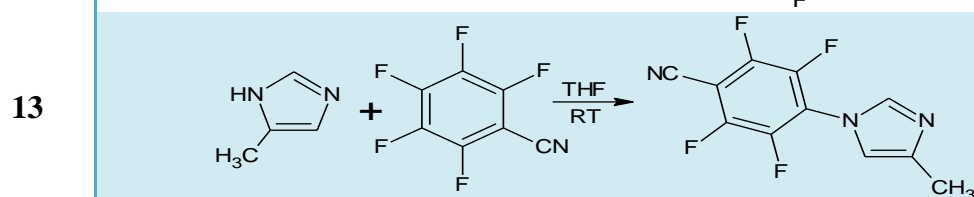
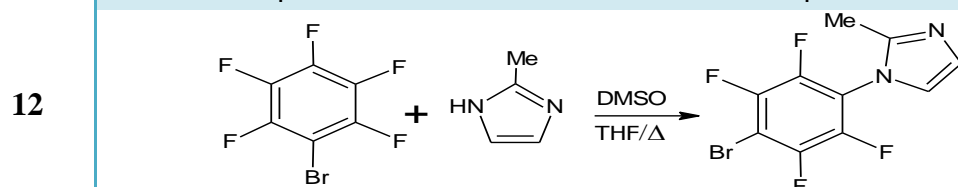
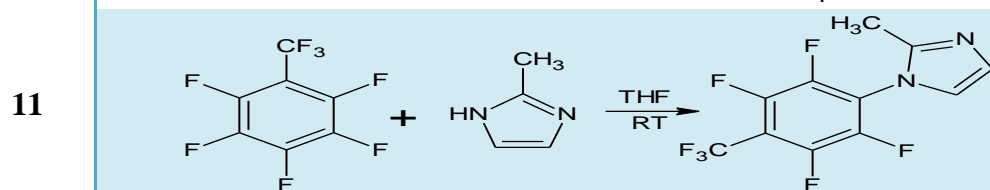
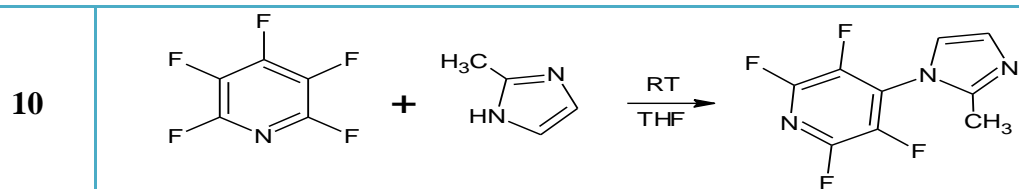


8

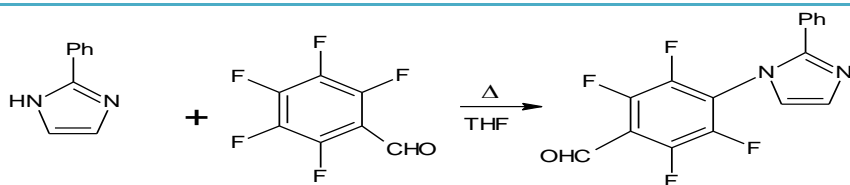


9

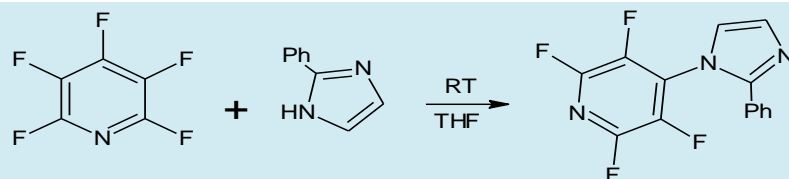




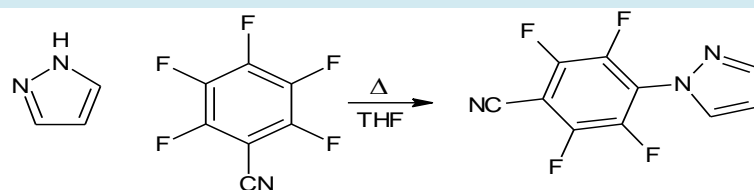
20



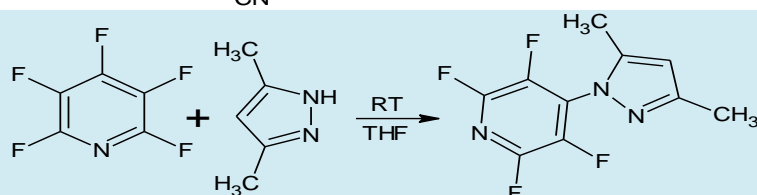
21



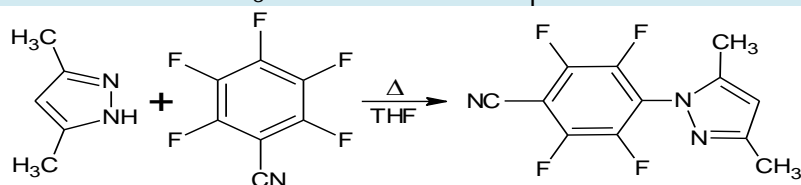
22



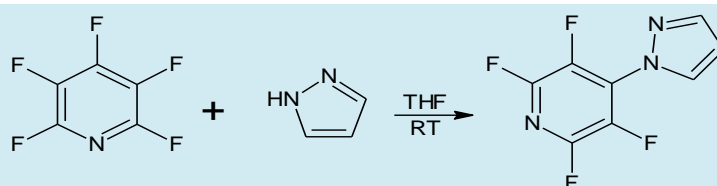
23



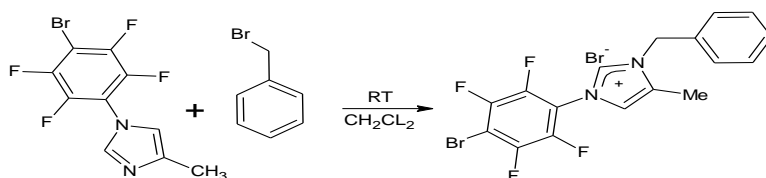
24



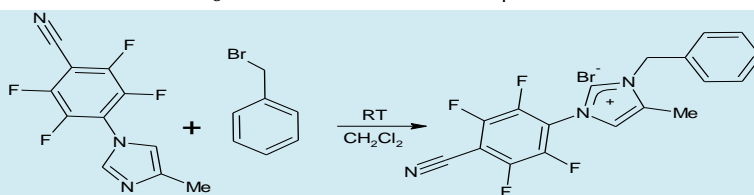
25



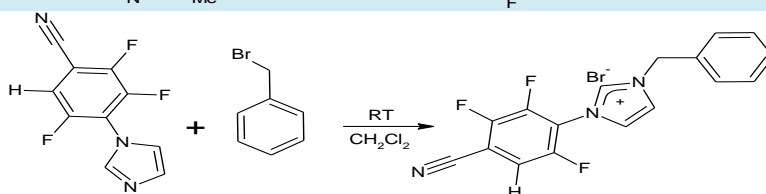
26



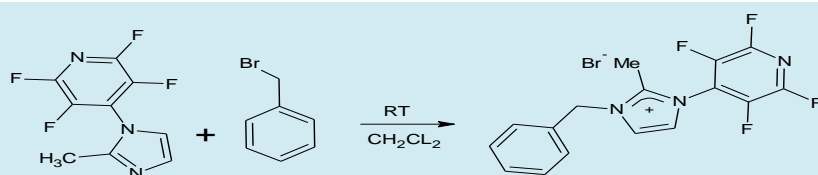
27



28



29



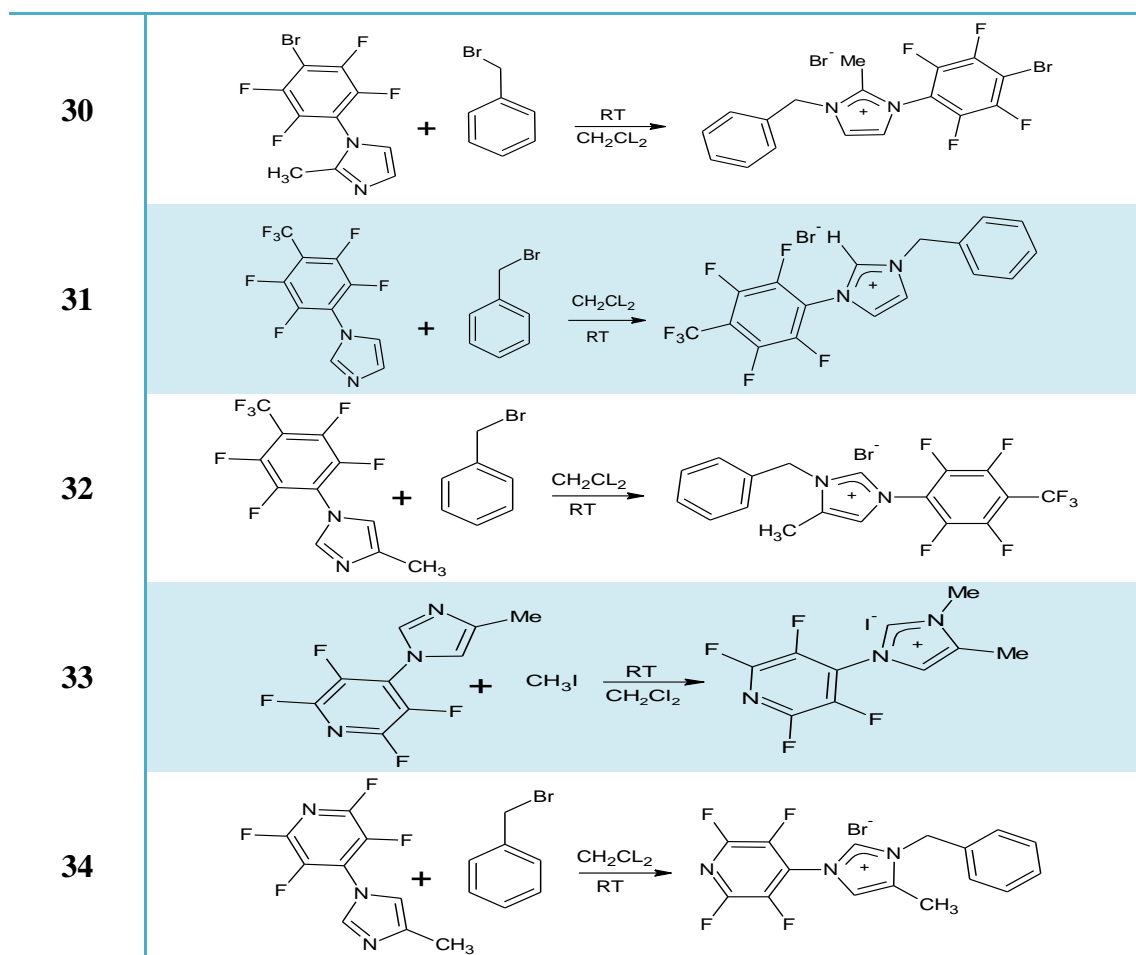


Table 4: Chemical reactions of PFB-R with imidazole, pyrazole and their derivatives, and the chemical reactions of these compounds to form imidazolium salts.

The treatment of 2,3,4,5-tetrafluorobenzonitrile, 2,3,5-trifluoropyridine and 4-bromo-2,3,5,6-tetrafluorobenzotrifluoride separately with imidazole afforded the compounds: 1-(2,3,6-trifluorobenzonitrile)imidazole (**1**), 1-(heptafluorotolyl)imidazole (**7**), and a mixture of 1-(5-bromo-3,4,6-trifluorobenzotrifluoride)imidazole (**8a**), and 1-(6-bromo-3,4,5-trifluorobenzotrifluoride)imidazole (**8b**) respectively. But the treatment of imidazole with 2,3,5,6-tetrafluoropyridine, 2,3,4-trifluorobenzonitrile, 2,3,5,6-tetrafluorobenzonitrile, octafluorotoluene and 2,4,5-trifluorobenzonitrile separately is expected to afford 1-(3,4,6-trifluoropyridyl)imidazole (**2**), 1-(2,3-

difluorobenzonitrile)imidazole (**3**), 1-(3,4,6-trifluorobenzonitrile)imidazole (**4**), 1-(4,6-difluoropyridyl)imidazole (**5**) and 1-(3,6-difluorobenzonitrile)imidazole (**6**) respectively.

The compounds 1-(2,3,5,6-tetrafluorobenzonitrile)-2-methylimidazole (**9**), 1-(2,3,5,6-tetrafluoropyridyl)-2-methylimidazole (**10**), 1-(heptafluorotolyl)-2-methylimidazole (**11**) and 1-(4-bromo-2,3,5,6-tetrafluorobenzyl)-2-methylimidazole (**12**) were formed through the treatment of 2-methylimidazole with each of pentafluorobenzonitrile, pentafluoropyridine, octafluorotoluene and bromopentafluorobenzene respectively, which, plus pentafluorobenzene and iodopentafluorobenzene, also have been treated with 4-methylimidazole to afford 1-(2,3,5,6-tetrafluorobenzonitrile)-4-methylimidazole (**13**), 1-(2,3,5,6-tetrafluoropyridyl)-4-methylimidazole (**14**), 1-(heptafluorotolyl)-4-methylimidazole (**15**), 1-(4-bromo-2,3,5,6-tetrafluorobenzyl)-4-methylimidazole (**16**), 1-(2,3,5,6-tetrafluorobenzyl)-4-methylimidazole (**17a & 17b**) and 1-(4-iodo-2,3,5,6-tetrafluorobenzyl)-4-methylimidazole (**18**).

The compounds that have been afforded through the reaction of 2-phenylimidazole with pentafluorobenzonitrile, pentafluorobenzaldehyde and pentafluoropyridine are 1-(2,3,5,6-tetrafluorobenzonitrile)-2-phenylimidazole (**19**), 1-(2,3,5,6-tetrafluorobenzaldehyde)-2-phenylimidazole (**20**) and 1-(2,3,5,6-tetrafluoropyridyl)-2-phenylimidazole (**21**). The treatment of pyrazole with pentafluorobenzonitrile lead to the formation of 1-(2,3,5,6-tetrafluorobenzonitrile)pyrazole (**22**), which also has been treated with 3,5-dimethylpyrazole to form 1-(2,3,5,6-tetrafluorobenzonitrile)-3,5-dimethylpyrazole (**23**), whereas, replacing pentafluorobenzonitrile with pentafluoropyridine afforded 1-(2,3,5,6-

tetrafluoropyridyl)-3,5-dimethylpyrazole (**24**). An attempt to synthesize 1-(2,3,5,6-tetrafluoropyridyl)pyrazole (**25**) was made through the treatment of pyrazole with pentafluoropyridine in THF at RT.

However, the treatment of benzyl bromide with the compounds **16**, **13**, **1**, **10**, **12**, **7** and **15** in CH₂Cl₂ lead to synthesis the imidazolium salts 1-(4-bromo-2,3,5,6-tetrafluorobenzyl)-3-benzyl-4-methylimidazolium bromide (**26**), 1-(2,3,5,6-tetrafluorobenzonitrile)-3-benzyl-4-methylimidazolium bromide (**27**), 1-(2,3,6-trifluorobenzonitrile)-3-benzyl-imidazolium bromide (**28**), 1-(2,3,5,6-tetrafluoropyridyl)-3-benzyl-2-methylimidazolium bromide (**29**), 1-(4-bromo-2,3,5,6-tetrafluorobenzyl)-3-benzyl-2-methylimidazolium bromide (**30**), Synthesis 1-(heptafluorotolyl)-3-benzyleimidazolium bromide (**31**) and 1-(heptafluorotolyl)-3-benzyl-4-methylimidazolium bromide (**32**) respectively. In contrast, compound **14** has not only been treated with benzyl bromide but also with methyl iodide to form 1-(2,3,5,6-tetrafluoropyridyl)-3-benzyl-4-methylimidazolium bromide (**33**) and 1-(2,3,5,6-tetrafluoropyridyl)-3,4-dimethylimidazolium iodide (**34**).

2.2. Preparation:

All reactions were performed by stirring the starting materials in THF at room temperature (with yields between 36% and 102%), except **8**, **12**, **16**, **17**, **18** and all salts from **26** to **34**. All salts have been formed in CH₂Cl₂ at RT (yields between 48% and 113%), and compounds **8**, **12**, **16**, **17** and **18** were formed under temperature from 60°C to 142°C in a mixture of DMSO and THF with yields between 30% and 110%, except **17** which was formed by heating at 55°C for three hours in DMSO with KOH as a base and yield 29%.

Some compounds have been synthesized by further steps than other compounds, such as compound **12**, which has been afforded by the treatment of 2-methylimidazole with 4-bromopentafluorobenzene in THF and DMSO, and then this mixture has been heated for three hours at 55°C. After the reaction mixture was poured into 500 ml of cold water, a white solid was deposited. Then it was collected and dissolved in 100 ml of CH₂Cl₂ with adding magnesium sulfate. The mixture was filtered; a white solid was obtained after evaporation under reduced pressure. The same steps in this reaction have been done again in the reactions of compounds **16**, **17** & **18**, but with different amount of distilled water, in which, 500 ml of water was used with compounds **12** & **16**, 300 ml with compound **17**, and 120 ml of water with compound **18**.

2.3. Characterization:

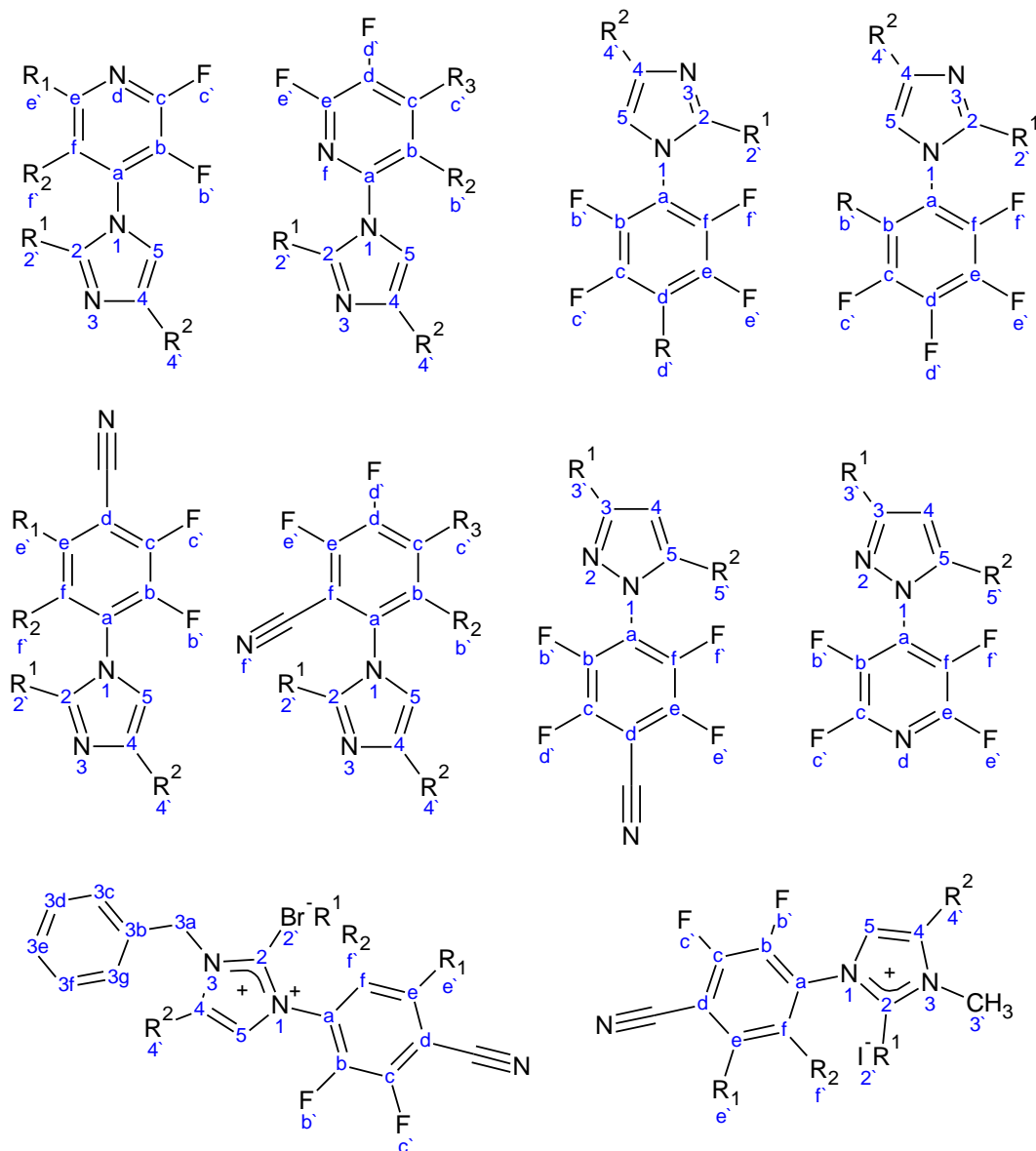


Figure 33: The labels that have been used to represent the NMR data of imidazole, pyrazole compounds and imidazolium salts ($R = \text{Br, I, F}$. $R^1, R^2 = \text{H, CH}_3$. $R_1, R_2, R_3 = \text{H, F}$).

All compounds and salts have been characterized by mass spectrometry (MS) and NMR spectroscopy. In MS, all compounds ($[\text{M} + \text{H}]^+$) and salts ($[\text{M}]^+$) gave the expected peak. For example, **1** and **2** show peaks at 224, **3** and **6** at 206, **8** and **27**

at 346, **9** and **13** at 256, **10** and **14** at 232, **11** and **15** at 299, **12** and **16** at 308, **23** and **33** at 246, **26** and **30** at 400, **29** and **34** at 322 m/z. Two multiplet or quartet peaks are exhibited in the ^{19}F NMR spectra for all compounds and salts at resonances ca. $\delta -86$ and $\delta -149$ ppm, except for **1**, **2**, **4**, **5**, **6**, **7**, **8**, **11**, **15**, **17** and **28** which have three peaks. The third peak is assigned to the CF_3 group ($\delta -55$ to -56 ppm) or to one fluorine atom in a different environment. The ^1H NMR spectrum of compound **35** shows a mixture of the expected product and unidentified compounds. All the hydrogen atoms that are attached directly to the imidazole or pyrazole ring resonate at $\delta 6-8$ ppm, whereas in the salts, these hydrogen atoms resonate from $\delta 7$ to 11 ppm. The ^1H NMR spectra possess a resonance from $\delta 2.36$ to 2.62 ppm characteristic of the three hydrogen atoms of the 2-methyl group (bonded to the carbon atom between the two nitrogen atoms) in compounds **9** to **12** and salts **29** and **30**, whereas compounds **13** to **18** with their imidazolium salts (**26**, **27**, **32**, **33**, **34**) which have a 4-methyl group display a lower resonance $\delta 2.12$ to 3.35 ppm. In salt **33** there are other three hydrogen atoms in the methyl group that are bonded directly to the nitrogen atom at the 3 position of the imidazole ring which resonate at $\delta 5.31$ ppm. The CH_2 group that is attached directly to nitrogen atom and phenyl ring in the imidazolium salts gives a single peak at the resonance of $\delta 5$ ppm.

The ^{13}C NMR spectra have been recorded for compounds **12** and **18**, the six carbon atoms of the benzyl ring in both compounds have shown multiple peaks at the resonances between δ 73 and 147 ppm, whereas, δ 116 to 145 are the resonances of the peaks of the three carbon atom in imidazole ring, and the carbon atom of 2- and 4-methyl group in both **12** and **18** give single resonances δ 31 ppm. Moreover, for **12** and **18**, the data of two dimensional NMR spectrum (HSQC and HMBC) have been collected are consistent with the chemical structures of **12** and **18**. For **12**, the HSQC spectrum shows that H-2' correlates with C-2', H-4 correlates with C-4, H-5 correlates with C-5 (Fig. 34). The HMBC spectrum shows that H-2' correlates with C-2' and C-2 and H-4 correlates with C-2, C-4, C-5 and H-5 correlates with C-2, C-4 and C-5 (Fig. 35). For **18**, the HSQC spectrum shows that H-4' correlates with C-4', H-2 correlates with C-2, H-5 correlates with C-5 (Fig. 36). The HMBC spectrum shows that H-4' correlates with C-4', C-4 and C-2, H-2 correlates with C-2, C-4 and C-5, H-5 correlates with C-2, C-4 and C-5 (Fig. 37).

The NMR data for the expected compounds 1-(3,4,6-trifluoropyridyl)imidazole (**2**), 1-(2,3-difluorobenzonitrile)imidazole (**3**), 1-(3,4,6-trifluorobenzonitrile)imidazole (**4**), 1-(4,6-difluoropyridyl)imidazole (**5**), 1-(3,6-difluorobenzonitrile)imidazole (**6**) show slow formation of the products, which need months to reach completion as shown in Figures 38, 39, 40, 41 and 42. Compounds and salts **1**, **12**, **14**, **16**, **18**, **19**, **16**, **30** and **34** have been analyzed by IR spectroscopy, which shows the expected peaks for all these compounds.

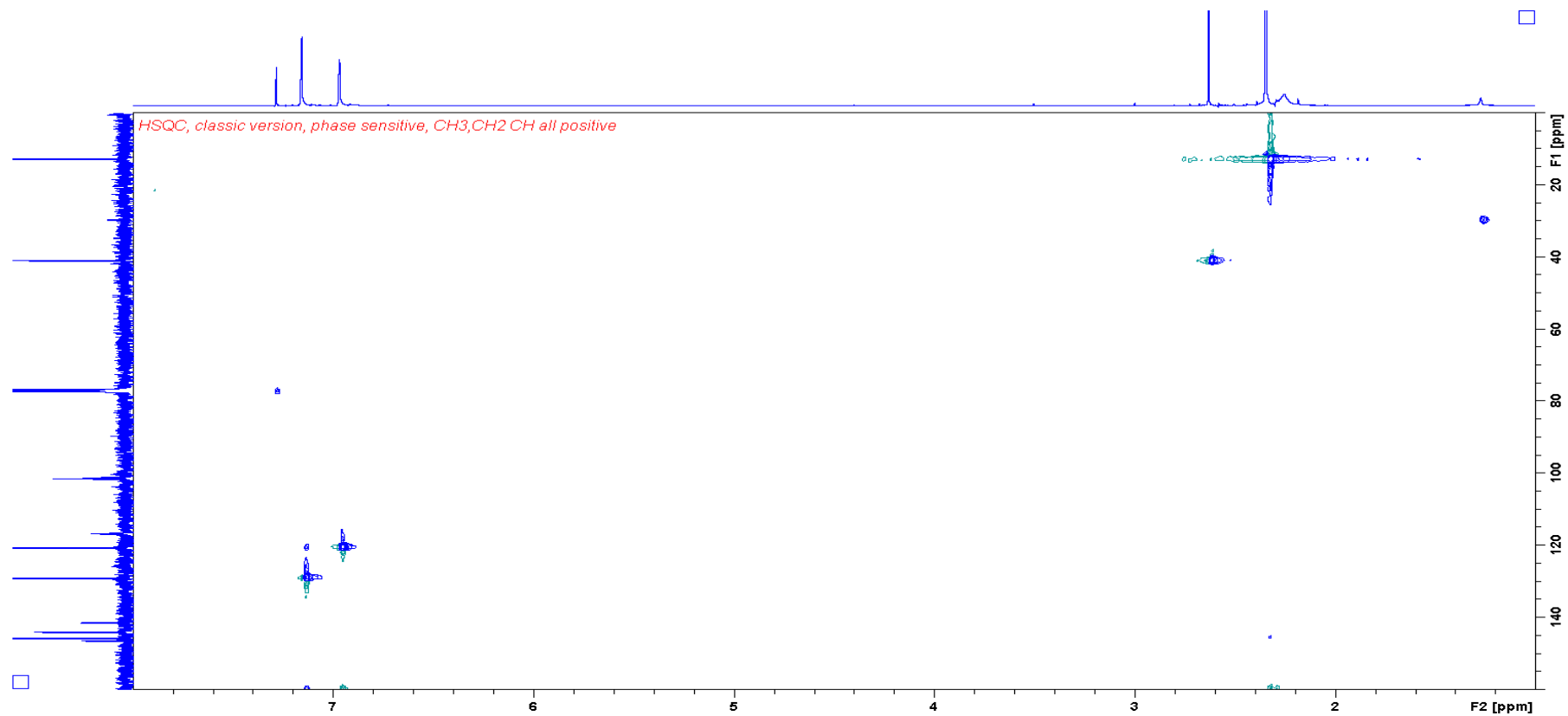


Figure 34: The HSQC spectrum of 1-(4-bromo-2,3,5,6-tetrafluorobenzyl)-2-methylimidazole **12**.

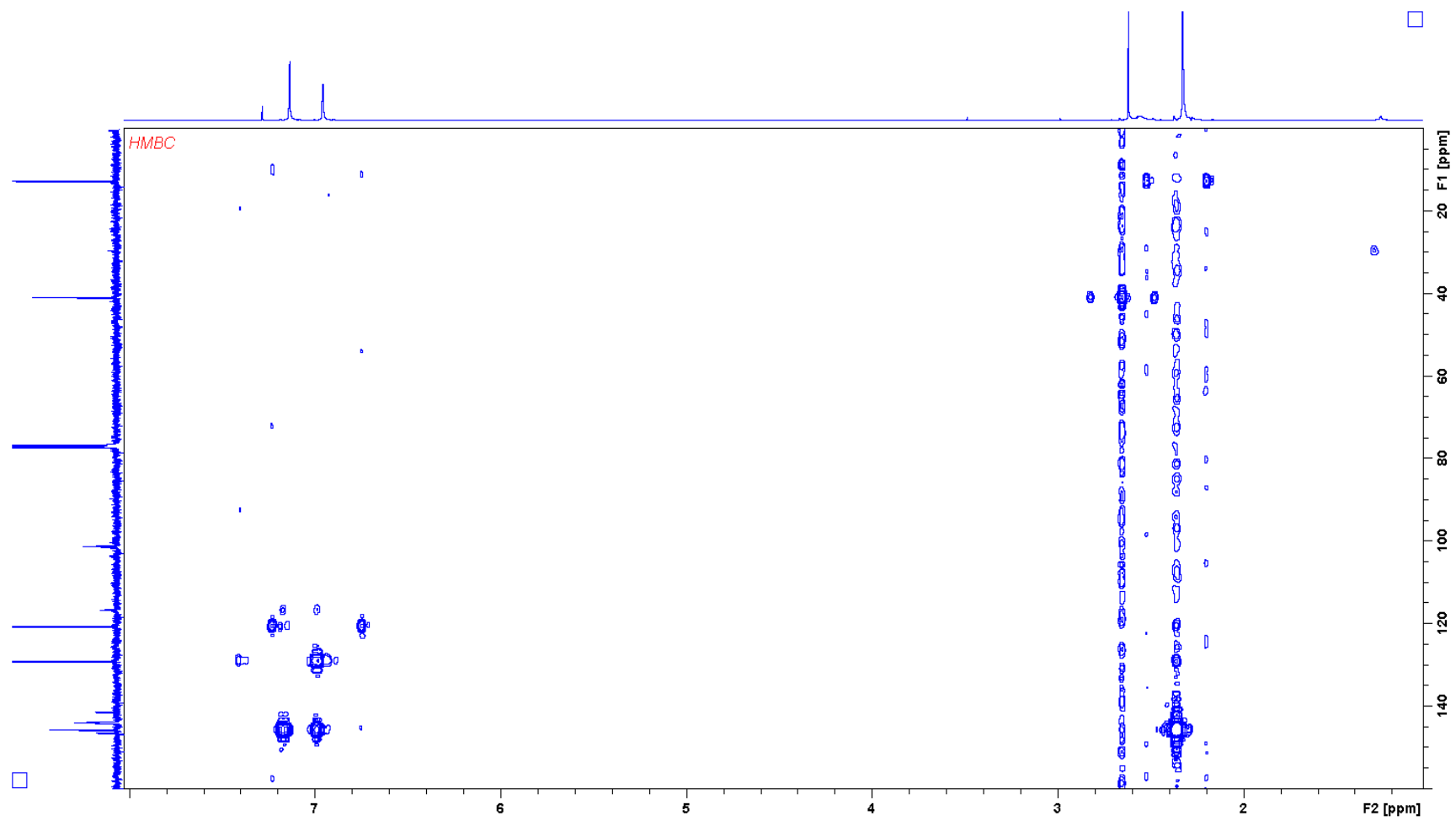


Figure 35: The HMBC spectrum of 1-(4-bromo-2,3,5,6-tetrafluorobenzyl)-2-methylimidazole **12**.

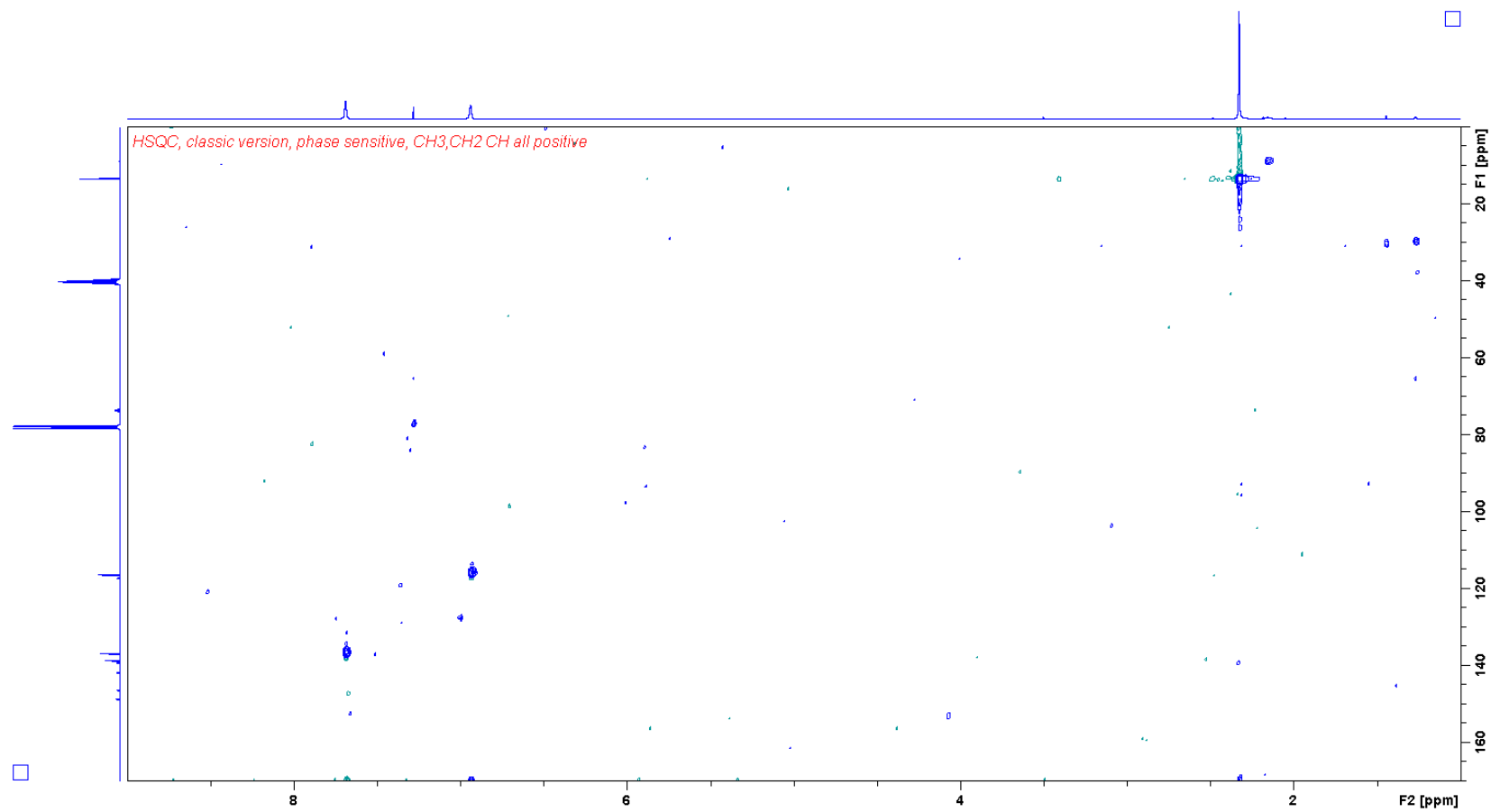


Figure 36: The HSQC spectrum of 1-(4-iodo-2,3,5,6-tetrafluorobenzyl)-4-methylimidazole **18**.

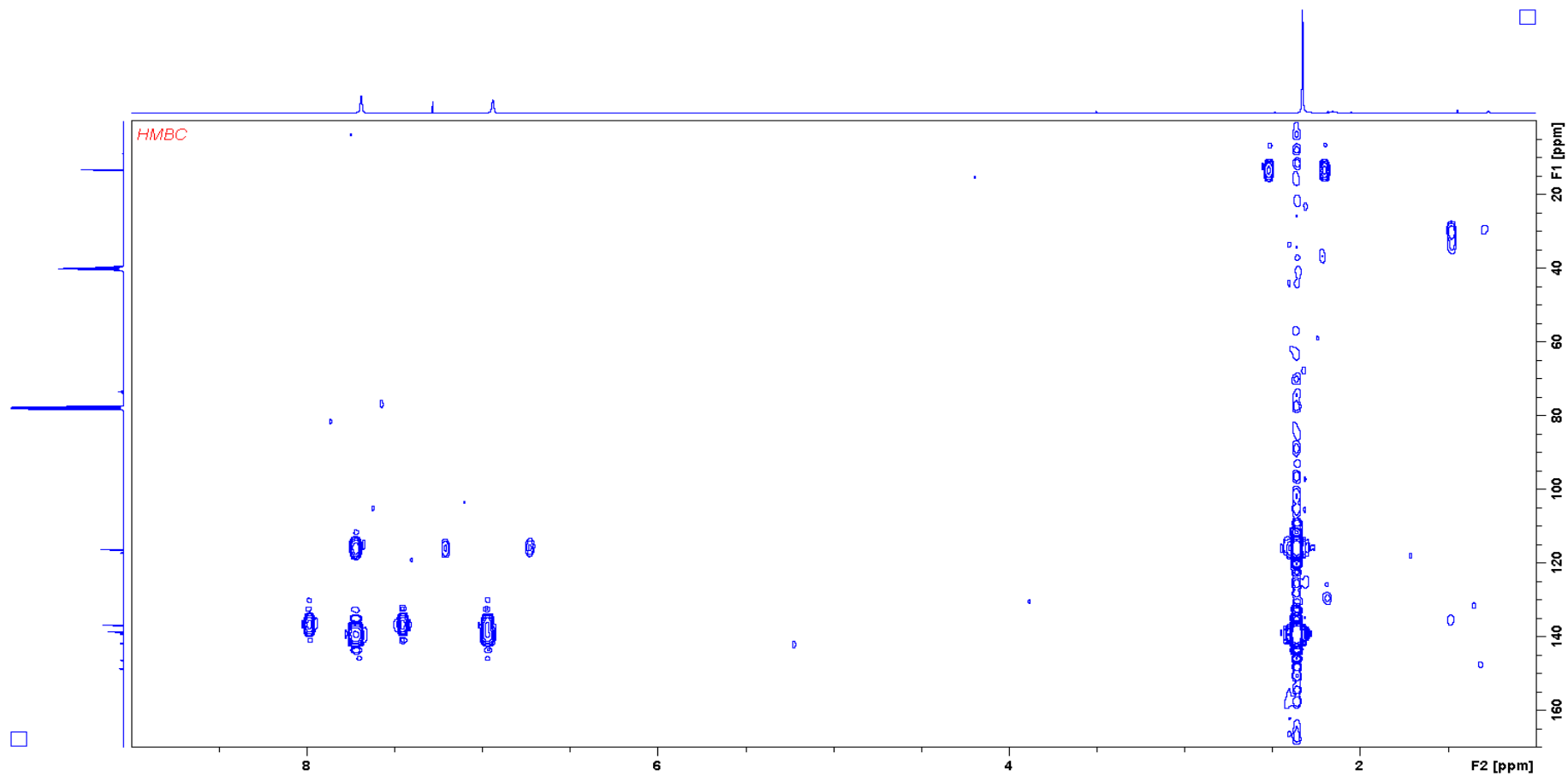


Figure 37: The HMBC spectrum of 1-(4-iodo-2,3,5,6-tetrafluorobenzyl)-4-methylimidazole **18**.

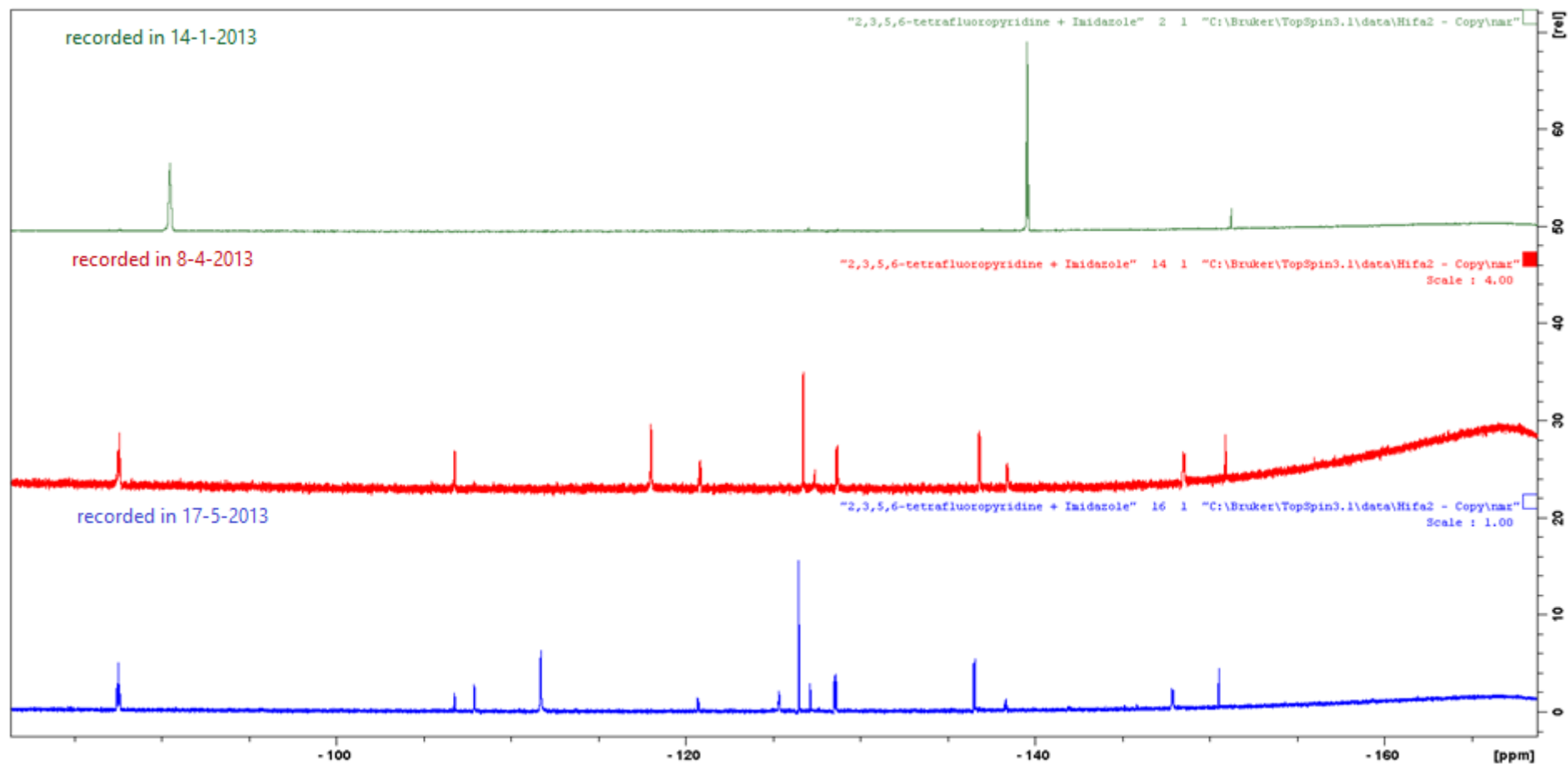


Figure 38: The formation of the expected compound 1-(3,4,6-trifluoropyridyl)imidazole **2** over months starting from green to blue.

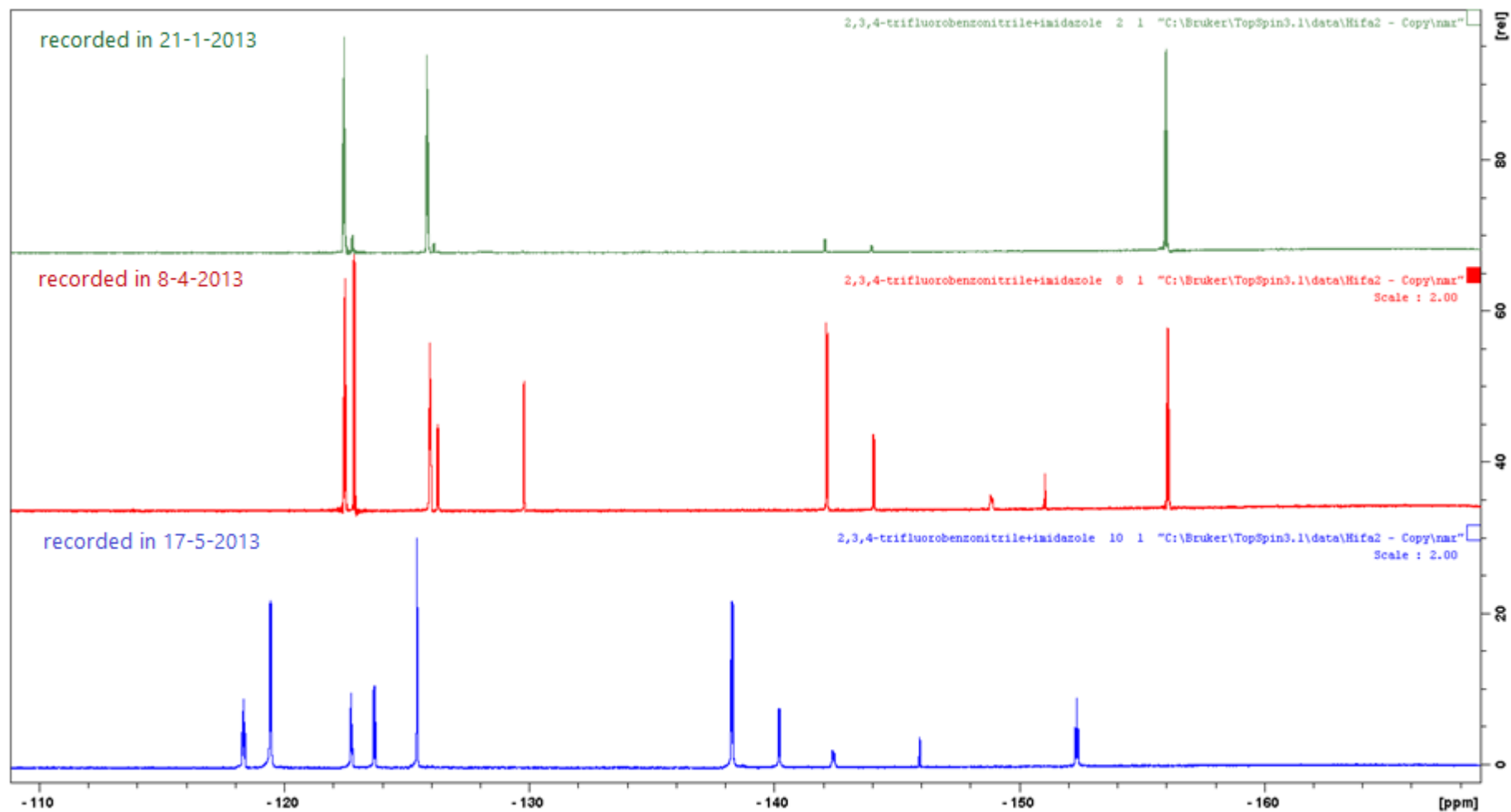


Figure 39: The formation of the expected compound 1-(2,3-difluorobenzonitrile)imidazole **3** over months starting from green to blue.

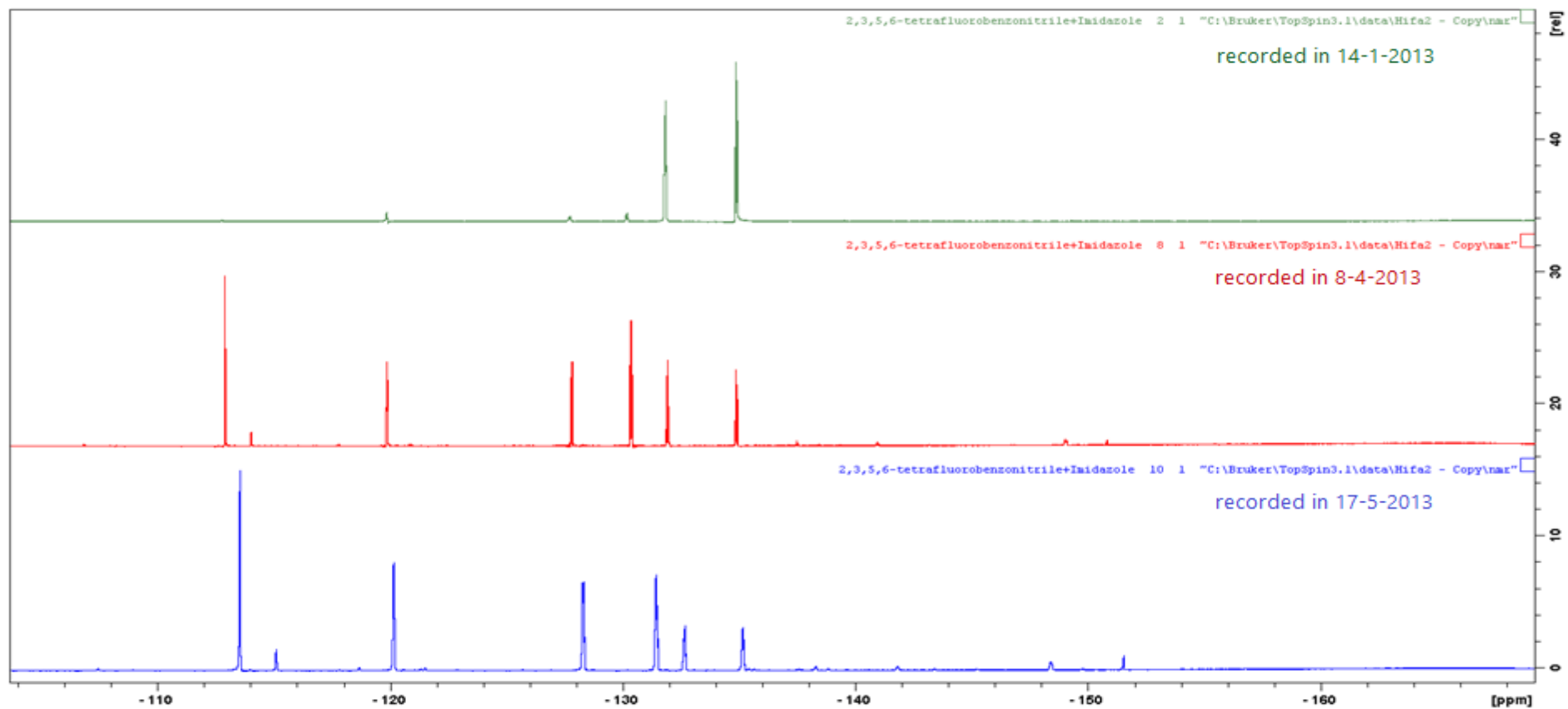


Figure 40: The formation of the expected compound 1-(3,4,6-trifluorobenzonitrile)imidazole **4** over months starting from green to blue.

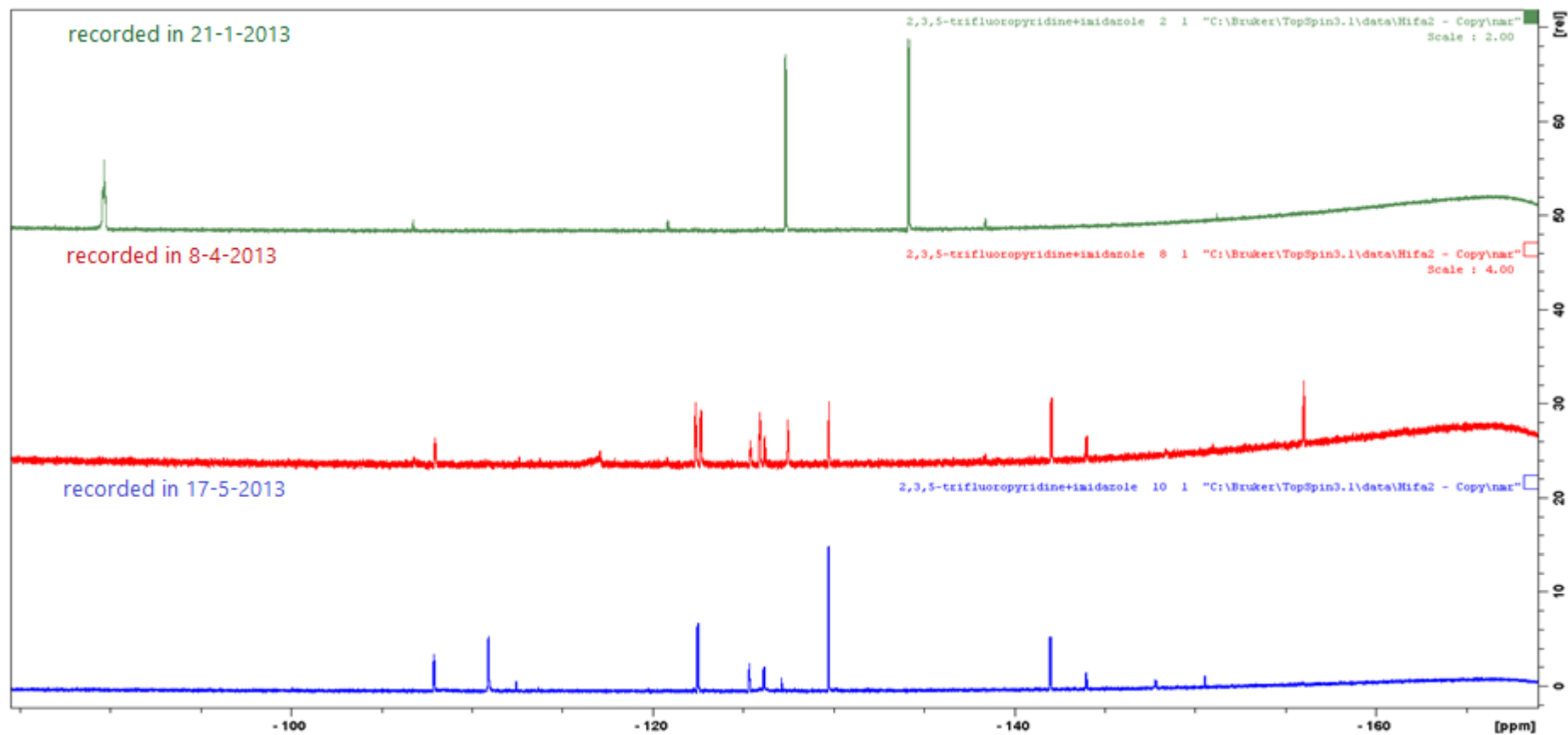


Figure 41: The formation of the expected compound 1-(4,6-difluoropyridyl)imidazole **5** over months starting from green to blue.

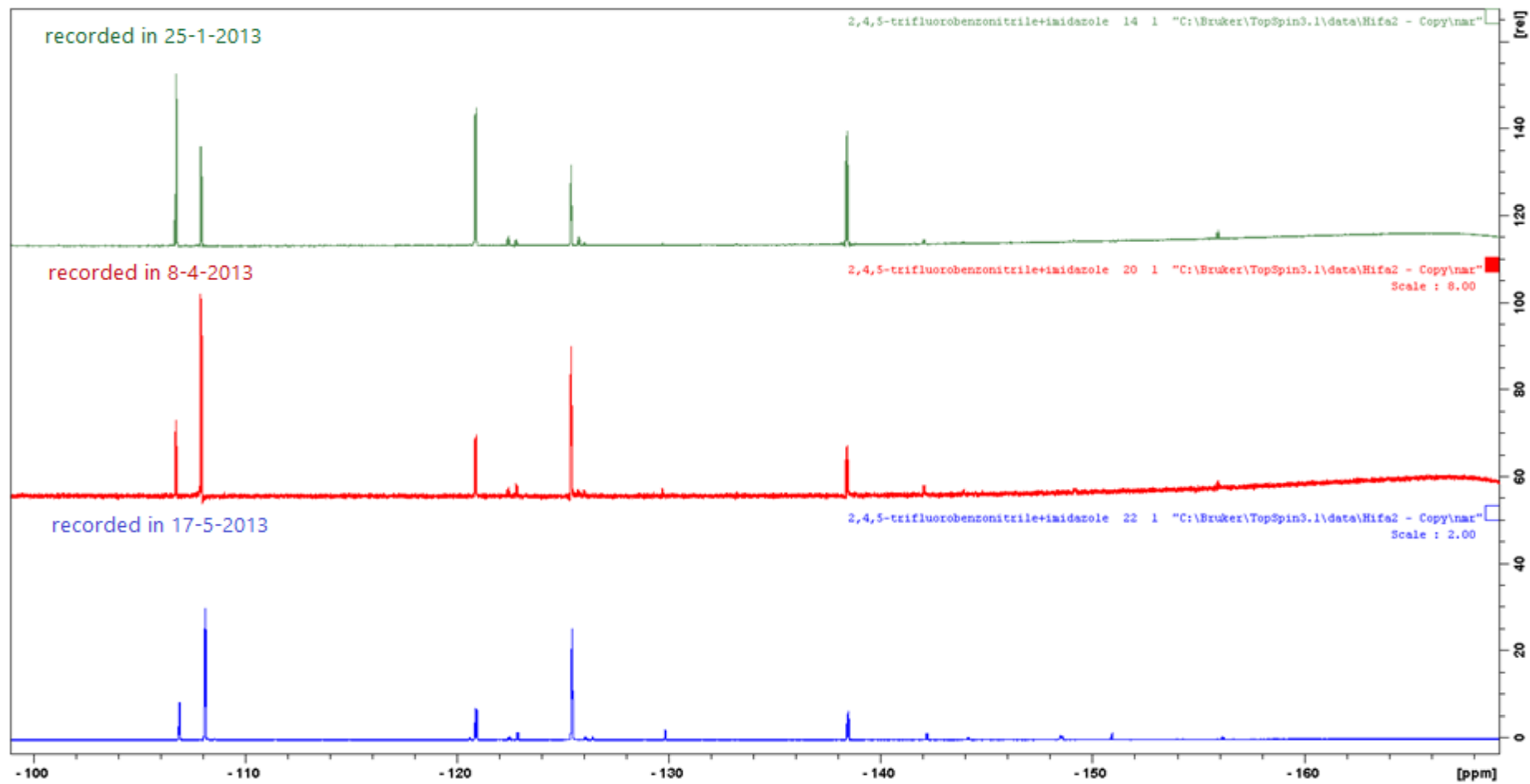


Figure 42: The formation of the expected compound 1-(3,6-difluorobenzonitrile)imidazole **6** over months starting from green to blue.

Crystallization of all the compounds was attempted by slow evaporation of the solution of these compounds in MeOH at room temperature, and this crystallization led to increase the purity of all the compounds but without giving the desired single crystals suitable to be analyzed by XRD, except salts **26** (Fig. 43) and **34** (Fig. 44), which gave colourless and brown crystals respectively. Single crystal X-ray diffraction studies show monoclinic crystal system with face to face geometry as a result of alternating stacking between polyfluoroaryl and aryl groups (Fig. 45&46). The crystals are in different space groups (I2/a in **26** and P21/c in **34**), centroid–centroid distance ($D_{\text{cent}} = 4.647 \text{ \AA}$ in **26** and $D_{\text{cent}} = 3.638 \text{ \AA}$ in **34**), angle ($\phi = 14.14^\circ$ in **26** and $\phi = 9.35^\circ$ in **34**), the hinge angle (C11–C10–N2) is $\alpha = 111.17^\circ$ in **26** and $\alpha = 111.57^\circ$ in **34**. The stack shift was $s = 0.00 \text{ \AA}$ in both (Fig. 47&48) (Crystallographic data for **26** and **34** has been shown in table 9 and table 10 respectively in chapter 5).

The columnar stacking in these crystals has been prevented by ions and the tick-shaped cations, and the planes of the complementary rings in both cannot be parallel. Further views of these crystals have been shown in figures 49 and 50. These two salts have the same structure with difference only in the nature of the fluoroaryl ring. Selected bond length (\AA) and bond and torsion angles ($^\circ$) for salts **26** and **34**, except those which relate to C17, Br2 and N3 atoms are given in Table 5, and those which relate to C17, Br2 and N3 atoms have been shown in Table 6. All bonds lengths between two atoms in **26** were almost identical to those of **34**, except the bonds length that were in fluoroaryl ring, which were attached (one to two bonds away) to the bromide atom in **26** or nitrogen atom in **34**, and these bonds are N3 C7 $1.302(4) \text{ \AA}$, N3 C8 $1.306(4) \text{ \AA}$, Br2 C17 $1.881(3) \text{ \AA}$, C17 C7

1.388(4) Å and C17 C8 1.382(4) Å. Identical angles to those of **26** are observed in **34**, and the range of these angles was from 106.3(2) of C2 C3 N2 to 131.8(3) of C2 C3 C4 in **26** and from 106.6(2) of C2 C3 N2 to 130.1(3) of C2 C3 C4 in **34**, except angles that are involved C17, Br2, and N3 atoms. The torsion angles in both **26** and **34** are similar. The experimental errors in **26** were almost similar to those of **34**. Hydrogen bonding between the bromide anion and acidic hydrogen H1 is suggested based on the distance between Br \cdots C1, which is 3.485 Å in **26** and 3.453 Å in **34**. Weaker interactions are suggested between the other hydrogen atom of the imidazolium ring and the bromide anion, which were C3 \cdots Br 3.584 Å in **26** and 3.683 Å in **34**.

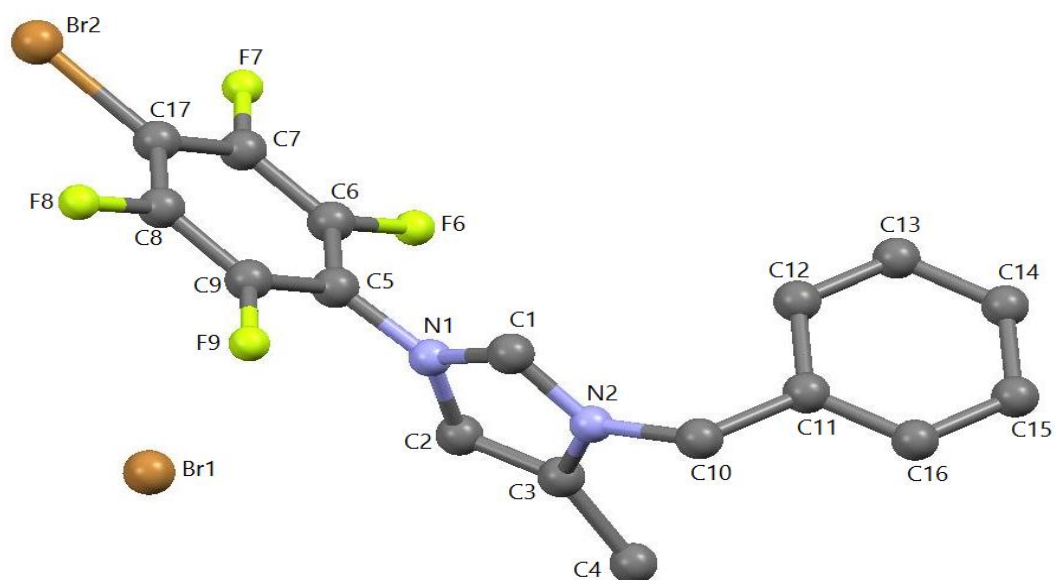


Figure 43: Structure of 1-(4-bromo-2,3,5,6-tetrafluorobenzyl)-3-benzyl-4-methylimidazolium bromide **26**.

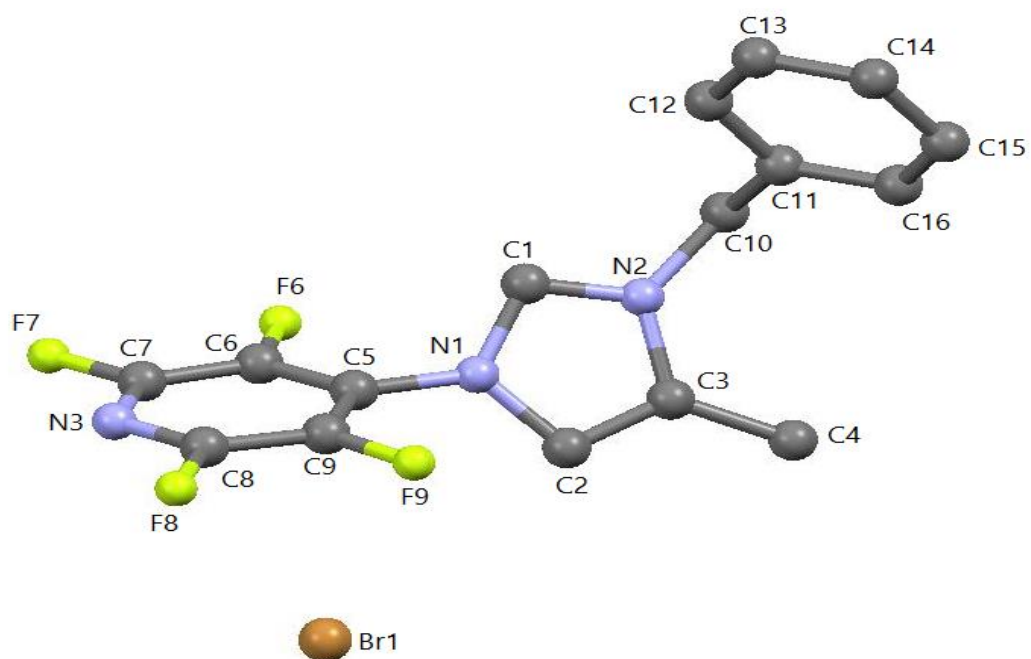


Figure 44: The structure of 1-(2,3,5,6-tetrafluoropyridyl)-3-benzyl-4-methylimidazolium bromide **34**.

| | Salt 26 | Salt 34 |
|------------|----------------|----------------|
| F6 C6 | 1.336(3) | 1.344(3) |
| F7 C7 | 1.347(3) | 1.340(3) |
| F8 C8 | 1.346(3) | 1.339(4) |
| F9 C9 | 1.343(3) | 1.338(3) |
| N1 C1 | 1.331(4) | 1.336(3) |
| N1 C2 | 1.390(4) | 1.386(3) |
| N1 C5 | 1.421(4) | 1.420(3) |
| N2 C1 | 1.321(4) | 1.320(3) |
| N2 C3 | 1.389(4) | 1.390(4) |
| N2 C10 | 1.469(3) | 1.483(3) |
| C2 C3 | 1.352(4) | 1.348(4) |
| C3 C4 | 1.488(4) | 1.484(4) |
| C5 C6 | 1.384(4) | 1.374(4) |
| C5 C9 | 1.383(4) | 1.379(4) |
| C6 C7 | 1.374(4) | 1.377(4) |
| C8 C9 | 1.377(4) | 1.381(4) |
| C10 C11 | 1.517(4) | 1.517(4) |
| C11 C16 | 1.394(4) | 1.385(4) |
| C11 C12 | 1.378(4) | 1.394(4) |
| C12 C13 | 1.397(4) | 1.393(4) |
| C13 C14 | 1.384(5) | 1.379(4) |
| C14 C15 | 1.380(5) | 1.383(5) |
| C15 C16 | 1.392(4) | 1.393(4) |
| | | |
| C1 N1 C2 | 109.4(2) | 109.1(2) |
| C1 N1 C5 | 123.5(2) | 124.1(2) |
| C2 N1 C5 | 127.0(2) | 126.7(2) |
| C1 N2 C3 | 110.0(2) | 109.6(2) |
| C1 N2 C10 | 124.1(2) | 122.7(2) |
| C3 N2 C10 | 125.8(2) | 127.7(2) |
| N2 C1 N1 | 107.7(2) | 107.8(2) |
| C3 C2 N1 | 106.7(2) | 106.8(2) |
| C2 C3 N2 | 106.3(2) | 106.6(2) |
| C2 C3 C4 | 131.8(3) | 130.1(3) |
| N2 C3 C4 | 121.8(2) | 123.2(3) |
| C6 C5 C9 | 118.4(3) | 117.8(3) |
| C6 C5 N1 | 121.0(3) | 121.2(3) |
| C9 C5 N1 | 120.5(2) | 121.0(3) |
| F6 C6 C5 | 119.8(3) | 120.9(3) |
| F6 C6 C7 | 119.6(3) | 120.4(3) |
| C5 C6 C7 | 120.6(3) | 118.7(3) |
| F7 C7 C6 | 118.8(2) | 119.2(3) |
| F8 C8 C9 | 118.7(2) | 118.6(3) |
| F9 C9 C5 | 119.5(2) | 120.8(3) |
| F9 C9 C8 | 119.8(2) | 121.0(3) |
| C5 C9 C8 | 120.7(3) | 118.2(3) |
| N2 C10 C11 | 111.2(2) | 111.6(2) |

| | | |
|-----------------|-----------|-----------|
| C16 C11 C12 | 119.0(3) | 119.1(3) |
| C16 C11 C10 | 120.9(3) | 121.7(3) |
| C12 C11 C10 | 120.1(2) | 119.2(3) |
| C13 C12 C11 | 120.6(3) | 120.5(3) |
| C14 C13 C12 | 120.0(3) | 120.1(3) |
| C13 C14 C15 | 119.9(3) | 119.5(3) |
| C14 C15 C16 | 119.9(3) | 120.8(3) |
| C11 C16 C15 | 120.6(3) | 120.0(3) |
| | | |
| C3 N2 C1 N1 | -0.8(3) | 0.7(3) |
| C10 N2 C1 N1 | 175.2(2) | -179.7(2) |
| C2 N1 C1 N2 | 0.9(3) | -0.6(3) |
| C5 N1 C1 N2 | -174.7(2) | 177.4(2) |
| C1 N1 C2 C3 | -0.7(3) | 0.2(3) |
| C5 N1 C2 C3 | 174.7(3) | -177.7(3) |
| N1 C2 C3 N2 | 0.2(3) | 0.2(3) |
| N1 C2 C3 C4 | 177.9(3) | -177.6(3) |
| C1 N2 C3 C2 | 0.4(3) | -0.5(3) |
| C10 N2 C3 C2 | -175.6(2) | 179.9(2) |
| C1 N2 C3 C4 | -177.6(2) | 177.5(3) |
| C10 N2 C3 C4 | 6.5(4) | -2.1(4) |
| C1 N1 C5 C6 | -63.6(4) | 61.5(4) |
| C2 N1 C5 C6 | 121.7(3) | -120.8(3) |
| C1 N1 C5 C9 | 113.7(3) | -119.0(3) |
| C2 N1 C5 C9 | -61.1(4) | 58.6(4) |
| C9 C5 C6 F6 | 178.7(2) | -178.4(2) |
| N1 C5 C6 F6 | -4.1(4) | 1.1(4) |
| C9 C5 C6 C7 | -1.1(4) | -0.1(4) |
| N1 C5 C6 C7 | 176.1(2) | 179.4(3) |
| F6 C6 C7 F7 | 0.7(3) | -1.8(4) |
| C5 C6 C7 F7 | -179.5(2) | 179.9(3) |
| C6 C5 C9 F9 | -180.0(2) | 179.0(2) |
| N1 C5 C9 F9 | 2.8(4) | -0.4(4) |
| C6 C5 C9 C8 | 0.9(4) | -0.5(4) |
| N1 C5 C9 C8 | -176.4(3) | -179.9(2) |
| F8 C8 C9 F9 | 0.4(4) | 0.9(4) |
| F8 C8 C9 C5 | 179.6(3) | -179.6(3) |
| C1 N2 C10 C11 | -100.7(3) | 87.1(3) |
| C3 N2 C10 C11 | 74.7(3) | -93.4(3) |
| N2 C10 C11 C16 | 38.9(4) | 103.0(3) |
| N2 C10 C11 C12 | -143.2(3) | -76.9(3) |
| C16 C11 C12 C13 | 0.2(5) | -0.7(4) |
| C10 C11 C12 C13 | -177.8(3) | 179.2(3) |
| C11 C12 C13 C14 | -0.5(5) | -0.1(4) |
| C12 C13 C14 C15 | 0.3(5) | 0.8(5) |
| C13 C14 C15 C16 | 0.4(5) | -0.5(5) |
| C12 C11 C16 C15 | 0.4(5) | 0.9(5) |
| C10 C11 C16 C15 | 178.3(3) | -179.0(3) |

| | | |
|-----------------|---------|---------|
| C14 C15 C16 C11 | -0.7(5) | -0.3(5) |
|-----------------|---------|---------|

Table 5: Selected bond lengths (Å) and bond and torsion angles (°) for salts **26** and **34**, except those related to C17, Br2 and N3.

| Salt 26 | Salt 34 |
|---------------------------|-----------------------|
| Br2 C17 1.881(3) | N3 C7 1.302(4) |
| C17 C7 1.388(4) | N3 C8 1.306(4) |
| C17 C8 1.382(4) | |
| | |
| C17 C8 F8 120.2(3) | C7 N3 C8 117.5(3) |
| C8 C17 C7 117.8(3) | N3 C7 F7 117.0(3) |
| C8 C17 Br2 121.6(2) | N3 C7 C6 123.8(3) |
| C7 C17 Br2 120.6(2) | N3 C8 F8 117.4(3) |
| F7 C7 C17 120.0(3) | N3 C8 C9 124.0(3) |
| C6 C7 C17 121.3(3) | |
| | |
| C7 C17 C8 C9 -0.6(4) | C8 N3 C7 F7 179.7(3) |
| Br2 C17 C8 C9 179.4(2) | C8 N3 C7 C6 -1.3(5) |
| C7 C17 C8 F8 179.8(2) | F6 C6 C7 N3 179.3(3) |
| Br2 C17 C8 F8 -0.2(4) | C5 C6 C7 N3 1.0(5) |
| C8 C17 C7 F7 -179.6(2) | C7 N3 C8 F8 -179.5(3) |
| Br2 C17 C7 F7 0.4(3) | C7 N3 C8 C9 0.7(5) |
| C8 C17 C7 C6 0.3(4) | N3 C8 C9 F9 -179.3(3) |
| Br2 C17 C7 C6 -179.69(19) | N3 C8 C9 C5 0.2(5) |
| C17 C7 C6 F6 -179.2(2) | C8 N3 C7 F7 179.7(3) |
| C17 C7 C6 C5 0.6(4) | |
| F9 C9 C8 C17 -179.2(3) | |
| C5 C9 C8 C17 0.0(4) | |

Table 6: Selected bond lengths (Å) and bond and torsion angles (°) for salts **26** and **34** that related to C17, Br2 and N3.

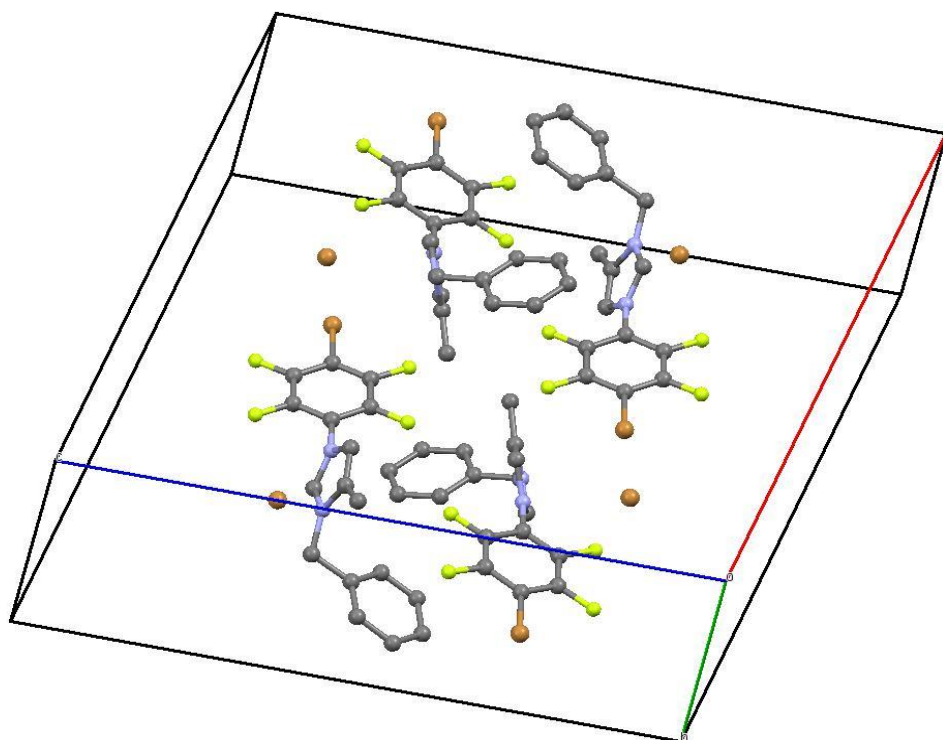


Figure 45: The monoclinic crystal system of 1-(4-bromo-2,3,5,6-tetrafluorobenzyl)-3-benzyl-4-methylimidazolium bromide **26**.

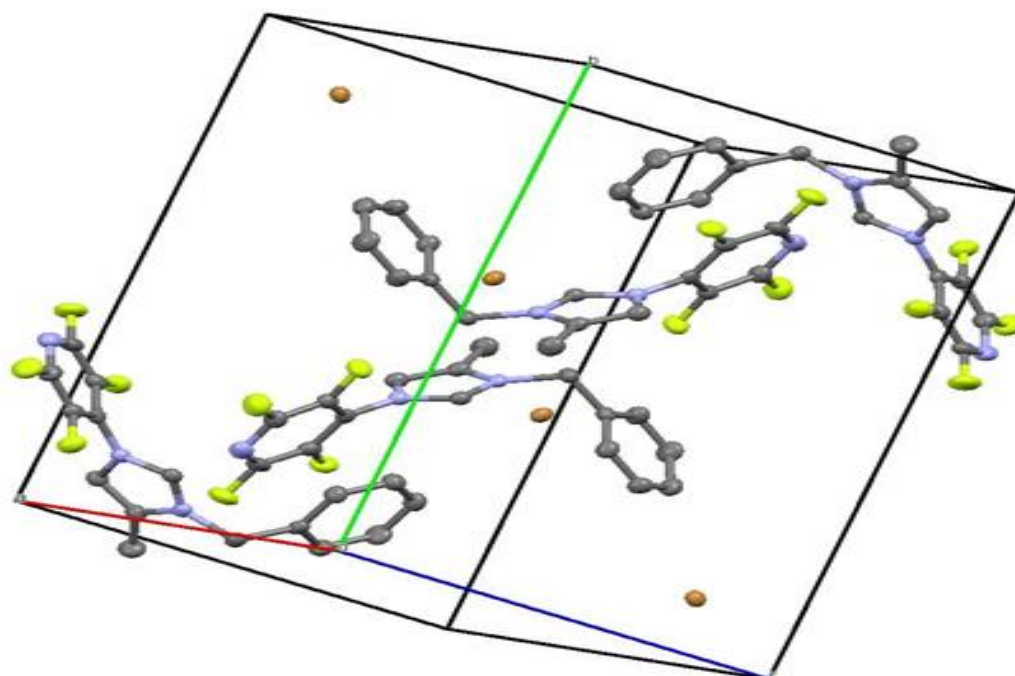


Figure 46: The monoclinic crystal system of 1-(2,3,5,6-tetrafluoropyridyl)-3-benzyl-4-methylimidazolium bromide **34**.

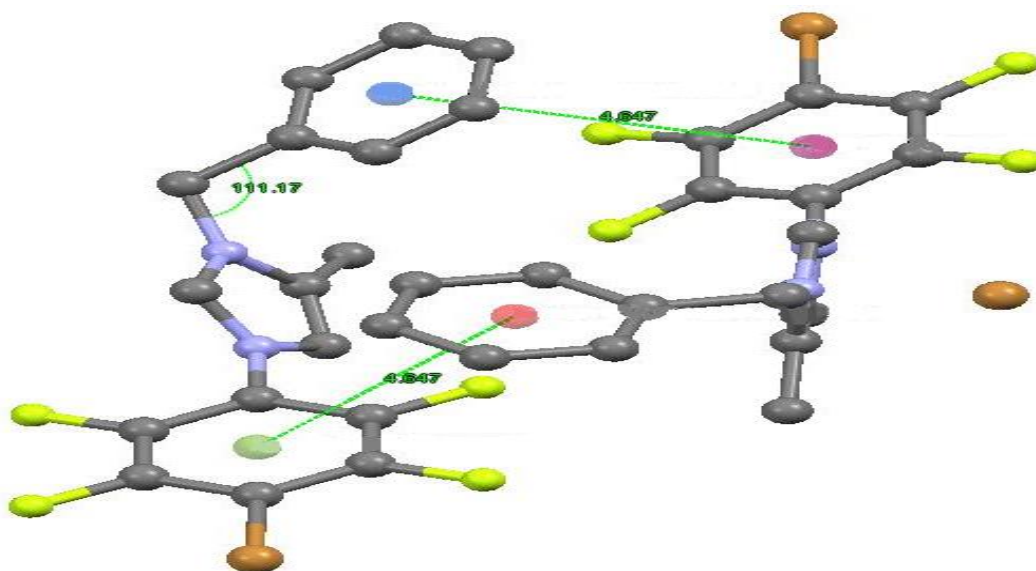


Figure 47: The π - π stacking of 1-(4-bromo-2,3,5,6-tetrafluorobenzyle)-3-benzyl-4-methylimidazolium bromide **26**.

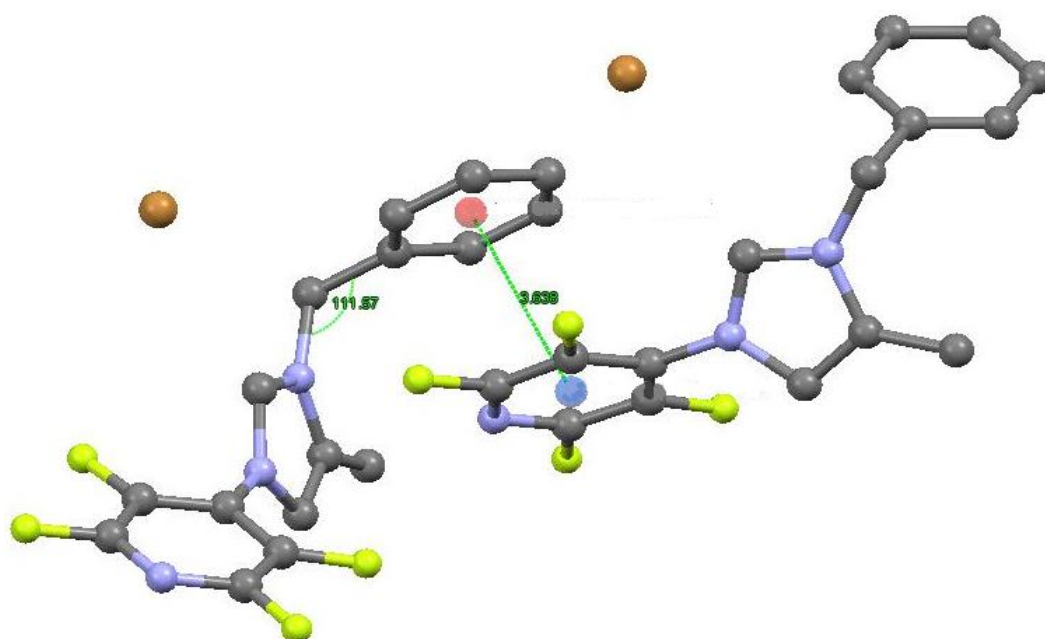


Figure 48: The π - π stacking of 1-(2,3,5,6-tetrafluoropyridyl)-3-benzyl-4-methylimidazolium bromide **34**.

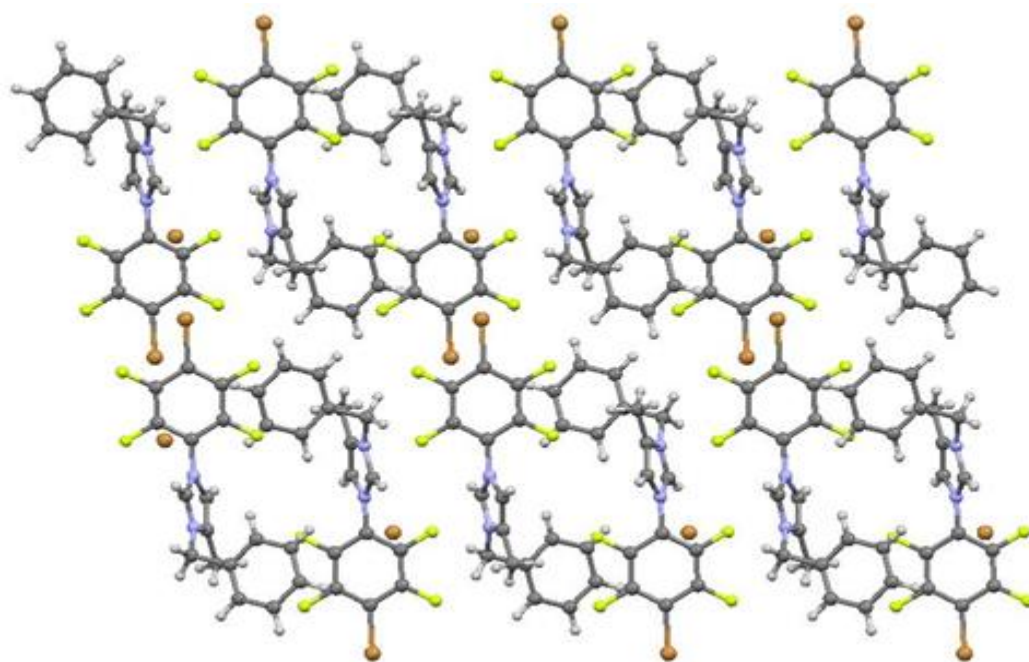
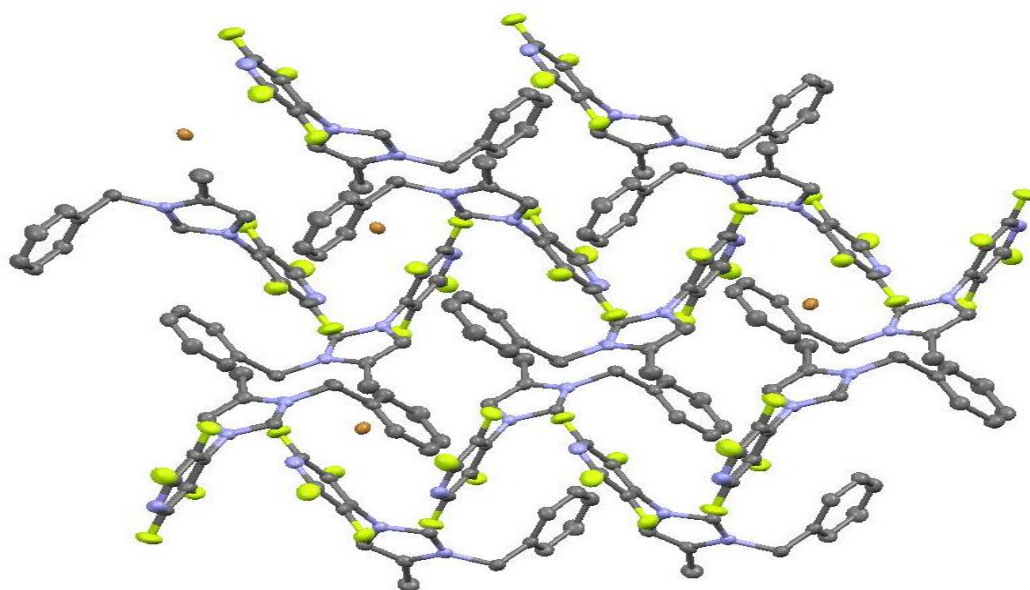
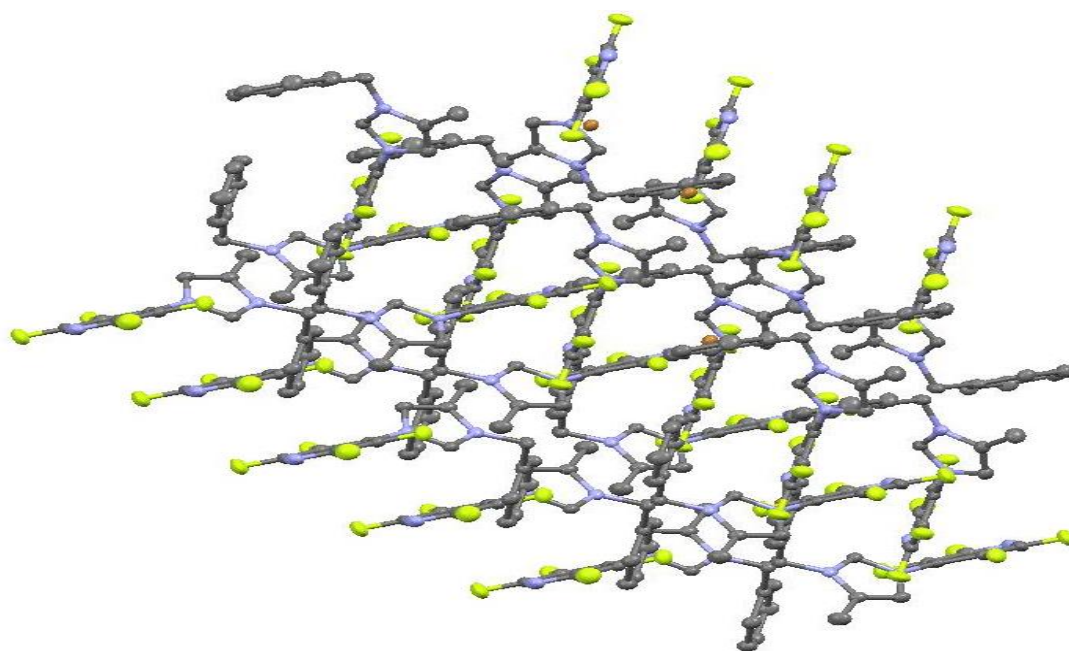


Figure 49: The crystal packing of 1-(4-bromo-2,3,5,6-tetrafluorobenzyle)-3-benzyl-4-methylimidazolium bromide **26** viewed along the b axis.



A



B

Figure 50: A & B The crystal packing of 1-(2,3,5,6-tetrafluoropyridyl)-3-benzyl-4-methylimidazolium bromide viewed along different axes.

3. Chapter Three:

3.1. Introduction:

The compounds and salts in this chapter were prepared similarly to those in chapter 2. Benzimidazole derivatives were dissolved in THF, then added to pentafluorobenzene derivatives, and left for different periods of time at room temperature. The solvent was then evaporated under reduced pressure. An NMR sample was prepared by adding CDCl₃, d₆-DMSO or both, to be analysed by ¹H and ¹⁹F NMR. Another sample was dissolved in MeOH to be analysed by MS. After the desired product was confirmed by these two analytical methods, the product was dissolved in CH₂Cl₂ and filtered, then the solvent has been removed by rotary evaporation and the product's yield was calculated. To crystalize the product, a small amount was dissolved in MeOH the solution left to evaporate slowly in air at ambient temperature. Salt **44** was achieved in the same way, using CH₂Cl₂ as a solvent.

3.2. Materials:

3.2.1. Pentafluorobenzene:

Pentafluorobenzene and its derivatives that were treated with imidazole, pyrazole and their derivatives in chapter 2 were also studied for their reaction with benzimidazole and its derivatives and indazole. These compounds are

tetrafluorophthalonitrile, pentafluorobenzaldehyde, chloro-tetrafluoropyridine, pentafluoropyridine, and octafluorotoluene. The chemical structure and the importance of pentafluorobenzene and its derivatives have been mentioned in chapters 1 and 2.

3.2.2. Benzimidazole:

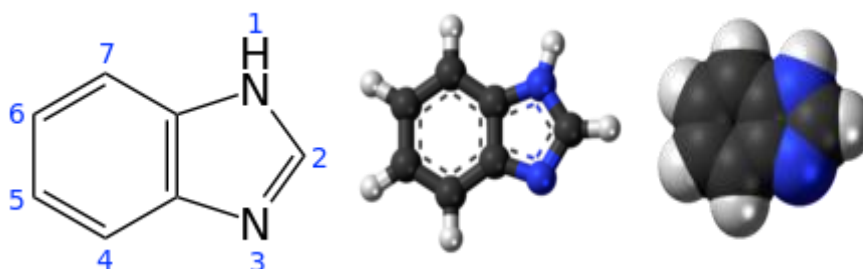


Figure 51: The chemical structure of benzimidazole ^[104].

Benzimidazole ($C_7H_6N_2$) was synthesized through the addition of a benzene ring to the carbon numbers 4 and 5 of the imidazole ring to give a product with a higher boiling and melting point than the starting materials ^[92]. In this project, benzimidazole and its derivatives were reacted with HFB and their derivatives, which have been used in the biological activity and possible use in the pharmaceutical industries. For instance, they have antiviral activity, such as 1-substituted-2-[(benzotriazol-1/2-yl) methyl] benzimidazole ^[105] and 2-phenylbenzimidazole derivatives ^[106], antiparasitic activity, such as 2-(trifluoromethyl)-benzimidazole derivatives ^[107], antimicrobial character, such as 2-alkylsulfanyl derivatives of 5-methylbenzimidazole ^[108], novel benzimidazole-hydrazone derivatives ^[109] and tetrahydronaphthalene benzimidazole derivatives ^[110], antiprotozoal properties, such as dicationic biphenyl benzimidazole derivatives ^[111] and as JNK3 inhibitors, such as 1,2-diaryl-1H-benzimidazole

derivatives (JNK3=c-Jan N-terminal kinases), which have been used to treat neurodegenerative diseases such as Alzheimer's, Parkinson's and ischemic injury [112].

3.2.3. Indazole:

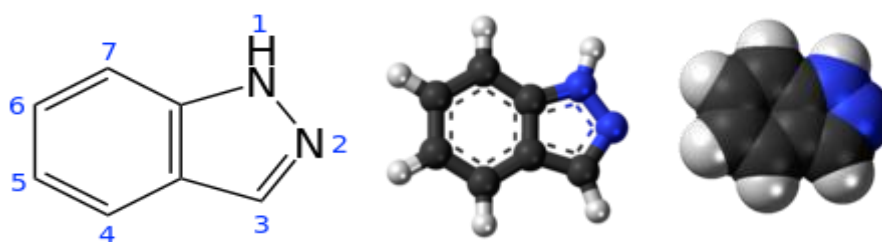


Figure 52: The chemical structure of indazole compound [113].

Indazole has the same chemical formula as benzimidazole ($C_7H_6N_2$) (Fig.52), but with a different position of the nitrogen atoms. Indazole and its derivatives have pharmaceutical and biological uses. For example, 4,5,6,7-tetrahydro-2H-indazole derivatives show anti-inflammatory activity [114], 3-cyano-2-(4-nitrophenyl)-2H-indazole N1-oxide and 2-(4-chlorophenyl)-3-cyano-2H-indazole N1-Oxide have antiepipimastigote activity and anti-T. cruzi activity with low cytotoxicity [115]. 3-[(N-carboalkoxy)ethylamino]-indazole-dione derivatives show inhibitor activity of the human carbonyl reductase [68], antifungal and antibacterial activity, such as 4,6-diphenyl-4,5-dihydro-3-hydroxy-2[H] indazole [116]. 4-(trifluoromethyl)-1H-indazole has shown activity against H460, A549, OS-RC-2, Lovo.HepG2, Bel-7402, SGC-7901 and MDA-MB-231 cancer cell lines [117], and as antichagasic drug, such as 1,2-disubstituted 5-nitroindazolinones [118].

Benzimidazole was treated with tetrafluorophthalonitrile, pentafluorobenzaldehyde, chloro-tetrafluoropyridine, pentafluoropyridine, and octafluorotoluene to afford 1-(2,3,6-trifluorophthalonitrile)benzimidazole (**35**), 1-(2,3,5,6-tetrafluorobenzaldehyde)benzimidazole (**36**), 1-(6-chloro-2,3,5-trifluoropyridyl)benzimidazole (**37**), 1-(2,3,5,6-tetrafluoropyridyl)benzimidazole (**38**) and 1-(heptafluorotolyl)benzimidazole (**39**) respectively. Octafluorotoluene, pentafluorobenzonitrile and pentafluoropyridine were treated with 2-methylbenzimidazole to give 1-(heptafluorotolyl)-2-methylbenzimidazole (**40**), 1-(2,3,5,6-tetrafluorobenzonitrile)-2-methylbenzimidazole (**41**) and 1-(2,3,5,6-tetrafluoropyridyl)-2-methylbenzimidazole (**42**). An attempt to synthesis 1-(2,3,5,6-tetrafluoropyridyl)indazole (**43**) in THF at RT was unsuccessful. A benzimidazolium salt 1-(2,3,5,6-tetrafluoropyridyl)-3-benzyl-benzimidazolium bromide (**44**) was afforded by the reaction of benzyl bromide with compound **38**.

| Comp or salt no | Chemical reaction |
|-----------------|-------------------|
| 35 | |
| 37 | |
| 36 | |
| 38 | |
| 39 | |
| 40 | |
| 41 | |
| 42 | |
| 43 | |
| 44 | |

Table 7: Chemical reactions of PFB-R with benzimidazole, indazole and their derivatives, and the chemical reactions of these compounds to form benzimidazolium salts.

3.3. Synthesis:

Compounds **35** to **43** were synthesized in THF at ambient temperature. The salt **44** was synthesized under room temperature in CH_2Cl_2 with yield of 67 %.

3.4. Characterization:

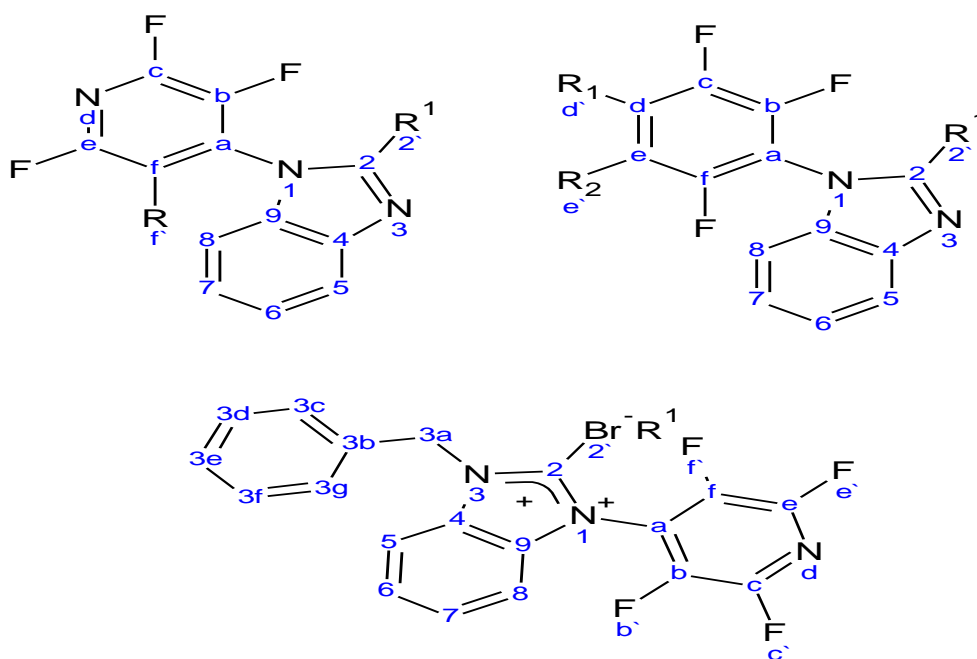


Figure 53: The labels that have been used to represent the NMR data of benzimidazole compounds and their salts. ($\text{R}_1 = \text{F}, \text{CF}_3, \text{CN}, \text{CHO}$, $\text{R}_2 = \text{F}, \text{CN}$, $\text{R} = \text{F}, \text{Cl}$ and $\text{R}^1 = \text{H}, \text{CH}_3$).

The mass spectra of all the compounds and exhibit the expected $[M + H]^+$ or $[M]^+$ peaks). The ^{19}F NMR spectra of all these compounds are similar to those of the compounds in the second chapter (compounds and salts **1** to **34**). The ^1H NMR spectra of compounds **36** to **39** possess a resonance at δ 8.00 characteristic of the acidic hydrogen atom of the 2 position (bonded to the carbon atom between the two nitrogen atoms), The resonances of the peaks of the 2'-methyl hydrogen atoms of compounds from **40** to **42** were similar to those of compounds **9** to **12** in the second chapter. But in benzimidazole, further hydrogen atoms have been exhibited as a result of the phenylene ring attached in positions 4 and 5 of the imidazole ring in these compounds, and the four hydrogen atoms of this ring have shown resonances from δ 7.9 and 7.0 ppm. The ^{13}C NMR spectra have been collected for compounds **38** and **42**, and they display similar resonances.

For example, C2 of **38** displayed a resonance at δ 147 and δ 150 for **42**, C5 displayed a resonance at δ 110 for **38** and 109 for **42**, C8 displayed a resonance at δ 121 for **38** and 119 for **42**, C9 and C4 displayed resonances at δ 132 for **38** and 134 for **42**. Similar resonances are displayed for the other carbon atoms of **38** and **42**, Ca gave 127, Cb with Cf and Cc with Ce, have shown two multiple peaks at the resonances of δ 144 and 136-138 ppm respectively and C6 gave 124 ppm. The difference between the compounds is the presence of methyl group in **42** in the 2' position and the carbon atom of this group has shown single peak with resonance at 13 ppm.

The chemical structures of **42** were confirmed through the data that has been collected by two dimensional NMR spectrum (HSQC and HMBC). For **42** in the HSQC spectrum H-2' correlates with C-2', H-5 correlates with C-5, H-6 and H-7 correlates with C-6 and C-7, and H-8 correlates with C-8 (Fig. 54). In the

HMBC spectrum H-2' correlates with C-2' and C-2, H-5 correlates with C-5, C-4, C-6 and C-7, H-6 and H-7 correlates with C-4, C-5, C-6, C-7, C-8 and C-9, H-8 correlates with C-6, C-7, C-8 and C-9 (Fig. 55). Salt **44** has shown instability, slowly decomposing in methanol over months as shown in Figure 56. The IR spectral data of **36**, **37**, **38**, **39**, **40**, **41**, **42** and **44** were as expected. The elemental composition of **42** was calculated to be C = 55.53 %, H = 2.51 % and N = 14.94 %, and found to be C = 55.55 %, H = 2.62 % and N = 15.03 %.

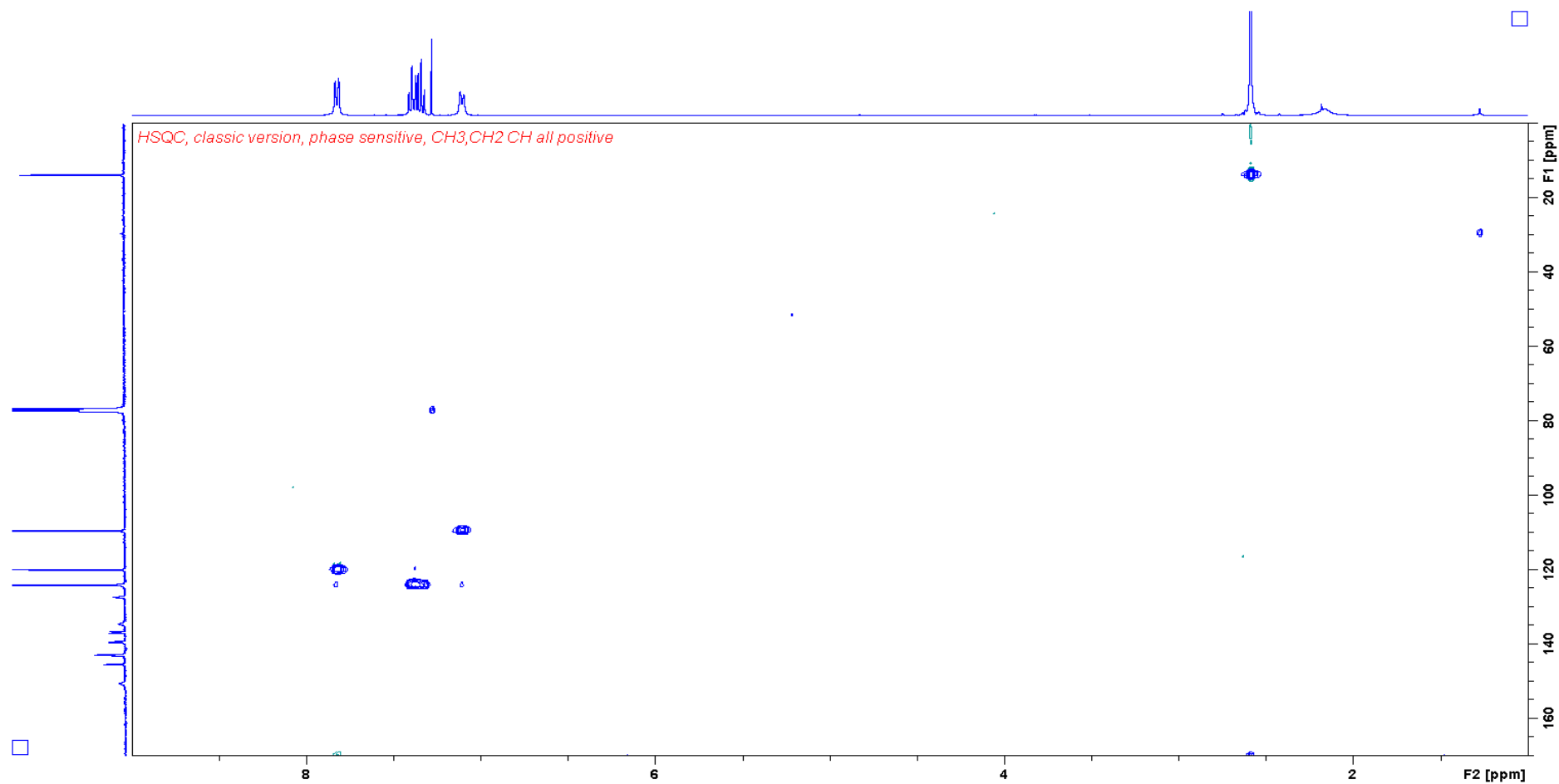


Figure 54: The HSQC spectrum of 1-(2,3,5,6- tetrafluoropyridyl)-2-methylbenzimidazole **42**.

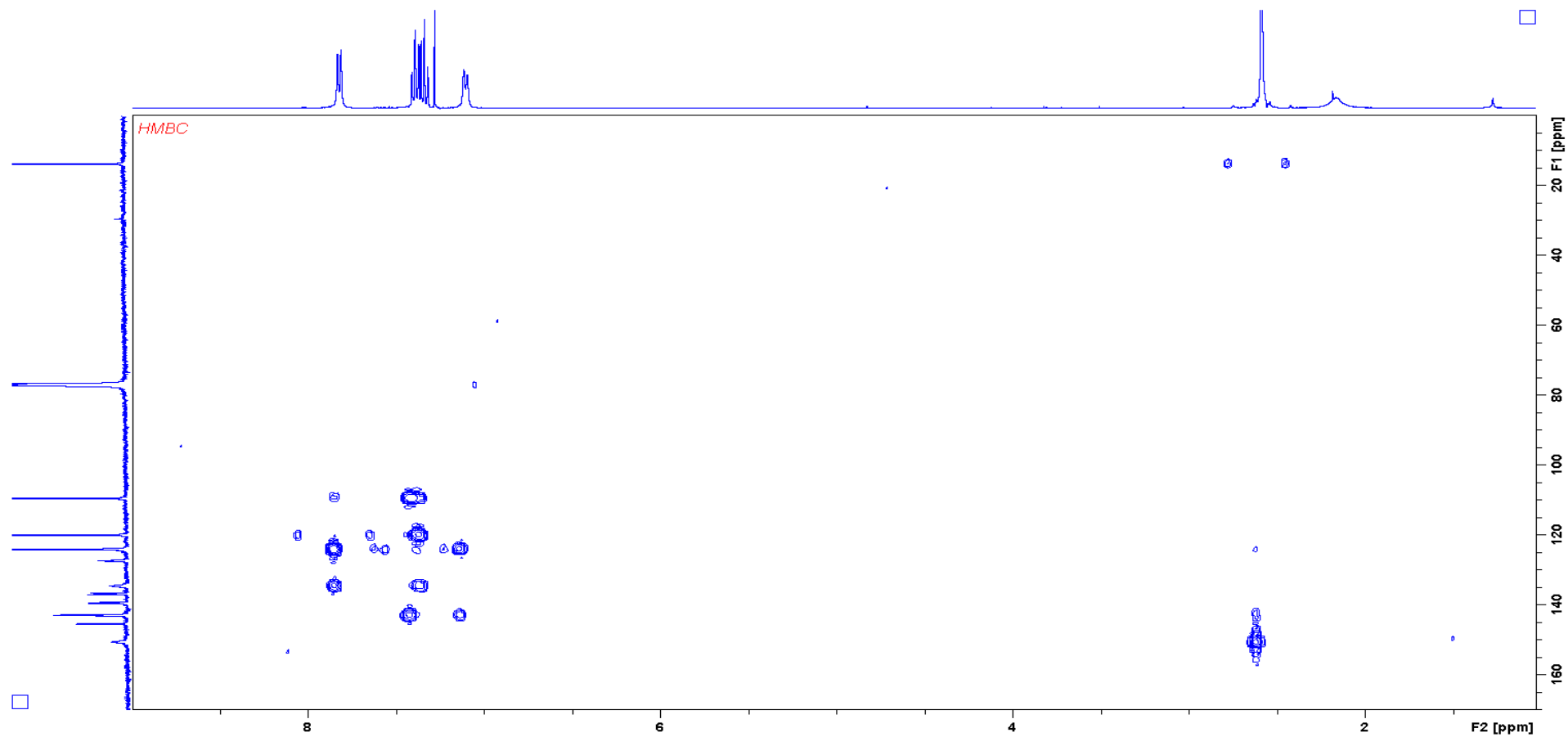


Figure 55: The HMBC spectrum of 1-(2,3,5,6- tetrafluoropyridyl)-2-methylbenzimidazole **42**.

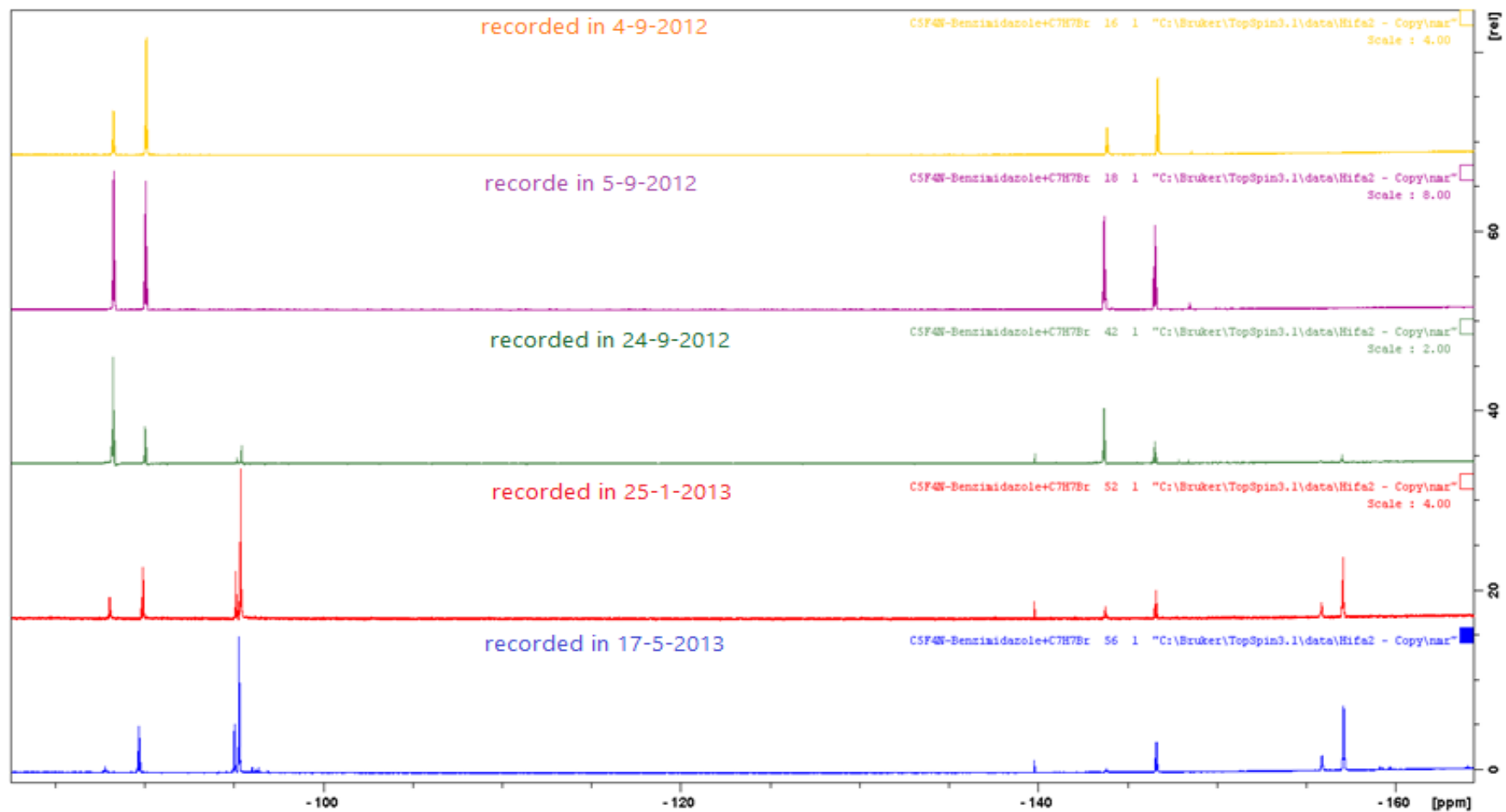


Figure 56: Decomposing of 1-(2,3,5,6-tetrafluoropyridyl)-3-benzyl-benzimidazolium bromide **44** over months from yellow to blue.

All the compounds were recrystallized from methanol by slow evaporation, but crystals suitable for single-crystal X-ray diffraction were obtained only for **42**, which crystallized in space group $Pca2_1$ in the orthorhombic crystal system with two independent molecules in the asymmetric unit (Crystallographic data for **42** has been shown in table 11, chapter 5). π - π stacking is evident shown in the crystal structure (Fig.58). The centroid-centroid distances are $D_{\text{cent}} = 3.623$ and 3.960 \AA , the angle $\phi = 5.96^\circ$, and the stack shift $s = 0.00 \text{ \AA}$ (Fig.59).

There are two values of slip angle as a result of rotated layers, $\theta = 49.29^\circ$ is the angle between the direction of the stack and the perpendiculars to the tetrafluoropyridyl ring, whereas, $\theta = 83.47^\circ$ is the angle between the direction of the stack and the perpendiculars to 2-methylbenzimidazole ring in this compound. Bond lengths and selected angles have been given in the table 8. The bonds lengths and angles of **42A** were very similar to those of **42B**.

The bonds lengths and angles of **42A** were very similar to those of **42B**. The range of bond lengths and experimental errors are $1.302(3) - 1.497(3) \text{ \AA}$ in compound **42A** and $1.306(3) - 1.486(3) \text{ \AA}$ in **42B**. The range of angles are from $106.05(19)^\circ$ of C1A-N2A-C3A to $132.6(19)^\circ$ of C5A-C4A-C3A in **42A** and from $105.45(18)^\circ$ of C1B-N2B-C3D to $132.3(2)^\circ$ C5B-C4B-N1B in **42B**. Some torsion angles of **42A** are similar to those of **42B**, such as the torsion angle of C9-N1-C4-C5, $1.5(4)^\circ$ in **42A** and $1.4(4)^\circ$ in **42B**. Other torsion angles are considerably different. For example, C1A-N1A-C9A-C13A of **42A** is $54.2(3)^\circ$, which differs significantly from C1B-N1B-C9B-C13B $128.2(2)^\circ$ of **42B** by *ca.* 74° .

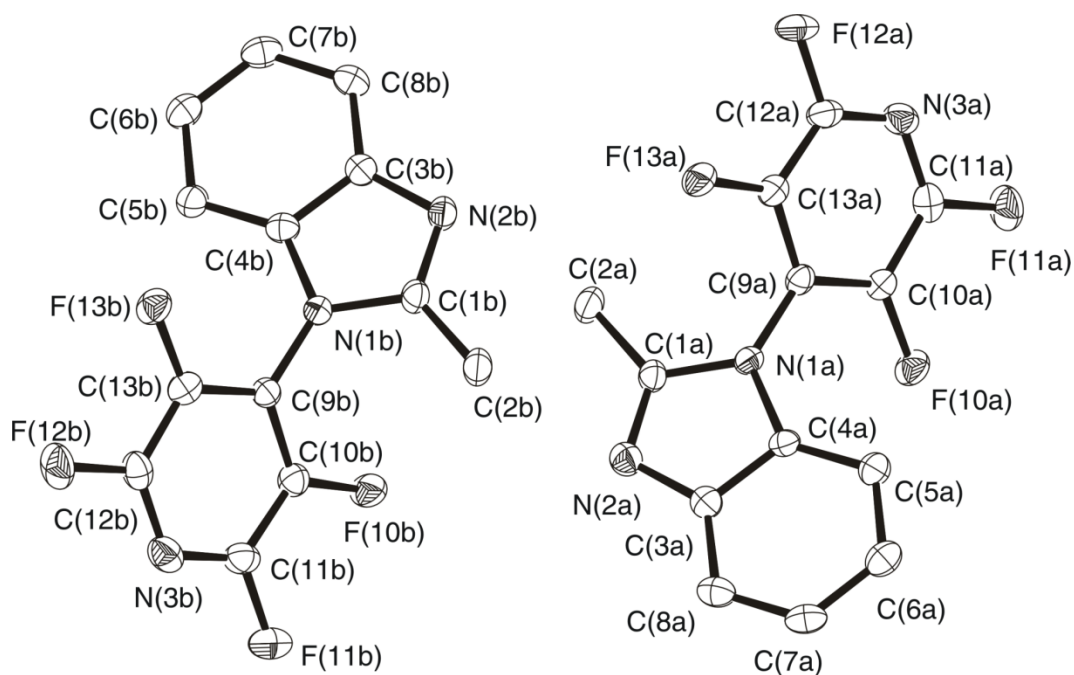


Figure 57: The crystal structure of 1-(2,3,5,6-tetrafluoropyridyl)-2-methylbenzimidazole **42**.

| Comp. 42A | Data of 42A | Comp. 42B | Data of 42B |
|-----------|-------------|-----------|-------------|
| F10A C10A | 1.336(3) | F10B C10B | 1.337(3) |
| F11A C11A | 1.335(3) | F11B C11B | 1.335(3) |
| F12A C12A | 1.341(3) | F12B C12B | 1.340(3) |
| F13A C13A | 1.334(3) | F13B C13B | 1.337(3) |
| N1A C9A | 1.400(3) | N1B C4B | 1.399(3) |
| N1A C1A | 1.403(3) | N1B C1B | 1.408(3) |
| N1A C4A | 1.403(3) | N1B C9B | 1.414(3) |
| N2A C1A | 1.302(3) | N2B C1B | 1.307(3) |
| N2A C3A | 1.392(3) | N2B C3B | 1.401(3) |
| N3A C11A | 1.304(3) | N3B C11B | 1.306(3) |
| N3A C12A | 1.313(3) | N3B C12B | 1.313(3) |
| C1A C2A | 1.497(3) | C1B C2B | 1.486(3) |
| C3A C8A | 1.399(4) | C3B C8B | 1.393(3) |
| C3A C4A | 1.403(3) | C3B C4B | 1.395(3) |
| C4A C5A | 1.393(3) | C4B C5B | 1.395(3) |
| C5A C6A | 1.388(3) | C5B C6B | 1.392(3) |
| C6A C7A | 1.402(4) | C6B C7B | 1.393(4) |
| C7A C8A | 1.386(4) | C9B C10B | 1.381(3) |
| C9A C13A | 1.392(3) | C9B C13B | 1.388(3) |
| C9A C10A | 1.394(3) | C7B C8B | 1.389(4) |
| C10A C11A | 1.381(3) | C10B C11B | 1.389(3) |
| C12A C13A | 1.378(3) | C12B C13B | 1.378(3) |

| | | | |
|-----------------|-------------|-----------------|------------|
| C9A N1A C1A | 127.05(19) | C1B N1B C9B | 126.75(19) |
| C9A N1A C4A | 126.54(19) | C4B N1B C9B | 126.64(19) |
| C1A N1A C4A | 106.37(18) | C4B N1B C1B | 106.61(18) |
| C1A N2A C3A | 106.05(19) | C1B N2B C3B | 105.45(18) |
| C11A N3A C12A | 117.1(2) | C11B N3B C12B | 117.2(2) |
| N2A C1A N1A | 112.33(19) | N2B C1B N1B | 112.16(19) |
| N2A C1A C2A | 124.8(2) | N2B C1B C2B | 124.7(2) |
| N1A C1A C2A | 122.9(2) | N1B C1B C2B | 123.1(2) |
| N2A C3A C8A | 129.4(2) | C8B C3B C4B | 120.0(2) |
| N2A C3A C4A | 110.6(2) | C8B C3B N2B | 128.9(2) |
| C8A C3A C4A | 120.0(2) | C4B C3B N2B | 111.1(2) |
| C5A C4A C3A | 122.8(2) | C5B C4B C3B | 123.0(2) |
| C5A C4A N1A | 132.6(2) | C5B C4B N1B | 132.3(2) |
| C3A C4A N1A | 104.63(19) | C3B C4B N1B | 104.70(19) |
| C6A C5A C4A | 116.4(2) | C6B C5B C4B | 115.8(2) |
| C5A C6A C7A | 121.7(2) | C5B C6B C7B | 122.0(2) |
| C8A C7A C6A | 121.6(2) | C10B C9B C13B | 117.2(2) |
| C7A C8A C3A | 117.5(2) | C10B C9B N1B | 121.7(2) |
| C13A C9A C10A | 116.4(2) | C13B C9B N1B | 121.2(2) |
| C13A C9A N1A | 121.96(19) | C8B C7B C6B | 121.3(2) |
| C10A C9A N1A | 121.6(2) | C7B C8B C3B | 117.9(2) |
| F10A C10A C11A | 120.7(2) | F10B C10B C9B | 121.3(2) |
| F10A C10A C9A | 120.1(2) | F10B C10B C11B | 119.9(2) |
| C11A C10A C9A | 119.2(2) | C9B C10B C11B | 118.8(2) |
| N3A C11A F11A | 117.2(2) | N3B C11B F11B | 117.2(2) |
| N3A C11A C10A | 124.0(2) | N3B C11B C10B | 123.9(2) |
| F11A C11A C10A | 118.9(2) | F11B C11B C10B | 118.9(2) |
| N3A C12A F12A | 116.8(2) | N3B C12B F12B | 117.2(2) |
| N3A C12A C13A | 124.5(2) | N3B C12B C13B | 124.2(2) |
| F12A C12A C13A | 118.7(2) | F12B C12B C13B | 118.7(2) |
| F13A C13A C12A | 120.6(2) | F13B C13B C12B | 120.3(2) |
| F13A C13A C9A | 120.7(2) | F13B C13B C9B | 121.0(2) |
| C12A C13A C9A | 118.7(2) | C12B C13B C9B | 118.7(2) |
| | | | |
| | | | |
| C3A N2A C1A N1A | 0.4(2) | C3B N2B C1B N1B | -0.7(2) |
| C3A N2A C1A C2A | 178.9(2) | C3B N2B C1B C2B | -178.3(2) |
| C9A N1A C1A N2A | 178.68(19) | C9B N1B C1B N2B | 178.96(19) |
| C4A N1A C1A N2A | 0.7(2) | C4B N1B C1B N2B | -0.3(2) |
| C9A N1A C1A C2A | 0.2(3) | C9B N1B C1B C2B | -3.4(3) |
| C4A N1A C1A C2A | 177.81(19) | C4B N1B C1B C2B | 177.3(2) |
| C1A N2A C3A C8A | 179.7(2) | C1B N2B C3B C8B | -179.2(2) |
| C1A N2A C3A C4A | -1.3(2) | C1B N2B C3B C4B | 1.5(2) |
| N2A C3A C4A C5A | -179.09(19) | N2B C3B C4B C5B | 178.8(2) |
| C8A C3A C4A C5A | 0.0(3) | C8B C3B C4B C5B | -0.5(3) |
| N2A C3A C4A N1A | 1.7(2) | N2B C3B C4B N1B | -1.7(2) |
| C8A C3A C4A N1A | -179.18(19) | C8B C3B C4B N1B | 179.00(18) |
| C9A N1A C4A C5A | 1.5(4) | C9B N1B C4B C5B | 1.4(4) |

| | | | |
|---------------------|-------------|---------------------|-------------|
| C1A N1A C4A C5A | 179.5(2) | C1B N1B C4B C5B | -179.4(2) |
| C9A N1A C4A C3A | -179.44(19) | C9B N1B C4B C3B | -178.07(19) |
| C1A N1A C4A C3A | -1.4(2) | C1B N1B C4B C3B | 1.2(2) |
| C3A C4A C5A C6A | 0.8(3) | C3B C4B C5B C6B | -0.9(3) |
| N1A C4A C5A C6A | 179.7(2) | N1B C4B C5B C6B | 179.8(2) |
| C4A C5A C6A C7A | -0.7(3) | C4B C5B C6B C7B | 1.0(3) |
| C5A C6A C7A C8A | -0.1(3) | C5B C6B C7B C8B | 0.1(4) |
| C6A C7A C8A C3A | 0.9(3) | C6B C7B C8B C3B | -1.5(3) |
| N2A C3A C8A C7A | 178.0(2) | N2B C3B C8B C7B | -177.5(2) |
| C4A C3A C8A C7A | -0.8(3) | C4B C3B C8B C7B | 1.7(3) |
| C1A N1A C9A C13A | 54.2(3) | C1B N1B C9B C13B | 128.2(2) |
| C4A N1A C9A C13A | -128.2(2) | C4B N1B C9B C13B | -52.7(3) |
| C1A N1A C9A C10A | -126.0(2) | C1B N1B C9B C10B | -52.1(3) |
| C4A N1A C9A C10A | 51.6(3) | C4B N1B C9B C10B | 127.0(2) |
| C13A C9A C10A F10A | 179.60(18) | C13B C9B C10B F10B | 177.07(19) |
| N1A C9A C10A F10A | -0.2(3) | N1B C9B C10B F10B | -2.6(3) |
| C13A C9A C10A C11A | -1.4(3) | C13B C9B C10B C11B | -2.8(3) |
| N1A C9A C10A C11A | 178.77(19) | N1B C9B C10B C11B | 177.5(2) |
| C12A N3A C11A F11A | -178.79(18) | C12B N3B C11B F11B | -179.5(2) |
| C12A N3A C11A C10A | 2.4(3) | C12B N3B C11B C10B | 0.3(3) |
| F10A C10A C11A N3A | 177.56(19) | F10B C10B C11B N3B | -177.1(2) |
| C9A C10A C11A N3A | -1.5(3) | C9B C10B C11B N3B | 2.8(4) |
| F10A C10A C11A F11A | -1.2(3) | F10B C10B C11B F11B | 2.6(3) |
| C9A C10A C11A F11A | 179.76(18) | C9B C10B C11B F11B | -177.5(2) |
| C11A N3A C12A F12A | 179.69(18) | C11B N3B C12B F12B | 177.8(2) |
| C11A N3A C12A C13A | -0.5(3) | C11B N3B C12B C13B | -3.2(3) |
| N3A C12A C13A F13A | 177.34(19) | N3B C12B C13B F13B | -176.4(2) |
| F12A C12A C13A F13A | -2.9(3) | F12B C12B C13B F13B | 2.6(3) |
| N3A C12A C13A C9A | -2.3(3) | N3B C12B C13B C9B | 3.0(4) |
| F12A C12A C13A C9A | 177.51(18) | F12B C12B C13B C9B | -177.98(19) |
| C10A C9A C13A F13A | -176.55(18) | C10B C9B C13B F13B | 179.59(19) |
| N1A C9A C13A F13A | 3.3(3) | N1B C9B C13B F13B | -0.7(3) |
| C10A C9A C13A C12A | 3.1(3) | C10B C9B C13B C12B | 0.2(3) |
| N1A C9A C13A C12A | -177.1(2) | N1B C9B C13B C12B | 179.9(2) |

Table 8: Selected bond lengths (Å) and bond and torsion angles (°) for compounds **42A** and **42B**.

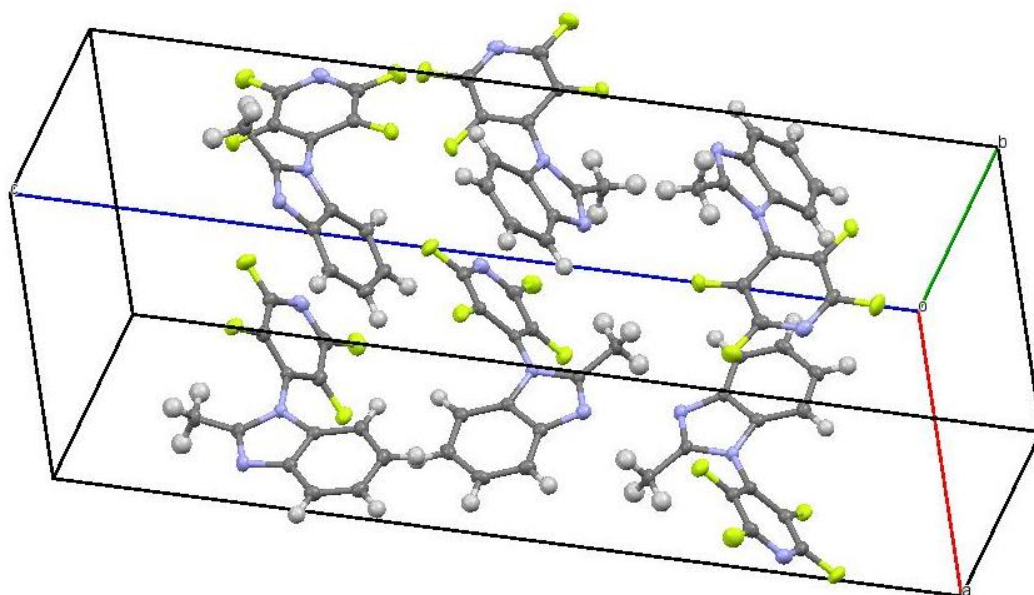


Figure 58: The orthorhombic crystal system of 1-(2,3,5,6-tetrafluoropyridyl)-2-methylbenzimidazole **42**.

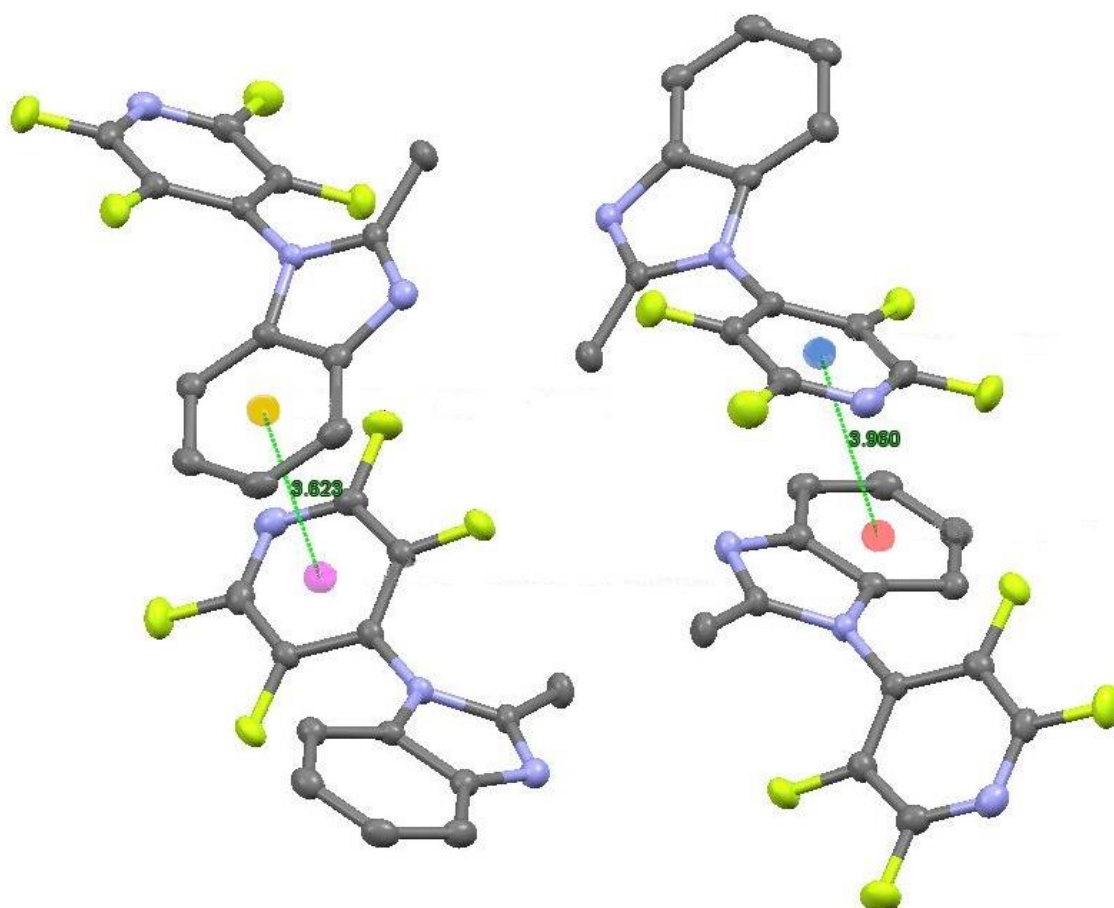


Figure 59: The crystal structure of 1-(2,3,5,6-tetrafluoropyridyl)-2-methylbenzimidazole **42**.

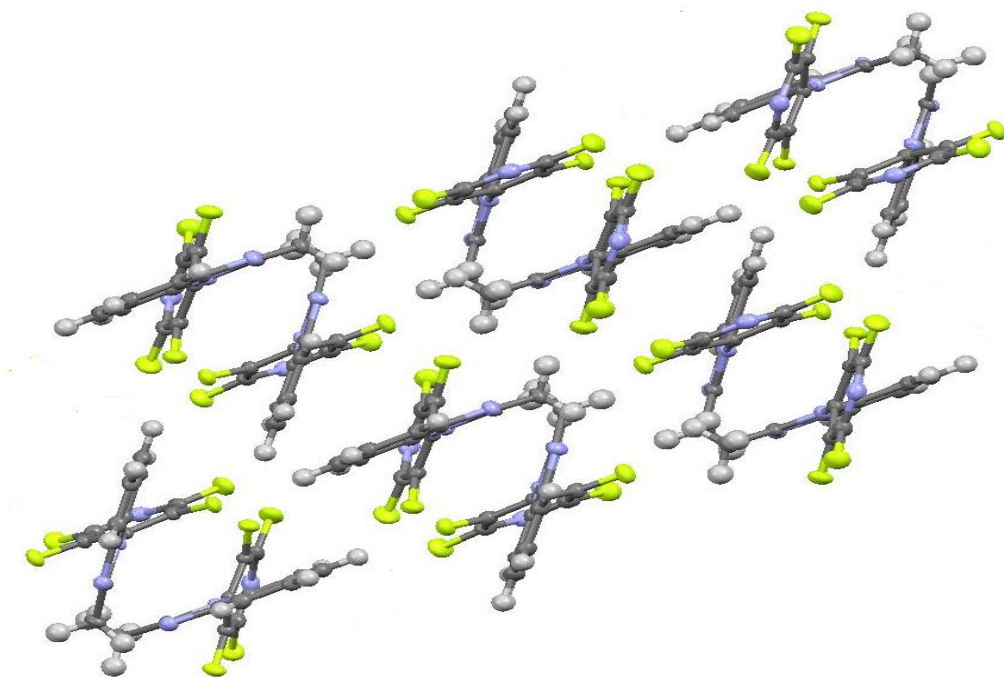


Figure 60: The crystal packing of 1-(2,3,5,6-tetrafluoropyridyl)-2-methylbenzimidazole **42** viewed along the C-C₅F₄N bond.

4. Chapter Four:

4.1. Conclusion:

In this project a number of new compounds containing both aryl and polyfluoroaryl groups have been synthesized in variable yields using nucleophilic aromatic substitution and subsequent functionalization. All the reactions have been done at ambient temperature except the reactions of the compounds **8**, **12**, **16**, **17** and **18** have been heated from 55° C to 142° C. The compounds were characterized by MS (micro-TOF), IR spectroscopy, micro-elemental analysis and NMR spectroscopy. Two dimensional spectra, such as HSQC and HMBC have been determined for compounds **12**, **18**, and **42**, which confirmed their characterization. The imidazolium salts, such as 1-(2,3,5,6-tetrafluoropyridil)-3-benzyl-4-methylimidazolium bromide (**34**), were recrystallized from methanol. The benzimidazolium salts, such as 1-(2,3,5,6-tetrafluoropyridyl)-3-benzylbenzimidazolium bromide (**44**) were not stable in methanol, decomposing slowly over months. Attempts were made to grow crystals suitable for single-crystal X-ray diffraction. Single crystals were obtained only for 1-(4-bromo-2,3,5,6-tetrafluorobenzyl)-3-benzyl-4-methylimidazolium bromide (**26**), 1-(2,3,5,6-tetrafluoropyridil)-3-benzyl-4-methylimidazolium bromide (**34**) and 1-(2,3,5,6-tetrafluoropyridyl)-2-methylbenzimidazole (**42**).

All three structures possess π - π stacking between the polyfluoroaryl group of one synthon and the aryl group of another. Attempts were made to synthesize 1-(2,3,5,6-tetrafluoropyridyl)pyrazole (**25**) and 1-(2,3,5,6-

tetrafluoropyridyl)indazole (**43**), which were envisaged to biological activity. In the future, more studying can be done to study the biological and pharmaceutical properties of these compounds with more interpretation of their role in crystal engineering. This project has established that a range of synthons for crystal engineering based on heterocycles bearing aryl and polyfluoroaryl groups may be readily prepared by the aromatic nucleophilic substitution reaction between the heterocycle and a polyfluoroarene. The π - π stacking exhibited by **26**, **34** and **42**, as well for similar compounds reported previously, appears to be a general and robust interaction.

5. Chapter Five:

5.1. General Synthesis:

The starting materials of all the compounds from **1** to **25** and from **35** to **43** were dissolved in THF, DMSO or both, and then stirred for different periods of time at temperatures between RT and 142°C, whereas the starting materials of the salts from **26** to **34** and salt **44** were dissolved in CH₂Cl₂ and stirred for a few days at room temperature. The solvents of these compounds and salts were removed by rotary evaporation. Their products were extracted into dichloromethane, which was then evaporated under reduced pressure to yield the products. The recrystallization of these products from methanol and of compounds **5** and **6** from diethyl ether led to an increase in purity, except for salts **26**, **34**, **44** and compound **42**. Crystals of **26**, **34** and **42** were grown from methanol and were analysed by XRD. In contrast, using methanol with salt **44** led to decomposition. The reactions of the expected compounds from **2** to **6** have not yet been completed. The slow rates of these reactions were shown by the NMR spectrum that was recorded over a period of months and the mass of these expected compounds was confirmed by MS analysis.

5.2. Imidazole:

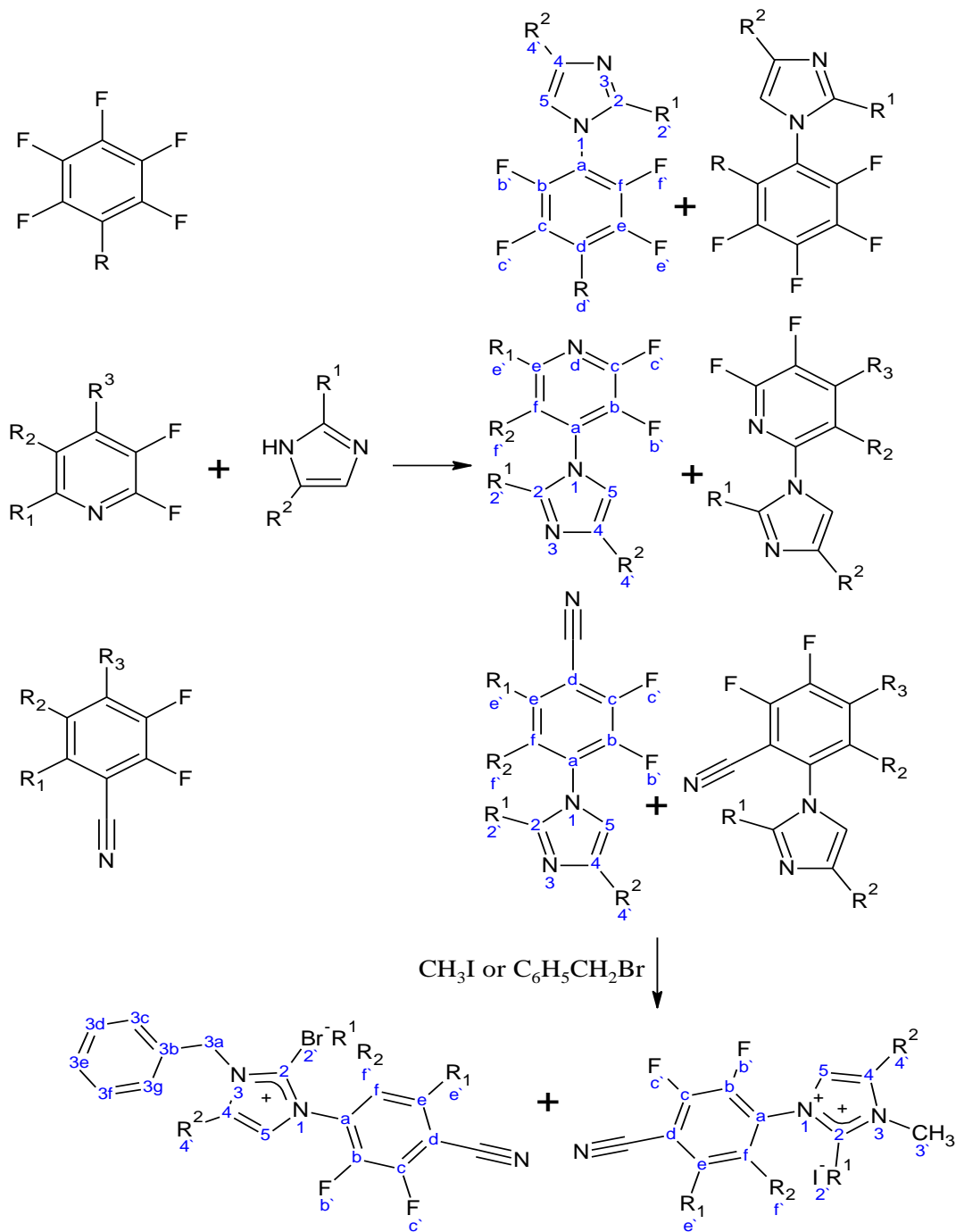


Figure 61: The general reaction of polyfluoroaryl and imidazole with their derivatives and examples of imidazolium salts (with the labels that have been used to represent the NMR data) (R = Br, I, F. R¹, R² = H, CH₃. R₁, R₂, R₃ = H, F).

5.2.1. 1-(2,3,6-Trifluorobenzonitrile)imidazole (1):

0.103 g of imidazole was dissolved in 50 ml of THF, which then was added to 0.151 g of 2,3,4,5- tetrafluorobenzonitrile, and then the solution was left at RT for a day. $C_{10}H_4F_3N_3$: 223.1569 $g \cdot mol^{-1}$. (93.28 % yield). MS: Calc. 224.0436. Found. 224.0490 m/z [$(M + H)^+$]. In $CDCl_3$ (400 MHz), 1H NMR: $\delta = 7.85$ (m, 1H, H-2), 7.43 (m, 1H, H-5) and 7.31 (q, $J = 0.77$ Hz, $J' = 0.77$ Hz, 2H, H-4 and H-e) ppm. ^{19}F NMR: $\delta = -121.33$ (t, $J = 10.39$ Hz, 12.52 Hz, 1F, F-f), -130.53 (m, 1F, F-c) and -137.92 (d, $J = 11.34$, 9.17 Hz, 1F, F-b) ppm. IR (KBr): 3157, 3006, 2240, 1643, 1619, 1517, 1495, 1467, 1400, 1375, 1349, 1303, 1275, 1255, 1233, 1175, 1111, 1087, 1062, 1048, 1029, 959, 916, 898, 876, 849, 827, 745, 714, 653, 615, 590, 574, 485, 468 and 449 cm^{-1} .

5.2.2. The Expected Compound 1-(3,4,6-Trifluoropyridyl)imidazole (2):

A solution of (0.086 g) of imidazole in THF was added to 0.165 g of 2,3,5,6-tetrafluoropyridine, and then the mixture was left for several months at RT. $C_8H_4F_3N_3$: 199.0357 $g \cdot mol^{-1}$. MS: Calc. 200.0436. Found. 200.9464 m/z [$(M + H)^+$]. NMR analysis has been recorded in $CDCl_3$ with (400 MHz) and show a slow rate of interaction (Fig. 38, chapter two).

5.2.3. The Expected Compound 1-(2,3-Difluorobenzonitrile)imidazole (3):

0.086 g of imidazole was dissolved in THF, and then added to 0.203 g of 2,3,4-trifluorobenzonitrile, then this mixture was left at RT for several months. $C_{10}H_5F_2N_3$: 205.1664 $g \cdot mol^{-1}$. MS: Calc. 206.0530. Found. 206.0483 m/z [$(M +$

H)⁺], NMR analysis has been recorded in CDCl₃ with (400 MHz) and show a slow rate of interaction (Fig. 39, chapter two).

5.2.4. The Expected Compound 1-(3,4,6-Trifluorobenzonitrile)imidazole (4):

0.039 g of imidazole was dissolved in THF, and then added to 0.117 g of 2,3,5,6-tetrafluorobenzonitrile, then this mixture was left at RT for several months. C₁₀H₄F₃N₃: 223.1569 g.mol⁻¹. MS: Calc. 224.0436. Found: 224.9958 m/z [(M + H)⁺]. NMR analysis has been recorded in CDCl₃ with (400 MHz) and show a slow rate of interaction (Fig. 40, chapter two).

5.2.5. The Expected Compound 1-(4,6-Difluoropyridyl)imidazole (5):

A solution of 0.086 g of imidazole and 0.180 g of 2, 3, 5-trifluoropyridine in THF was left for several months at RT. C₈H₅F₂N₃: 181.0452 g.mol⁻¹. MS: Calc. 182.0530. Found. 182.0914 m/z [(M + H)⁺]. NMR analysis has been recorded in CDCl₃ with (400 MHz) and show a slow rate of interaction (Fig. 41, chapter two).

5.2.6. The Expected Compound 1-(3,6-Difluorobenzonitrile)imidazole (6):

0.050 g of imidazole was dissolved in 50 ml of THF then added to 0.115 g of 2,4,5-trifluorobenzonitrile, Then it was left for several months at RT. C₁₀H₅F₂N₃: 205.1664 g.mol⁻¹. MS: Calc. 206.0530. Found. 206.0385 m/z [(M + H)⁺]. NMR

analysis has been recorded in CDCl_3 with (400 MHz) and show a slow rate of interaction (Fig. 42, chapter two).

5.2.7. 1-(Heptafluorotolyl)imidazole (7):

0.179 g of imidazole was dissolved in 50 ml of THF then added to 0.595 g of 1,2,3,4,5-pentafluoro-6-(trifluoromethyl)benzene, Then it was left for a day at RT. $\text{C}_{10}\text{H}_3\text{F}_7\text{N}_2$: 284.1359 $\text{g}\cdot\text{mol}^{-1}$. (36.87% yield). MS: Calc. 285.0263. Found. 285.3625 m/z [$(M + \text{H})^+$]. In CDCl_3 (400 MHz), ^1H NMR: $\delta = 7.85$ (m, 1H, H-2), 7.31 (m, 1H, H-5), 7.29 (m, 1H, H-4) ppm. ^{19}F NMR: $\delta = -56.19$ (t, $J = 21.74$ Hz, 3F, F-d'), -137.94 (m, 2F, F-c' and F-e') and -146.19 (m, 2F, F-b' and F-f') ppm.

5.2.8. 1-(5-Bromo-3,4,6-trifluorobenzotrifluoride)imidazole (8a) and 1-(6-Bromo-3,4,5-trifluorobenzotrifluoride)imidazole (8b):

A solution of imidazole (0.157 g) in THF was added to 0.508 g of 4-bromo-2,3,5,6-tetrafluorobenzotrifluoride, then this was heated at 80°C for 8 days. $\text{C}_{10}\text{H}_3\text{F}_6\text{N}_2\text{Br}$: 345.0415 $\text{g}\cdot\text{mol}^{-1}$. (60.83 % yield) MS: Calc. 346.9558. Found. 346.9389 m/z [$(M + \text{H})^+$]. In CDCl_3 (400 MHz), ^1H NMR: $\delta = 7.13$ (d, $J = 0.99$ Hz, 2H, H-2, in **a** and **b**), 7.01 (d, $J = 0.66$ Hz, 4H, H-4 & H-5, in **a** and **b**) ppm. ^{19}F NMR: $\delta = -55.47$ (m, 3F, F-b or F-e, in **a** or **b**), -56.18 (d, $J = 13.56$, $J = 12.44$ Hz, 3F, F-b or F-e, in **a** or **b**), -130.70 (m, 1F, F-f' in **a** or **b**), -130.91 (m, 2F, F-c' & F-d' in **a** or **b**), -144.59 (m, 1F, F-f' in **a** or **b**), -146.98 (m, 2F, F-c' & F-d' in **a** or **b**) ppm.

5.2.9. 1-(2,3,5,6-Tetrafluorobenzonitrile)-2-methylimidazole (9):

0.162 g of 2-methylimidazole was dissolved in 50 ml of THF then added to 0.375 g of pentafluorobenzonitrile, then left for three days at room temperature. $C_{11}H_5F_4N_3$: 255.1742 $g \cdot mol^{-1}$. (72.65 % yield). MS: Calc. 256.0498. Found. 256.0382 $m/z[(M + H)^+]$. In $CDCl_3$ (400 MHz), 1H NMR: $\delta = 7.18$ (d, $J = 1.58$ Hz, 1H, H-5), 6.98 (q, $J = 1.54$ Hz, $J = 1.21$ Hz, 1H, H-4), 2.36 (t, $J = 1.09$ Hz, 3H, H-2) ppm. ^{19}F NMR: $\delta = -192.94$ (m, 2F, F-c' and F-e') and -142.15 (m, 2F, F-b' and F-f') ppm.

5.2.10. 1-(2,3,5,6-Tetrafluoropyridyl)-2-methylimidazole (10):

0.270 g of 2-methylimidazole was dissolved in 50 ml of THF then added to 0.540 g of pentafluoropyridine, then the solution was left over night at RT. $C_9H_5F_4N_3$: 231.1522 $g \cdot mol^{-1}$. (95.24 % yield). MS: Calc. 232.0498. Found. 232.0513 $m/z[(M + H)^+]$. In $CDCl_3$ (400 MHz), 1H NMR: $\delta = 7.21$ (d, $J = 1.65$ Hz, 1H, H-5), 7.05 (q, $J = 1.32$ Hz, $J = 1.32$ Hz, 1H, H-4), 2.43 (t, $J = 1.21$ Hz, 3H, H-2) ppm. ^{19}F NMR: $\delta = -86.10$ (m, 2F, F-c' and F-e') and -146.10 (m, 2F, F-b' and F-f') ppm.

5.2.11. 1-(Heptafluorotolyl)-2-methylimidazole (11):

0.188 g of 2-methylimidazole was dissolved in THF, and then added to 0.540 g of octafluorotoluene, and then this mixture was left at RT for 2 days. $C_{11}H_5F_7N_2$:

298.1627 g.mol⁻¹. (76.44 % yield). MS: Calc. 299.0419. Found. 299.0258 m/z [(M + H)⁺]. In CDCl₃ (400 MHz), ¹H NMR: δ = 7.11 (d, J = 0.56 Hz, 1H, H-5), 6.95 (m, 1H, H-4) and 5.27 (t, J = 0.35 Hz, 0.43 Hz, 3H, H-2') ppm. ¹⁹F NMR: δ = -56.49 (t, J = 21.92 Hz, 3F, F-d'), -138.87 (m, 2F, F-c' and F-e') and -143.95 (m, 2F, F-b' and F-f') ppm.

5.2.12. 1-(4-Bromo-2,3,5,6-tetrafluorobenzyl)-2-methylimidazole (12):

1.65 g of 2-methylimidazole was dissolved in 10 ml of THF and 20 ml of DMSO then added to 4.95 g of bromopentafluorobenzene, then the solution was heated at 80°C for 8 days. C₁₀H₅F₄N₂Br: 309.0605 g.mol⁻¹. (30 % yield). MS: Calc. 308.9650. Found. 308.9621 m/z [(M + H)⁺]. In CDCl₃ (400 MHz), ¹H NMR: δ = 7.13 (d, J = 1.54 Hz, 1H, H-5), 6.95 (q, J = 0.66 Hz, J' = 0.88 Hz, 1H, H-4) and 2.62 (s, J = 6.99 Hz, 3H, H-2') ppm. ¹⁹F NMR: δ = -130.70 (m, 2F, F-c' and F-e') and -144.58 (m, 2F, F-b' and F-f') ppm. ¹³C NMR: δ = 145.77 (s, J = 23.85 Hz, 1C, C-2), 145.27 (dm, J = 249.53 Hz, 2C, C-b & C-f), 142.82 (dm, J = 254.27 Hz, C-c & C-e), 129.10 (s, J = 16.28 Hz, 1C, C-5), 120.64 (s, J = 29.24 Hz, 1C, C-4), 116.70 (m, 1C, C-a), 101.38 (t, J = 22.41 Hz, 1C, C-d) and 12.81 (s, J = 22.61 Hz, 1C, C-2') ppm. The HSQC spectrum shows that H-2' correlates with C-2', H-4 correlates with C-4, H-5 correlates with C-5 (Fig. 34, chapter two). The HMBC spectrum shows that H-2' correlates with C-2' and C-2 and H-4 correlates with C-2, C-4, C-5 and H-5 correlates with C-2, C-4 and C-5 (Fig. 35, chapter two). IR (KBr): 3437, 1587, 1493, 1395, 1319, 1300, 1209, 1165, 1132, 1082, 1021, 973, 850, 792, 733, 686, 663, 630, 614, 470 and 441 cm⁻¹.

5.2.13. 1-(2,3,5,6-Tetrafluorobenzonitrile)-4-methylimidazole (13):

0.157 g of 4-methylimidazole was dissolved in 50 ml of THF then added to 0.370 g of pentafluorobenzonitrile, then left for 24 hrs at room temperature. $C_{11}H_5F_4N_3$: 255.1742 g.mol⁻¹. (100 % yield). MS: Calc. 256.0498. Found. 256.0400 m/z [(M + H)⁺]. In CDCl₃ (400 MHz), ¹H NMR: δ = 7.77 (m, 1H, H-2), 6.99 (m, 1H, H-5), 2.19 (m, 3H, H-4') ppm. ¹⁹F NMR: δ = -130.95 (m, 2F, F-c' and F-e') and -145.36 (m, 2F, F-b' and F-f') ppm.

5.2.14. 1-(2,3,5,6-Tetrafluoropyridyl)-4-methylimidazole (14):

0.307 g of 4-methylimidazole was dissolved in THF then added to 0.576 g of pentafluoropyridine, then the solution was left a week at RT. $C_9H_5F_4N_3$: 231.1522 g.mol⁻¹. (102 % yield) MS: Calc. 232.0498. Found. 232.0506 m/z [(M + H)⁺]. In CDCl₃ (400 MHz), ¹H NMR: δ = 7.96 (d, J = 0.77 Hz, J' = 0.88 Hz, 1H, H-2), 7.14 (m, 1H, H-5) and 2.36 (d, 0.54 Hz, 3H, H-4') ppm. ¹⁹F NMR: δ = -87.06 (m, 2F, F-c' and F-e') and -149.30 (m, 2F, F-b' and F-f') ppm. IR (KBr): 3436, 1631, 1527, 1481, 1392, 1264, 1150, 1084, 971, 744, 657, 625, and 483 cm⁻¹.

5.2.15. 1-(Heptafluorotolyl)-4-methylimidazole (15):

To 0.576 g of octafluorotoluene, 0.200 g of 4-methylimidazole in 50 ml of THF has been added, and then it was left at RT for 48 hrs. $C_{11}H_5F_7N_2$: 298.1627

$\text{g}\cdot\text{mol}^{-1}$. (75.67 % yield). MS: Calc. 299.0419. found. 299.0316 m/z [$(M + H)^+$]. In CDCl_3 and DMSO (400 MHz), ^1H NMR: $\delta = 7.75$ (q, $J = 0.82$ Hz, $J' = 1.88$ Hz, 1H, H-2), 6.99 (m, 1H, H-5) and 2.32 (d, $J = 0.55$ Hz, 3H, H-4') ppm. ^{19}F NMR: $\delta = -56.21$ (t, $J = 21.72$ Hz, 3F, F-d'), -138.34 (m, 2F, F-c' and F-e') and -146.48 (m, 2F, F-b' and F-f') ppm.

5.2.16. 1-(4-Bromo-2,3,5,6-tetrafluorobenzyl)-4-methylimidazole (16):

1.65 g of 4-methylimidazole was dissolved in 10 ml of THF and 20 ml of DMSO then added to 4.95 g of bromopentafluorobenzene, and then the solution was heated at 80°C for 4 days. $\text{C}_{10}\text{H}_5\text{F}_4\text{N}_2\text{Br}$: 309.0605 $\text{g}\cdot\text{mol}^{-1}$. (42 % yield). MS: Calc. 308,9650. Found. 308.9555 m/z [$(M + H)^+$]. In CDCl_3 (400 MHz), ^1H NMR: $\delta = 7.72$ (m, 1H, H-2), 6.94 (m, 1H, H-5) and 2.63 (s, $J = 3.16$ Hz, 3H, H-4') ppm. ^{19}F NMR: $\delta = -130.836$ (m, 2F, F-c' and F-e') and -146.937 (m, 2F, F-b' and F-f') ppm. IR (KBr): 3434, 3118, 2930, 1638, 1519, 1494, 1448, 1376, 1303, 1289, 1253, 1233, 1212, 1150, 1031, 1004, 974, 831, 792, 742, 661, 633, 608 and 423 cm^{-1} .

5.2.17. 1-(2,3,5,6-Tetrafluorobenzyl)-4-methylimidazole (17):

1.75 g of pentafluorobenzene was added to a solution of 4-methylimidazole (0.867g) and KOH (0.638 g) in 5 ml of DMSO, and then the mixture was heated at 55°C for 3 hrs. $\text{C}_{10}\text{H}_6\text{F}_4\text{N}_2$: 230.1644 $\text{g}\cdot\text{mol}^{-1}$. (29.46 % yield). MS: Calc. 231.0545. Found. 231.0486 m/z [$(M + H)^+$]. In CDCl_3 (400 MHz), ^1H NMR: $\delta =$

7.66 (m, 1H, H-2, in **a** or **b**), 7.49 (d, $J = 0.39$ Hz, 1H, H-2, in **a** or **b**), 7.26 (m, 1H, H-5, in **a** or **b**), 7.14 (m, 1H, H-5, in **a** or **b**), 6.97 (t, $J = 1.00$ Hz, 1H, H-d' or H-f', in **a** or **b**), 6.92 (m, 1H, H-d' or H-f', in **a** or **b**), 2.60 (s, $J = 6.36$ Hz, 3H, H-4', in **a** or **b**), 2.30 (d, $J = 0.44$ Hz, 3H, H-4', in **a** or **b**) ppm. ^{19}F NMR: $\delta = -131.08$ (m, 1F, F-e', in **b**), -136.75 (m, 1F, F-d', in **b**), -136.93 (m, 2F, F-c' & F-e', in **a**), -146.28 (m, 1F, F-c', in **b**), -147.05 (m, 1F, F-b', in **b**) and -148.60 (m, 2F, F-b' & F-f', in **a**) ppm.

5.2.18. 1-(4-Iodo-2,3,5,6-tetrafluorobenzyl)-4-methylimidazole (**18**):

A solution of iodopentafluorobenzene (2.98 g) in 10 ml of THF was added to a solution of 4-methylimidazole (0.863 g) in 10 ml of DMSO, and then the mixture was heated for 45 hrs at 80°C. $\text{C}_{10}\text{H}_5\text{F}_4\text{N}_2\text{I}$: $356.061 \text{ g}\cdot\text{mol}^{-1}$. (92.50 % yield). MS: Calc. 356.9512. Found. 356.9573 m/z [$(M + H)^+$]. In CDCl_3 (400 MHz), ^1H NMR: $\delta = 7.68$ (m, 1H, H-2), 6.93 (m, 1H, H-5), 2.32 (d, $J = 0.99$ Hz, 3H, H-4') ppm. ^{19}F NMR: $\delta = -114.53$ (m, 2F, F-c' and F-e') and -142.37 (q, $J = 13.67$ Hz, $J' = 8.65$ Hz, 2F, F-b' and F-f') ppm. ^{13}C NMR: $\delta = 147.54$ (dm, $J = 244.03$ Hz, 2C, C-b & C-f), 140.58 (dm, $J = 254.88$ Hz, 2C, C-c & C-e), 138.68 (s, $J = 28.32$ Hz, 1C, C-2), 136.87 (s, $J = 34.24$ Hz, 1C, C-5), 117.22 (t, $J = 13.90$ Hz, 1C, C-a), 116.38 (s, $J = 30.68$ Hz, 1C, C-4), 73.57 (t, $J = 28.62$ Hz, 1C, C-d) and 13.38 (s, $J = 16.60$ Hz, 1C, C-4') ppm. The HSQC spectrum shows that H-4' correlates with C-4', H-2 correlates with C-2, H-5 correlates with C-5 (Fig. 36, chapter two). The HMBC spectrum shows that H-4' correlates with C-4', C-4 and C-2, H-2 correlates with C-2, C-4 and C-5, H-5 correlates with C-2, C-4 and C-5 (Fig. 37, chapter two). IR (KBr): 1636, 1578, 1484, 1309, 1248, 1227,

1211, 1146, 1081, 1034, 1004, 967, 866, 821, 804, 775, 748, 649, 628, 611 and 428 cm^{-1} .

5.2.19. 1-(2,3,5,6-Tetrafluorobenzonitrile)-2-phenylimidazole (19):

0.372 g of 2-phenylimidazole was dissolved in 50 ml of THF then added to 0.506 g of pentafluorobenzonitrile and then the solution was heated at 60°C for 92 hrs. $\text{C}_{16}\text{H}_7\text{F}_4\text{N}_3$: 317.245 $\text{g}\cdot\text{mol}^{-1}$. (61.24 % yield). MS: Calc. 318.0654. Found. 318.0641 m/z [$M + \text{H}$]⁺. In CDCl_3 (400 MHz), ^1H NMR: $\delta = 7.91$ (m, 1H, H-5), 7.41 (m, 1H, H-4) and 7.24 (dd, $J = 39.85$ Hz, $J' = 6.98$ Hz, 5H, H-ph) ppm. ^{19}F NMR: $\delta = -129.85$ (m, 2F, F-c' and F-e') and -141.97 (m, 2F, F-b' and F-f') ppm. IR (KBr): 1505, 1462, 1417, 1106, 948, 769, 738, 705, and 684 cm^{-1} .

5.2.20. 1-(2,3,5,6-Tetrafluorobenzaldehyde)-2-phenylimidazole (20):

0.322 g of 2-phenylimidazole and 0.433 g of pentafluorobenzaldehyde were dissolved in 60 ml of THF, then heated for 167 hrs, with the temperature increasing gradually from 85°C to 142°C. $\text{C}_{16}\text{H}_8\text{F}_4\text{N}_2\text{O}$: 320.2456 $\text{g}\cdot\text{mol}^{-1}$. (82.61 % yield). MS: Calc. 321.0651. Found. 321.0721 m/z [$M + \text{H}$]⁺. In CDCl_3 (400 MHz), ^1H NMR: $\delta = 7.88$ (m, 1H, H-d'), 7.41 (m, 1H, H-5), 7.17 (m, 1H, H-4) and 6.99 (d, $J = 0.54$ Hz, 5H, H-ph) ppm. ^{19}F NMR; $\delta = -143.15$ (m, 2F, F-c' and F-e') and -144.18 (m, 2F, F-b' and F-f') ppm.

5.2.21. 1-(2,3,5,6-Tetrafluoropyridyl)-2-phenylimidazole (21):

0.445 g of 2-phenylimidazole was dissolved in 50 ml of THF then added to 0.516 g of pentafluoropyridine, and then it was left two days at RT. $C_{14}H_7F_4N_3$: 293.223 $g \cdot mol^{-1}$. (49.85 % yield). MS: Calc. 294.0654. Found. 294.0663 $m/z [(M + H)^+]$. IR (KBr): 3053, 2992, 2828, 1570, 1505, 1462, 1416, 1397, 1302, 1185, 1137, 1106, 948, 913, 769, 738, 684 and 444 cm^{-1} . In $CDCl_3$ and DMSO (400 MHz), 1H NMR: $\delta = 7.87$ (m, 1H, H-5), 7.41 (m, 1H, H-4), 7.17 (s, $J = 7.63$ Hz, 5H, H-ph) ppm. ^{19}F NMR: $\delta = -86.27$ (m, 2F, F-c' and F-e') and -145.88 (m, 2F, F-b' and F-f') ppm.

5.3. Pyrazole:

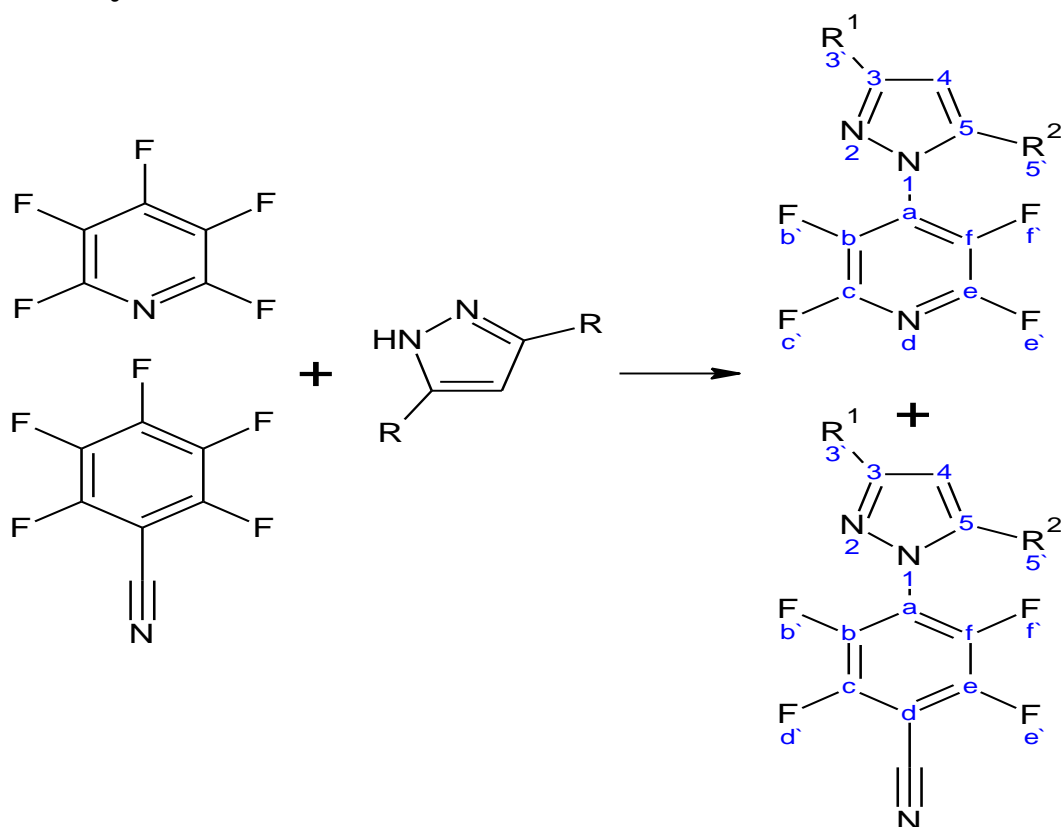


Figure 62: The general reaction of polyfluoroaryl and pyrazole and their derivatives (with the labels that have been used to represent the NMR data, R^1 , R^2 = H, CH_3).

5.3.1. 1-(2,3,5,6-Tetrafluorobenzonitrile)pyrazole (22):

0.129 g of pyrazole was dissolved in THF then added to 0.370 g of pentafluorobenzonitrile, and then the solution was heated for 93 hrs, with increase the temperature gradually from 95°C to 140°C. $C_{10}H_3F_4N_3$: 241.1474 $g \cdot mol^{-1}$. (33.51 % yield). MS: Calc. 242.0341. Found. 242.1665 $m/z [(M + H)^+]$. In $CDCl_3$ and DMSO (400 MHz), 1H NMR: $\delta = 7.92$ (m, 1H, H-5), 7.83 (m, 1H, H-3) and 6.62 (m, 1H, H-4) ppm. ^{19}F NMR: $\delta = -130.86$ (m, 2F, F-c` and F-e`) and -144.63 (m, 2F, F-b` and F-f`) ppm. Crystals were obtained by the slow evaporation of 1-(2,3,5,6-tetrafluorobenzonitrile)pyrazole in methanol, but the purity of these crystals was not enough to be analyzed by ^{13}C NMR and XRD.

5.3.2. 1-(2,3,5,6-Tetrafluorobenzonitrile)-3,5-dimethylpyrazole (23):

0.233 g of 3,5-dimethylpyrazole was dissolved in THF, then added to 0.473 g of pentafluorobenzonitrile, and then the solution was heated at 85°C for 28 hrs. $C_{12}H_7F_4N_3$: 269.201 $g \cdot mol^{-1}$. (110 % yield). MS: Calc. 270.0654. Found. 270.0639 $m/z [(M + H)^+]$. In $CDCl_3$ and DMSO (400 MHz), 1H NMR: $\delta = 6.11$ (m, 1H, H-4), 2.32 (m, 3H, H-5`) and 2.23 (m, 3H, H-3`) ppm. ^{19}F NMR: $\delta = -131.20$ (m, 2F, F-c` and F-e`) and -141.95 (m, 2F, F-b` and F-f`) ppm.

5.3.3. 1-(2,3,5,6-Tetrafluoropyridyl)-3,5-dimethylpyrazole (24):

0.354 g of 3,5-dimethylpyrazole was dissolved in 50 ml of THF then added to 0.570 g of pentafluoropyridine, then the solution was left for 17 days at RT. $C_{10}H_7F_4N_3$: 245.179 g.mol⁻¹. (62.80 % yield). MS: Calc. 246.0654. Found. 246.0661 m/z [(M + H)⁺]. In CDCl₃ (400 MHz), ¹H NMR: δ = 6.13 (s, J = 14.44 Hz, 1H, H-4), 2.33 (s, J = 9.70 Hz, 3H, H-5') and 2.27 (d, J = 0.90 Hz, 3H, H-3') ppm. ¹⁹F NMR: δ = -87.78 (m, 2F, F-c' and F-e') and -146.03 (m, 2F, F-b' and F-f) ppm.

5.3.4. Attempt to synthesize 1-(2,3,5,6-Tetrafluoropyridyl)pyrazole (25):

0.213 g of pyrazole was dissolved in THF then added to 0.563 g of pentafluoropyridine, and then the solution was left for a week at RT.

5.4. Imidazolium Salts:

5.4.1. 1-(4-Bromo-2,3,5,6-tetrafluorobenzyl)-3-benzyl-4-methylimidazolium bromide (**26**):

To 0.545 g of 1-(4-bromo-2,3,5,6-tetrafluorobenzyl)-4-methylimidazole (**16**) in CH₂Cl₂ was added 0.322 g of benzyl bromide has been added, and then this was left for two days at RT. C₁₇H₁₂F₄N₂Br₂: 480.0968 g.mol⁻¹. (93.26 % yield). MS: Calc. 400.0198 Found. 400.0157 m/z [(M - Br)⁺]. In CDCl₃ and DMSO (400 MHz), ¹H NMR: δ = 9.77 (s, J = 11.13 Hz, 1H, H-2), 7.97 (s, J = 12.37 Hz, 1H, H-5), 7.43 (m, 5H, H-3c,3d,3e,3f,3g), 5.61 (s, J = 10.31 Hz, 2H, H-3a) and 3.35 (s, J = 9.25 Hz, 3H, H-4') ppm. ¹⁹F NMR: δ = -132.25 (m, 2F, F-c' and F-e') and -145.58 (m, 2F, F-b' and F-f') ppm. IR (KBr): 3884, 3436, 3125, 3089, 3025, 2969, 2940, 2825, 2405, 2307, 1904, 1877, 1809, 1770, 1622, 1613, 1568, 1502, 1454, 1445, 1426, 1392, 1369, 1349, 1329, 1307, 1264, 1247, 1209, 1196, 1165, 1148, 1075, 1047, 1024, 1002, 978, 877, 804, 769, 755, 726, 697, 677, 630, 618, 571, 472, 426, 449, 429 and 419 cm⁻¹. Crystallographic data for **26** has been shown in table 9.

Crystallographic data for 1-(1-bromo-2,3,5,6-tetrafluorophenyl)-4-methylbenzimidazolium bromide

| | |
|---|--|
| Formula | C ₁₇ H ₁₂ Br ₂ F ₄ N ₂ |
| Formula weight | 480.11 |
| Crystal system | monoclinic |
| Space group | <i>I</i> 2/a |
| <i>a</i> , Å | 23.6805(3) |
| <i>b</i> , Å | 7.13235(7) |
| <i>c</i> , Å | 21.0790(2) |
| <i>B</i> , ° | 103.6307(11) |
| <i>V</i> , Å ³ | 3459.92(6) |
| <i>Z</i> | 8 |
| <i>D</i> _c (g cm ⁻³) | 1.843 |
| <i>μ</i> (mm ⁻¹) | 6.353 |
| <i>θ</i> range (°) | 3.84 → 73.57 |
| Total reflections | 17663 |
| Unique reflections (<i>R</i> _{int}) | 3447(0.0515) |
| Observed reflections [<i>I</i> > 2σ(<i>I</i>)] | 3419 |
| Parameters | 226 |
| Final <i>R</i> indices [<i>I</i> > 2σ(<i>I</i>)] | <i>R</i> ₁ 0.0372, <i>wR</i> ₂ = 0.0376 |
| <i>R</i> indices (all data) | <i>R</i> ₁ = 0.1025, <i>wR</i> ₂ = 0.1029 |
| Weighting scheme | $w = 1/[\sigma^2(F_o)^2 + \{0.0607 (F_o^2 + 2F_c^2)/3\}^2 + 11.1404 (F_o^2 + 2F_c^2)/3]$ |
| Max., min. Δρ (eÅ ⁻³) | 0.829, -1.327 |
| Goodness of fit on <i>F</i> ² | 1.550 |

Table 9: Estimated standard deviations are given in parentheses. Data were collected at 100(2) K with graphite monochromated copper radiation ($\lambda = 1.54184$ Å).

5.4.2. 1-(2,3,5,6-Tetrafluorobenzonitrile)-3-benzyl-4-methylimidazolium bromide (27):

To 0.200 g of benzyl bromide was added 0.100 g of 1-(2,3,5,6-tetrafluorobenzonitrile)-4-methylimidazole (**13**) in 50 ml of CH₂Cl₂, and then it was left at RT for 48 hrs. C₁₈H₁₂F₄N₃Br: 426.2105 g.mol⁻¹. (113 % yield). MS: Calc. 346.0967. Found. 346.1087 m/z [(M - Br)⁺]. In CDCl₃ (400 MHz), ¹H NMR: δ = 7.35 (m, 7H, H-2,5,3c,3d,3e,3f,3g), 5.73 (s, J = 80.12 Hz, 2H, H-3a) and 2.12 (s, J = 5.40 Hz, 3H, H-4') ppm. ¹⁹F NMR: δ = -127.82 (q, J = 6.77 Hz, J' = 4.44 Hz, 2F, F-c' and F-e') and -141.98 (m, 2F, F-b' and F-f') ppm.

5.4.3. 1-(2,3,6-Trifluorobenzonitrile)-3-benzyl-imidazolium bromide (28):

0.065 g of 1-(2,3,6-trifluorobenzonitrile)imidazole (**1**) was dissolved in CH₂Cl₂ 0.0693 g of benzyl bromide was added and this mixture was left for two days at RT. C₁₇H₁₁F₃N₃Br: 394.1932 g.mol⁻¹. (97.55 % yield). MS: Calc. 314.0905, Found. 314.0765 m/z [(M - Br)⁺]. In CDCl₃ and DMSO (400 MHz), ¹H NMR: δ = 9.93 (s, J = 12.40 Hz, 1H, H-2), 8.20 (m, 2H, H-4,5), 7.47 (m, 7H, H-f',3c,3d,3e,3f,3g) and 5.62 (s, J' = 9.80 Hz, 2H, H-3a) ppm. ¹⁹F NMR: δ = -122.03 (d, J = 4.57Hz, J' = 9.20 Hz, 1F, F-f'), -133.35 (m, 1F, F-c') and -137.76 (d, J = 10.30 Hz, 1F, F-b') ppm.

5.4.4. 1-(2,3,5,6-Tetrafluoropyridyl)-3-benzyl-2-methylimidazolium bromide

(29):

0.267 g of benzyl bromide has been added to 0.314 g of 1-(2,3,5,6-tetrafluoropyridyl)-2-methylimidazole (**10**) in CH₂Cl₂, which was left for 48 hrs. at RT. C₁₆H₁₂F₄N₃Br: 402.1885 g.mol⁻¹. (92.07 % yield). MS: Calc. 322.0967 Found. 322.0968 m/z [(M - Br)⁺]. In CDCl₃ and DMSO (400 MHz), ¹H NMR: δ = 8.06 (m, 2H, H-4,5), 7.45 (m, 5H, H-3c,3d,3e,3f,3g), 5.56 (s, J = 9.10 Hz, 2H, H-3a) and 3.35 (s, J = 10.47 Hz, 3H, H-2') ppm. ¹⁹F NMR: δ = -88.11 (m, 2F, F-b' & F-f') and -144.24 (m, 2F, F-c' & F-e') ppm.

5.4.5. 1-(4-Bromo-2,3,5,6-tetrafluorobenzyl)-3-benzyl-2-methylimidazolium bromide (30):

0.221 g of benzyl bromide was added to a solution of 0.353 g of 1-(4-bromo-2,3,5,6-tetrafluorobenzene)-2-methylimidazole (**12**) in CH₂Cl₂, which was left for 48 hr, at RT. C₁₇H₁₂F₄ N₂Br₂: 480.0968 g.mol⁻¹. (112 % yield). MS: Calc. 400.0198. Found. 400.0144 m/z [(M - Br)⁺]. In CDCl₃ and DMSO (400 MHz), ¹H NMR: δ = 8.07 (s, J = 2.53 Hz, 2H, H-4,5), 7.45 (m, 5H, H-3c,3d,3e,3f,3g), 5.58 (s, J = 8.40 Hz, 2H, H-3a), 3.44 (s, J = 42.82 Hz, 3H, H-2') ppm. ¹⁹F NMR: δ = -132.39 (m, 2F, F-c' & F-e') and -145.25 (q, J = 16.00 Hz, J' = 8.00 Hz, 2F, F-b' & F-f') ppm. IR (KBr): 3446, 3185, 3166, 3120, 3070, 3033, 2951, 1697, 1640, 1581, 1534, 1511, 1496, 1428, 1395, 1375, 1334, 1319, 1300, 1261, 1244, 1227, 1209, 1197, 1165, 1147, 1132, 1098, 1082, 1041, 1031, 1021, 975, 917, 850, 838, 793, 760, 748, 734, 723, 702, 695, 688, 650, 621, 613, 547, 472, 451, 442 and 413 cm⁻¹.

5.4.6. 1-(Heptafluorotolyl)-3-benzylimidazolium bromide (31):

A solution of 0.135 g of 1-(heptafluorotolyl)imidazole (**7**) and 0.152 g of benzyl bromide in CH₂Cl₂ was left for two days at RT. C₁₇H₁₀F₇N₂Br: 455.1722 g.mol⁻¹. (98.84 % yield). MS: Calc. 375.0732, Found. 375.0558 m/z [(M - Br)⁺]. In CDCl₃ and DMSO (400 MHz), ¹H NMR: δ = 10.07 (s, J = 11.14 Hz, 1H, H-2), 8.20 (m, 1H, H-5), 7.53 (m, 1H, H-4), 7.38 (m, 5H, H-3c,3d,3e,3f,3g), 5.67 (s, J = 7.75 Hz, 2H, H-3a) ppm. ¹⁹F NMR: δ = -55.93 (t, J = 21.75 Hz, 3F, F-d'), -139.49 (m, 2F, F-c' and F-e') and -143.82 (m, 2F, F-b' and F-f') ppm.

5.4.7. 1-(Heptafluorotolyl)-3-benzyl-4-methylimidazolium bromide (32):

To a solution of (0.516 g) 1-(heptafluorotolyl)-4-methylimidazole (**15**) in CH₂Cl₂, 0.307 g of benzyl bromide was added, and then this mixture was left for two days at RT. C₁₈H₁₂F₇N₂Br: 469.199 g.mol⁻¹. (97.40 % yield). MS: Calc. 389.0889. Found. 389.0722 m/z [(M - Br)⁺]. In CDCl₃ and DMSO (400 MHz), ¹H NMR; δ = 11.27 (s, J = 13.67 Hz, H, H-2), 7.56 (s, J = 11.51 Hz, H, H-5), 7.24 (m, 5H, H-3c,3d,3e,3f,3g), 5.84 (s, J = 10.18 Hz, 2H, H-3a), 2.37 (d, J = 0.54 Hz, H, H-4') ppm. ¹⁹F NMR: δ = -56.44 (m, 3F, F-d'), -136.13 (m, 2F, F-c' and F-e') and -143.55 (m, 2F, F-b' and F-f') ppm.

5.4.8. 1-(2,3,5,6-Tetrafluoropyridyl)-3,4-dimethylimidazolium iodide (33):

0.193 g of iodomethane in 50 ml of CH₂Cl₂ was added to (0.196 g) of 1-(2,3,5,6-tetrafluoropyridyl)-4-methylimidazole (**14**) and then the mixture has been left for

two days at RT. $C_{10}H_8F_4N_3I$: $373.0914 \text{ g}\cdot\text{mol}^{-1}$. (51.19 % yield). MS: Calc. 246.0654. Found. 246.0711 m/z [$(M - I)^+$]. In DMSO (400 MHz), 1H NMR: $\delta = 7.95$ (m, 1H, H-2), 7.14 (s, $J = 18.62$ Hz, 1H, H-5), 5.31 (s, $J = 6.70$ Hz, 3H, H-3') and 2.35 (d, $J = 0.49$ Hz, 3H, H-4') ppm, ^{19}F NMR: -86.96 (m, 2F, F-c' and F-e') and -149.26 (m, 2F, F-b' and F-f') ppm.

5.4.9. 1-(2,3,5,6-Tetrafluoropyridyl)-3-benzyl-4-methylimidazolium bromide (34):

A solution of 0.775 g of 1-(2,3,5,6-tetrafluoropyridyl)-4-methylimidazole (**14**) and 0.636 g of benzyl bromide in CH_2Cl_2 was left for two days at RT. $C_{16}H_{12}F_4N_3Br$: $402.1885 \text{ g}\cdot\text{mol}^{-1}$. (48.55 % yield). MS: Calc. 322.0967. Found. 322.0490 m/z [$(M - Br)^+$]. In $CDCl_3$ and DMSO (400 MHz), 1H NMR: $\delta = 9.99$ (s, $J = 20.06$ Hz, 1H, H-2), 8.08 (m, 1H, H-5), 7.45 (m, 5H, H-3c,3d,3e,3f,3g), 5.68 (s, $J = 14.01$ Hz, 2H, H-3a) and 3.35 (s, $J = 13.39$ Hz, 3H, H-4') ppm. ^{19}F NMR: $\delta = -88.79$ (m, 2F, F-c' and F-e') and -146.87 (m, 2F, F-b' and F-f') ppm. IR (KBr): 3886, 3436, 3121, 3087, 3067, 3024, 2930, 2825, 2775, 2524, 2396, 2014, 1910, 1839, 1770, 1654, 1625, 1614, 1572, 1498, 1480, 1454, 1442, 1432, 1420, 1404, 1387, 1368, 1342, 1327, 1263, 1250, 1210, 1199, 1166, 1155, 1133, 1084, 1036, 1006, 969, 932, 890, 844, 825, 815, 786, 778, 729, 705, 693, 667, 632, 610, 571, 524, 470 and 460 cm^{-1} . Crystallographic data for **34** has been shown in table 10.

Crystallographic data for 1-(2,3,5,6-tetrafluoropyridyl)-3-benzyl-4-methylimidazolium bromide.

| | |
|---|---|
| Formula | C ₁₆ H ₁₂ Br ₂ F ₄ N ₃ |
| Formula weight | 402.20 |
| Crystal system | monoclinic |
| Space group | <i>P</i> 2 ₁ / <i>c</i> |
| <i>a</i> , Å | 7.9987(4) |
| <i>b</i> , Å | 16.4596(9) |
| <i>c</i> , Å | 12.9003(7) |
| <i>B</i> , ° | 106.104(2) |
| <i>V</i> , Å ³ | 1631.75(15) |
| <i>Z</i> | 4 |
| <i>D</i> _c (g cm ⁻³) | 1.637 |
| Crystal size (mm ³) | 0.25 × 0.12 × 0.12 |
| <i>μ</i> (mm ⁻¹) | 2.563 |
| <i>θ</i> range (°) | 2.06 → 27.99 |
| Total reflections | 21297 |
| Unique reflections (<i>R</i> _{int}) | 3936(0.0590) |
| Observed reflections [<i>I</i> > 2σ(<i>I</i>)] | 2957 |
| Parameters | 217 |
| Final <i>R</i> indices [<i>I</i> > 2σ(<i>I</i>)] | <i>R</i> ₁ 0.0363, <i>wR</i> ₂ = 0.0847 |
| <i>R</i> indices (all data) | <i>R</i> ₁ = 0.0576, <i>wR</i> ₂ = 0.0918 |
| Weighting scheme | $w = 1/[\sigma^2(F_o)^2 + \{0.0403(F_o^2 + 2F_c^2)/3\}^2 + 0.9492(F_o^2 + 2F_c^2)/3]$ |
| Max., min. Δρ (eÅ ⁻³) | 0.631, -0.593 |
| Goodness of fit on <i>F</i> ² | 1.029 |

Table 10: Estimated standard deviations are given in parentheses. Data were collected at 89(2) K with graphite monochromated radiation ($\lambda = 0.71073$ Å).

5.5. Benzimidazole:

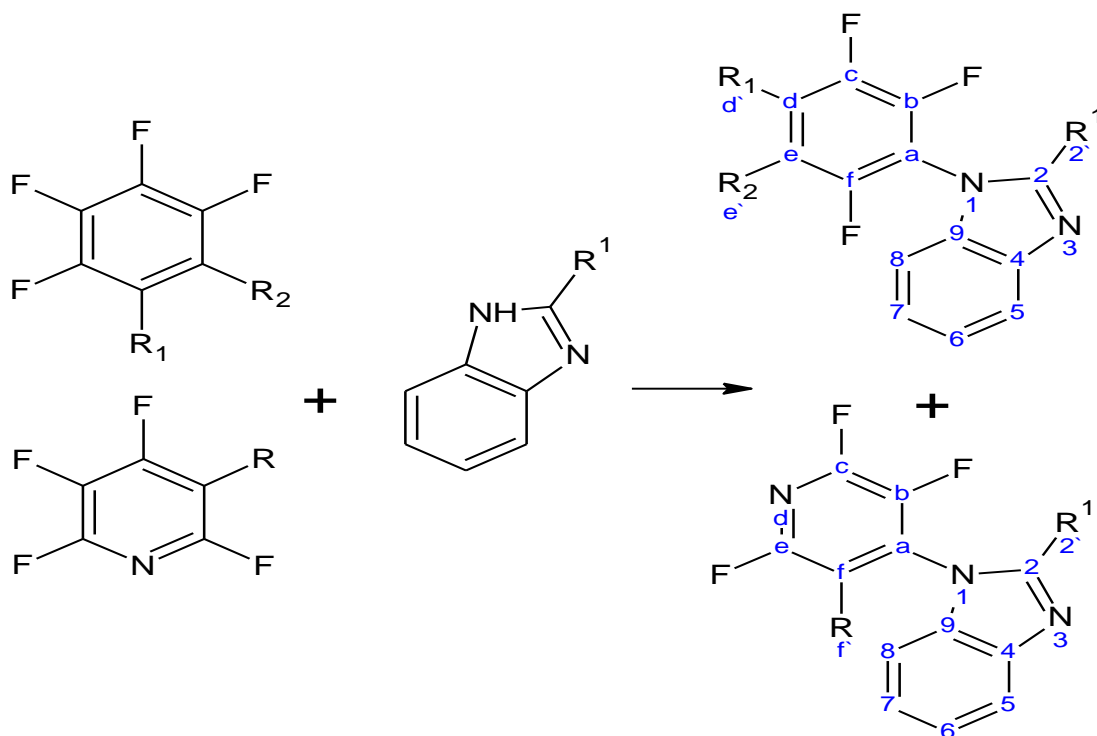


Figure 63: The general reaction of polyfluoroarene and benzimidazole derivatives (with the labels that have been used to represent the NMR data), ($R_1 = F, CF_3, CN, CHO$), $R_2 = F, CN$, $R = F, Cl$ and $R^1 = H, CH_3$).

5.5.1. 1-(2,3,6-Trifluorophthalonitrile)benzimidazole (35):

0.155 g of benzimidazole was dissolved in about 60 ml of THF, and this solution was added to 0.198 g of tetrafluorophthalonitrile, then mixture was left for two days at room temperature. $C_{15}H_5F_3N_4$; 298.2265 $g \cdot mol^{-1}$. (165.5 % yield). MS: Calc. 299.0545. Found. 299.0401 $m/z [(M + H)^+]$. In $CDCl_3$ and DMSO (400 MHz), ^{19}F NMR: $\delta = -109.66$ (m, 1F, F-c'), -125.30 (m, 1F, F-b') and -140.23 (m, 1F, F-f) ppm. 1H NMR spectra show a mixture of the expected product and unidentified compounds.

5.5.2. 1-(2,3,5,6-Tetrafluorobenzaldehyde)benzimidazole (36):

0.339 g of benzimidazole was dissolved in 70 ml of THF then added to 0.580 g of pentafluorobenzaldehyde, and then the solution was left for two days. $C_{14}H_6F_4N_2O$: 294.2078 g.mol⁻¹. (50.00 % yield). MS: Calc. 295.0495. Found. 295.0382 m/z [(M + H)⁺]. In CDCl₃ (400 MHz), ¹⁹F NMR: δ = -142.92 (q, J = 4.55 Hz, J' = 10.80 Hz, 2F, F-c' and F-e') and -144.28 (q, J = 4.58 Hz, J' = 11.44 Hz, 2F, F-b' and F-f') ppm. ¹H NMR: δ = 8.23 (s, J = 24.59 Hz, 1H, H-d'), 7.76 (m, 1H, H-2) and 7.31 (m, 4H, H-5, 6, 7 & 8) ppm. IR (KBr): 3133, 1706, 1651, 1610, 1521, 1492, 1454, 1405, 1341, 1306, 1266, 1213, 1158, 1131, 1106, 1067, 1012, 970, 942, 890, 826, 798, 769, 753, 668, 619, 480 and 432 cm⁻¹.

5.5.3. 1-(6-Chloro-2,3,5-trifluoropyridyl)benzimidazole (37):

0.172 g of benzimidazole was dissolved in 50 ml of THF then added to 0.295 g of 3-chloro-2,4,5,6-tetrafluoropyridine, then the solution was left for 48 hrs at room temperature. $C_{12}H_5F_3N_3Cl$: 283.6398 g.mol⁻¹. (48.45% yield). MS: Calc. 284.0202. Found. 284.0091 m/z [(M + H)⁺]. CDCl₃ and DMSO (400 MHz), ¹H NMR: δ = 8.24 (s, J = 13.00 Hz, 1H, H-2), 7.96 (m, 1H, H-8), 7.46 (m, 2H, H-6 and H-7) and 7.24 (m, 1H, H-5) ppm. ¹⁹F NMR: δ = -69.01 (q, J = 14.83, J' = 12.62 Hz, 1F, F-c'), -84.17 (q, J = 8.03, J' = 12.59 Hz, 1F, F-e') and -145.50 (q, J = 6.88, J' = 20.58 Hz, 1F, F-b') ppm. IR (KBr): 3071, 1623, 1609, 1492, 1454, 1443, 1407, 1350, 1324, 1303, 1282, 1259, 1234, 1180, 1153, 1085, 1071, 1010,

939, 895, 887, 831, 782, 764, 747, 674, 640, 624, 575, 549, 505, 470 and 429 cm^{-1} .

5.5.4. 1-(2,3,5,6-Tetrafluoropyridyl)benzimidazole (38):

0.419 g of benzimidazole was dissolved in 50 ml of THF then added to 0.578 g of penatfluoropyridine, and then it was left two days at RT. $\text{C}_{12}\text{H}_5\text{F}_4\text{N}_3$: 267.1852 $\text{g}\cdot\text{mol}^{-1}$. (75.12% yield). MS: Calc. 268.0498. Found. 268.0520 m/z [$(M + H)^+$]. In CDCl_3 (400 MHz), ^1H NMR: δ = 8.13 (t, J = 1.98 Hz, 1H, H-2), 7.94 (m, 1H, H-8), 7.46 (m, 2H, H-6 and H-7), 7.34 (m, 1H, H-5). ^{19}F NMR: δ = -86.16 (m, 2F, F-c' and F-e') and -145.80 (m, 2F, F-b' and F-f') ppm. ^{13}C NMR: 144.33 (dm, J = 247.18 Hz, 3C, C-b, C-f & C-2), 141.34 (m, 1C, C-2), 136.77 (dm, J = 268.36 Hz, 2C, C-c & C-e), 132.22 (s, J = 15.87 Hz, 1C, C-9), 127.16 (m, 1C, C-a), 125.18 (s, J = 21.60 Hz, 1C, C-7), 124.35 (s, J = 21.05 Hz, 1C, C-6), 121.19 (s, J = 17.27 Hz, 1C, C-8) and 110.4 (t, J = 2.95 Hz, 1C, C-5) ppm. IR (KBr): 3074, 1645, 1615, 1532, 1451, 1415, 1337, 1305, 1249, 1194, 1155, 1119, 1081, 1011, 968, 887, 834, 783, 765, 749, 696, 631, 621, 474 and 430 cm^{-1} .

5.5.5. 1-(Heptafluorotolyl)benzimidazole (39):

0.551 g of octafluorotoluene was added to a dissolved 0.272 g of benzimidazole in THF, which then left for two days at RT. $\text{C}_{14}\text{H}_5\text{F}_7\text{N}_2$: 334.1957 $\text{g}\cdot\text{mol}^{-1}$. (84.25% yield). MS: Calc. 335.0419. Found. 335.1400 m/z [$(M + H)^+$]. In CDCl_3 and DMSO (400 MHz), ^1H NMR: δ = 7.48 (s, J = 16.47 Hz, 1H, H-2), 7.02 (m,

2H, H-5 & H-8) and 6.62 (m, 2H, H-6 & H-7) ppm. ^{19}F NMR: $\delta = -51.13$ (t, J = 21.75 Hz, 3F, F-d'), -134.25 (m, 2F, F-c' & F-e') and -138.59 (m, 2F, F-b' & F-f') ppm. IR (KBr): 3474, 3114, 3096, 3062, 3038, 3003, 2968, 2945, 2861, 2796, 2741, 2621, 2541, 1934, 1897, 1862, 1816, 1771, 1737, 1682, 1661, 1620, 1587, 1530, 1509, 1496, 1478, 1458, 1409, 1364, 1346, 1325, 1301, 1273, 1245, 1201, 1162, 1135, 1112, 1086, 1003, 996, 958, 933, 914, 898, 887, 847, 810, 795, 768, 746, 716, 673, 634, 626, 617, 578, 542, 584 and 419 cm^{-1} .

5.5.6. 1-(Heptafluorotolyl)-2-methylbenzimidazole (40):

To a solution of 0.341 g of 2-methylbenzimidazole in THF, 0.587 g of octafluorotoluene was added, and left for three days at RT. $\text{C}_{15}\text{H}_7\text{F}_7\text{N}_2$: 348.2225 $\text{g}\cdot\text{mol}^{-1}$. (65.66% yield). In CDCl_3 and DMSO (400 MHz), MS: Calc. 349.2909. Found. 349.2909 m/z [$(M + H)^+$]. ^1H NMR: $\delta = 7.43$ (m, 2H, H-8 and H-5), 7.11 (m, 2H, H-6 and H-7) and 2.55 (m, 3H, H-2') ppm. ^{19}F NMR: $\delta = -56.07$ (t, J = 21.73 Hz, 3F, F-d'), -138.16 (m, 2F, F-c' and F-e') and -141.90 (m, 2F, F-b' and F-f') ppm. IR (KBr): 3461, 3179, 3113, 3063, 2997, 2919, 2877, 2849, 2790, 2724, 2680, 2543, 1921, 1879, 1764, 1624, 1592, 1508, 1488, 1451, 1418, 1387, 1361, 1318, 1272, 1220, 1197, 1155, 1120, 1069, 1044, 1028, 1004, 924, 896, 850, 834, 765, 749, 732, 674, 625, 618, 492, 480 and 434 cm^{-1} .

5.5.7. 1-(2,3,5,6-Tetrafluorobenzonitrile)-2-methylbenzimidazole (41):

0.322 g of 2-methylbenzimidazole was dissolved in 50ml of THF then added to 0.475 g of 2,3,4,5,6 pentafluorobenzonitrile and then heated at 60°C for 65:11 h. $C_{15}H_7F_4N_3$: 305.234 $g \cdot mol^{-1}$. (81.53% yield). MS: Calc. 306.0654. Found. 306.0627 m/z [$(M + H)^+$]. In $CDCl_3$ (400 MHz), 1H NMR: $\delta = 7.80$ (m, 1H, H-8), 7.38 (m, 2H, H-6,7), 7.04 (m, 1H, H-5) and 3.51 (s, $J = 4.91$ Hz, 3H, H-2') ppm. ^{19}F NMR: $\delta = -129.48$ (m, 2F, F-c' and F-e') and -140.01 (m, 2F, F-b' and F-f') ppm. IR (KBr): 3436, 2924, 2855, 2248, 1651, 1613, 1504, 1457, 1386, 1324, 1296, 1269, 1230, 1200, 1163, 1051, 1019, 990, 933, 875, 831, 814, 771, 748, 678, 656, 544, 499 and $437 cm^{-1}$.

5.5.8. 1-(2,3,5,6-Tetrafluoropyridyl)-2-methylbenzimidazole (42):

0.504 g of 2-methylbenzimidazole was dissolved in 50 ml of THF then added to 0.598 g of pentafluoropyridine, and the solution was left for 17 days at RT. $C_{13}H_7F_4N_3$: 281.212 $g \cdot mol^{-1}$. (84.85% yield). MS: Calc. 282.0654. Found. 282.0659 m/z [$(M + H)^+$]. In $CDCl_3$ (400 MHz), 1H NMR: $\delta = 7.81$ (dm, $J = 8.03$ Hz, 1H, H-8), 7.35 (m, 2H, H-6 and H-7), 7.04 (dm, $J = 7.72$ Hz, 1H, H-5), 3.51 (s, $J = 9.54$ Hz, 3H, H-2') ppm. ^{19}F NMR: $\delta = -129.49$ (m, 2F, F-c' and F-e') and (m, 2F, F-b' and F-f') ppm. ^{13}C NMR: $\delta = 150.55$ (m, 1C, C-2), 144.15 (dm, $J = 249.96$ Hz, 2C, C-b & C-f), 138.07 (dm, $J = 260.54$ Hz, 2C, C-c & C-e), 134.49 (m, 1C, C-9), 127.30 (m, 1C, C-a), 124.05 (d, $J = 16.07$ Hz, 2C, C-6 & C-7), 119.95 (s, $J = 32.17$ Hz, 1C, C-8), 109.48 (s, $J = 41.61$ Hz, 1C, C-5) and 13.85 (s, $J = 42.45$ Hz, 1C, C-2) ppm. IR (KBr): 3401, 1642, 1616, 1516, 1482, 1454, 1416, 1390, 1368, 1342, 1312, 1283, 1256, 1152, 1136, 1100, 1022, 1013, 978, 928, 868, 830, 764, 743, 695, 672, 649, 628, 522 and $437 cm^{-1}$. Elemental

analysis, C = Found. 55.55 (Calc. 55.53) %, H = Found. 2.62 (Calc. 2.51) % and N = Found. 15.03 (Calc.14.94) %. In 2D NMR, the HSQC spectrum shows that H-2' correlates with C-2', H-5 correlates with C-5, H-6 and H-7 correlates with C-6 and C-7, and H-8 correlates with C-8 (Fig. 52, chapter two). In the HMBC spectrum shows that H-2' correlates with C-2' and C-2, H-5 correlates with C-5, C-4, C-6 and C-7, H-6 and H-7 correlates with C-4, C-5, C-6, C-7, C-8 and C-9, H-8 correlates with C-6, C-7, C-8 and C-9 (Fig. 53, chapter two). Crystallographic data for **42** has been shown in table 11.

Crystallographic data for 1-(2,3,5,6-tetrafluoropyridyl)-2-methylbenzimidazole

| | |
|---|---|
| Formula | C ₁₃ H ₇ F ₄ N ₃ |
| Formula weight | 281.22 |
| Crystal system | orthorhombic |
| Space group | <i>Pca</i> 2 ₁ |
| <i>a</i> , Å | 11.0582(4) |
| <i>b</i> , Å | 7.4614(2) |
| <i>c</i> , Å | 28.1810(10) |
| <i>B</i> , ° | — |
| <i>V</i> , Å ³ | 2325.20(13) |
| <i>Z</i> | 8 |
| <i>D</i> _c (g cm ⁻³) | 1.607 |
| Crystal size (mm ³) | 0.38 × 0.35 × 0.32 |
| <i>μ</i> (mm ⁻¹) | 0.144 |
| <i>θ</i> range (°) | 1.45 → 28.01 |
| Total reflections | 15814 |
| Unique reflections (<i>R</i> _{int}) | 5112(0.0394) |
| Observed reflections [<i>I</i> > 2σ(<i>I</i>)] | 4556 |
| Parameters | 361 |
| Final <i>R</i> indices [<i>I</i> > 2σ(<i>I</i>)] | <i>R</i> ₁ 0.0389, <i>wR</i> ₂ = 0.1044 |
| <i>R</i> indices (all data) | <i>R</i> ₁ = 0.0443, <i>wR</i> ₂ = 0.1086 |
| Weighting scheme | $w = 1/[\sigma^2(F_o)^2 + \{0.0592(F_o^2 + 2F_c^2)/3\}^2 + 0.6334(F_o^2 + 2F_c^2)/3]$ |
| Max., min. Δρ (eÅ ⁻³) | 0.360, -0.425 |
| Goodness of fit on <i>F</i> ² | 1.040 |

Table 11: Estimated standard deviations are given in parentheses. Data were collected at 89(2) K with graphite monochromated radiation ($\lambda = 0.71073$ Å).

5.6. Indazole:

5.6.1. Attempt to synthesize 1-(2,3,5,6-Tetrafluoropyridyl)indazole (43):

0.378 g of indazole was dissolved in 50 ml of THF then added to 0.535 g of pentafluoropyridine, and then the solution was left for a week at RT.

5.7. Benzimidazolium Salt:

5.7.1. 1-(2,3,5,6-Tetrafluoropyridyl)-3-benzyl-benzimidazolium bromide (44):

0.312 g of 1-(2,3,5,6-tetrafluoropyridyl)benzimidazole **38** was dissolved in 50 ml of CH₂Cl₂ with 0.218 g of benzyl bromide, and then the solution was left for two days at RT. C₁₉H₁₂F₄N₃Br: 438.2215 g.mol⁻¹. (67.40 % yield). MS: Calc. 358.0967. Found. 358.0963 m/z [(M - Br)⁺]. In DMSO (400 MHz), ¹H NMR: δ = 10.46 (s, J = 7.74 Hz, 1H, H-2), 8.60 (m, 4H, H-5,6,7 and 8), 7.34 (m, 5H, H-3c,3d,3e,3f,3g) and 5.73 (s, J = 1.97 Hz, 2H, H-3a) ppm. ¹⁹F NMR: δ = -90.09 (m, 2F, F-c' & F-e') and -146.68 (m, 2F, F-b' & F-f') ppm. IR (KBr): 3639, 3399, 3125, 3058, 3028, 2959, 2926, 1971, 1849, 1805, 1720, 1650, 1622, 1608, 1590, 1562, 1481, 1458, 1444, 1427, 1407, 1361, 1347, 1325, 1265, 1250, 1212, 1203, 1192, 1162, 1130, 1084, 1031, 976, 919, 888, 840, 819, 780, 757, 746, 723, 697, 649, 634, 595, 572, 542, 523, 513, 459 and 421 cm⁻¹.

References:

- [1] J. A. K. H. Andrei S. Batsanov, Todd B. Marder² and Edward G. Robins., *Acta Cryst.* 2001, 1303-1305.
- [2] Y. I. Bagryanskaya, Gatilov, V. Y., Maksimov, M. A., Platonov, E. V., & Zibarev, V. A., *Journal of fluorine Chemistry* 2005, 126, 1281-1287.
- [3] E. C. Smith, Smith, S. P., Thomas, L. R., Robins, G. E., Collings, C. J., Dai, C., Scott, J. A., Borwick, S., Batsanov, S. A., Watt, W. S., Clark, J. S., Viney, C., Howard, K. A. J., Clegg, W., & Marder, B. T., *Journal of Materials Chemistry.* 2004, 14, 413 – 420.
- [4] C. J. Collings, Batsanov, S. A., Howard, A. K. J., & Marder, B. T., *Canadian Journal of Chemistry.* 2006, 84, 238-242.
- [5] C. G. Saunders, *CrystEngComm.* 2011, 13, 1801-1803.
- [6] W. G. Coates, Dunn, R. A., Henling, M. L., Dougherty, A. D., & Grubbs, H. R., *Angewandte Chemie.* 1997, 36, 248.
- [7] Y. I. Bagryanskaya, Gatilov, V. Y., Lork, E. Mews, R., Shakirov, M. M., Watson, G. P., & Zibarev, V. A., *Journal of Fluorine Chemistry* 2002, 116, 149-156.
- [8] L. M. E. Salonen, Manuel; Diederich, François., *Angew. Chem. Int. Ed.* 2011, 50, 4808 – 4842.
- [9] J. C. R. Collings, Karl P; Robins, Edward G; Batsanov, Andrei S; Stimson, Lorna M; Howard, Judith A. K; Clark, Stewart J and Marder, Todd B., *New J. Chem.* 2002, 26, 1740-1746.
- [10] K. S. G. a. L. G. Christophorou, *The Journal of Chemical Physics* 1976, 65, 2977-2981.
- [11] T. T. Korenaga, Hikaru; Ema, Tadashi; Sakai, Takashi., *Journal of Fluorine Chemistry.* 2003, 122, 201- 205
- [12] V. R. N. Vangala, Ashwini; Lynch, Vincent M., *Chemical communications (Cambridge, England).* 2002, 1304-1305.
- [13] R. P. S. Sharma, Anju; Singh, Sukhjinder; Venugopalan, Paloth; Harrison, William T.A., *Journal of Fluorine Chemistry.* 2010, 131, 456 - 460
- [14] J. C. B. Collings, Andrei S; Howard, Judith A.K; Dickie, Diane A; Clyburne, Jason A.C; Jenkins, Hilary A and Marder, Todd B, *Journal of Fluorine Chemistry* 2005, 126, 513 - 517

- [15] J. C. Collings, Roscoe, K. P., Robins, E. G., Andrei, S., Batsanov, A. S., Stimson, L. M., Howard, J. A. K., Clark, S. J., & Marder, T. B., *New Journal of Chemistry*. 2002, 26, 1740-1746.
- [16] J. C. Collings, A. S. Batsanov, J. A. K. Howard and T. B. Marder, *Crystal Engineering* 2002, 5, 37-46.
- [17] J. M. S. S. Becerra, Ortega, S. H., Morales, D. M., & Marti´nez, J. V., *CrystEngComm*. 2009, 11, 226–228.
- [18] S. FUJII, MAKI, Y., & KIMOTO, H., *Journal of Fluorine Chcmistr*), 1989, 43, 131-144.
- [19] K. A. Wheeler, *Molecular Crystals and Liquid Crystals* 2011, 548, 295-296.
- [20] L.-l. Ooi, 2010.
- [21] E. R. T. a. Z.-S. Tiekink, J´ulio., 2012.
- [22] M. L. Waters, *Current Opinion in Chemical Biology* 2002, 6, 736-741.
- [23] K. Pluhackova, P. Jurecka and P. Hobza, *Physical Chemistry Chemical Physics* 2007, 9, 755-760.
- [24] Y.-C. C. Chang, Yu-Da; Chen, Chih-Hsin; Wen, Yuh-Sheng; Lin, Jiann T; Chen, Hsing-Yin., *The Journal of organic chemistry*. 2008, 73, 4608–4614.
- [25] C. A. L. Hunter, Kevin R; Perkins, Julie; Urch, Christopher J., *Journal of the Chemical Society, Perkin Transactions 2*. 2001, 651 - 669
- [26] C. ZHANG., *J Comput Chem*. 2010, 32.
- [27] S. A. a. S. Arnstein, C David., *Physical chemistry chemical physics : PCCP*. 2008, 10, 2646-2655.
- [28] a. K. T. Take-aki Koizumi, [a] and Koji Tanaka., *Eur. J. Org. Chem*. 2003, 4528-4532.
- [29] S. E. H. Snyder, Bin-Syuan; Chu, Yu W; Lin, Huei-Shian; Carey, James R., *Chemistry : a European journal*. 2012, 18, 12663–12671.
- [30] J.-I. K. Seo, Inkoo; Lee, Yoon Sup., *Chemical Physics Letters*. 2009, 474, 101 - 106
- [31] M. J. Rashkin and M. L. Waters, *Journal of the American Chemical Society* 2002, 124, 1860-1861.
- [32] M. J. a. W. Rashkin, Marcey L., *Journal of the American Chemical Society*. 2002, 124, 1860–1861.

- [33] S. L. H. Cockroft, Christopher A; Perkins, Julie; Zonta, Cristiano; Adams, Harry; Spey, Sharon E; Low, Caroline M. R.; Vinter, Jeremy G; Lawson, Kevin R; Urch, Christopher J and Hunter, Christopher A., *Organic & biomolecular chemistry*. 2007, 5, 1062-1080.
- [34] S. L. H. Cockroft, Christopher A; Lawson, Kevin R; Perkins, Julie; Urch, Christopher J., *Journal of the American Chemical Society*. 2005, 127, 8594 - 8595
- [35] M. D. Weck, Alex R; Matsumoto, Kozo; Coates, Geoffrey W; Lobkovsky, Emil B; Grubbs, Robert H., *Angewandte Chemie International Edition*. 1999, 38, 2741-2745
- [36] A. S. H. Batsanov, J A; Marder, T B; Robins, E G., *Acta Crystallographica Section C*. 2001, 57, 1303-1305.
- [37] N. Barbero, C. Barolo, D. Marabello, R. Buscaino, G. Gervasio and G. Viscardi, *Dyes and Pigments* 2012, 92, 1177-1183.
- [38] D. L. D. Reger, Agota; Smith, Mark D., *Inorganic chemistry*. 2011, 50, 11754–11764.
- [39] D. L. D. Reger, Agota; Reinecke, Bryn; Rassolov, Vitaly; Smith, Mark D; Semeniuc, Radu F., *Inorganic chemistry*. 2009, 48, 8911–8924.
- [40] L. C. Zhao, Xu-Dong; Mak, Thomas C. W., *Inorganic chemistry*. 2008, 27, 2483 - 2489.
- [41] X. L. Yang, Jiang; Zhao, Xin-Hua; Wang, Hai-Wen and Shan, Yong-Kui., *Crystal Structure Communications*. 2007, C63, m171-m173.
- [42] J. G. Santos, Bruno; Illescas, Beatriz M; Guldi, Dirk M; Martín, Nazario., *Chemical Communications*. 2008, 5993-5995.
- [43] Y.-Q. S. Zheng, Jie; Lin, Jian-Li., *Zeitschrift für anorganische und allgemeine Chemie*. 2000, 626, 1274 - 1276
- [44] M. a. Z. Du, Xiao-Jun., *Acta Crystallographica Section E Structure Reports Online*. 2004, 60, o439 - o441
- [45] S. I. M. Sheby M. George, Jinkwon Kim., *Inorganic Chemistry Communications*. 2010, 13, 429–432.
- [46] J. W. Junwei Ye, Ying Wu, Ling Ye, Ping Zhang., *Journal of Molecular Structure*. 2008, 873, 35–40.
- [47] Y.-T. H. He, Kun-Lin; Hu, Chang-Wen; Pan, Wan-Long; Chi, Ying-Nan., *Crystal Structure Communications*. 2007, C63, m161-m162.
- [48] a. T. K.-S. Yusaku Suenaga, a Masahiko Maekawab and Megumu Munakataa., 1999, 2737–2741.

- [49] Y. W. a. M.-H. Yang., *Synthesis and Reactivity in Inorganic, Metal-Organic, and Nano-Metal Chemistry*. 2009, 39, 520–524.
- [50] S. E.-D. H. E. a. M. M. EL-BENDARY., *Journal of Coordination Chemistry*. 2010, 63, 1038–1051.
- [51] H. A.-J. Ali-Boucetta, Khuloud T; McCarthy, David; Prato, Maurizio; Bianco, Alberto; Kostarelos, Kostas., *Chemical communications*. 2008.
- [52] F. H. Liu, Wei; Tang, Chao; Chen, Qing-Quan; Shi, Fei-Fei; Wu, Hong-Bin ; Xie, Ling-Hai; Peng, Bo; Wei, Wei; Cao, Yong and Huang, Wei., *J. Phys. Chem. C*. 2009, 113, 4641–4647.
- [53] A. F. Sygula, Frank R; Sygula, Renata; Rabideau, Peter W; Olmstead, Marilyn M., *J. AM. CHEM. SOC.* 2007, 129, 3842-3843.
- [54] J. C. C. Noveron, Biswaroop; Arif, Atta M; Stang, Peter J., *JOURNAL OF PHYSICAL ORGANIC CHEMISTRY*. 2003, 16, 420-425.
- [55] L. M. a. W. Tang, Yu Jiang., *Chinese Chemical Letters*. 2009, 20, 1259-1262.
- [56] M. S. M. a. R. M. B. Lionel E. Cheruzel, *Chem. Commun.* 2005, 2223-2225.
- [57] X.-M. F. Shi, Ming-Jin; Liu, Hong-Jiang; He, Xiang; Shao, Min; Li, Ming-Xing., *Journal of Coordination Chemistry*. 2010, 63, 3743–3752.
- [58] S. B. M. Raj, Packianathan Thomas; Rychlewska, Urszula; Warzajtis, Beata; Bocelli, Gabriele; O'lla, Rita., *Acta Crystallographica Section E Structure Reports Online*. 2003, 59, m46 - m49
- [59] C. Shao, *Inorganic Chemistry Communications*. 2002, 5, 667-670.
- [60] S.-L. L. Lee, Nai-Ti; Liao, Wei-Chih; Chen, Chun-hsien; Yang, Hsiao-Ching; Luh, Tien-Yau., *CHEMISTRY A EUROPEAN JOURNAL*. 2009, 15, 11594 – 11600.
- [61] X.-J. a. J. Zheng, Lin-Pei., *Polyhedron*. 2003, 22, 2617-2624.
- [62] H. Zheng and J. Gao, *Angewandte Chemie International Edition* 2010, 49, 8635-8639.
- [63] E. A. Meyer, Castellano, R. K., & Diederich, F., *Angewandte Chemie*. 2003, 42, 1210 – 1250.
- [64] H. T. Yuki, Yoshikazu; Hata, Masayuki; Ishikawa, Hidenori; Neya, Saburo; Hoshino, Tyuji, *Journal of Computational Chemistry* 2007, 28, 1091 - 1099
- [65] L. W. Mao, Yanli; Hu, Xiche., *The Journal of Physical Chemistry B*. 2003, 107, 3963 -3971

- [66] D. D. F. Boehr, Adam R; Wright, Gerard D; Cox, James R., *Chemistry & Biology*. 2002, 9, 1209 -1217
- [67] C. D. M. a. W. Churchill, Stacey D., *J. Phys. Chem. B*. 2009, 113, 16046–16058.
- [68] S. S. Berhe, Andrew; Luster, Choice; Charlier, Jr, Henry A; Warner, Don L; Zalkow, Leon H; Burgess, Edward M; Enwerem, Nkechi M and Bakare, Oladapo., *Bioorganic & Medicinal Chemistry*. 2010, 18, 134–141.
- [69] K. a. R. Tiefenbacher, Jr, Julius., *Journal of the American Chemical Society*. 2012, 134, 2914-2917.
- [70] L. E. R.-R. Martikainen, Minna; Neshybova, Silvie; Lahtela-Kakkonen, Maija; Raunio, Hannu; Juvonen, Risto O, *European journal of pharmaceutical sciences* 2012, 47, 996–1005.
- [71] D.-W. F. Lee, Jason; Morey, Timothy; Dennis, Donn; Partch, Richard; Baney, Ronald, *Journal of Pharmaceutical Sciences* 2005, 94, 373 - 381
- [72] S. A. A. Nawaz, Muhammad; Brandt, Wolfgang; Wessjohann, Ludger A; Westermann, Bernhard, *Biochemical and Biophysical Research Communications* 2011, 404, 935–940.
- [73] J. Y. C. Chung, Seung Joo; Cho, Art E; Hah, Jung-Mi, *Bioorganic & Medicinal Chemistry Letters* 2012, 22, 3278–3283.
- [74] Y. Z. Yang, Ying-Ming; Chen, Yong; Zhao, Di; Chen, Jia-Tong; Liu, Yu, *Chem. Eur. J.* 2012, 18, 4208 – 4215.
- [75] J. G. Clayden, Nick; Warren, Stuart G., 2012.
- [76] L. M. a. C. Harwood, Timothy D. W., 1997, 43, 64.
- [77] en.wikipedia.org, 2013.
- [78] H. Debus, *Justus Liebigs Ann. Chem.* 1858, 107 199–208.
- [79] P. P. Ambalavanan, K; Ponnuswamyand, M. N; Thirumuruhan, R. A; Yathirajan, H. S; Prabhuswamy, B; Raju, C. R; Nagaraja, P; Mohana, K. N., *Mol. Cryst. Liq. Cryst.* 2003, 393, 75–82.
- [80] W. Z. Y. R. T. K. H. N. R. F. T. E. M. Sellers., *Drug Metabolism and Disposition*. 2002, 30, 314–318.
- [81] D. M. Zampieri, Maria Grazia; Laurini, Erik; Scialino, Giuditta; Banfi, Elena; Vio, Luciano., *Bioorganic & Medicinal Chemistry*. 2008, 16, 4516-4522.
- [82] D. N. Sharma, Balasubramanian; Kumar, Pradeep; Judge, Vikramjeet; Narang, Rakesh; De Clercq, Erik; Balzarini, Jan., *European Journal of Medicinal Chemistry*. 2009, 44, 2347–2353.

- [83] M. S. S. Khan, Shafi Ahmad; Siddiqui, Mohammad Shaik Rafi Ahmad; Goswami, Usha; Srinivasan, Kumar Venkatraman; Khan, Muhammad Islam., *Chem Biol Drug Des.* 2008, 72, 197–204.
- [84] L. R. a. Y. Swett, T O., *Journal of medicinal chemistry.* 1970, 13, 968 - 970.
- [85] A. J. Basu, Kalsariya; Jayaprakash, Venkatesan; Mishra, Nibha; Ojha, P; Bhattacharya, S., *European Journal of Medicinal Chemistry.* 2009, 44, 2400–2407.
- [86] V. S. Sorrenti, L; Di Giacomo, C; Acquaviva, R; Siracusa, M.A; Vanella, A., *Nitric Oxide.* 2006, 14, 45–50.
- [87] J. K. Lee, Hwan; Yu, Hana; Chung, Jae Yoon; Oh, Chang-Hyun; Yoo, Kyung Ho, Sim; Taebo, Hah, Jung-Mi., *Bioorganic & medicinal chemistry letters.* 2010, 20, 1573 - 1577.
- [88] R. S. Wang, Hong-Fan; Zhao, Jing-Feng; He, Yan-Ping; Zhang, Hong-Bin; Liu, Jian-Ping., *Bioorganic & Medicinal Chemistry Letters.* 2013, 23, 1760–1762.
- [89] A. A. Assadieskandar, Mohsen; Ostad, Seyed Nasser; Riazi, Gholam Hossein; Cheraghi-Shavi, Tayebe; Shafiei, Bentolhoda and Shafiee Abbas., *Bioorganic & Medicinal Chemistry.* 2013.
- [90] A. K. R. Jain, V; Sisodiya, Madhvi; Agrawal, R. K., *Asian Pacific Journal of Tropical Medicine.* 2010, 3, 471-474.
- [91] T. K. Nakamura, Hiroyuki; Umemiya, Hiroki; Amada, Hideaki; Miyata, Noriyuki; Taniguchi, Kazuo; Bando, Kagumi; Sato, Masakazu., *Bioorganic & Medicinal Chemistry Letters.* 2004, 14, 333-336.
- [92] C. Hofmann in *Imidazoles.*, Vol. 6 John Wiley & Sons, Inc., 2008, pp. 327-367.
- [93] en.wikipedia.org, 2013.
- [94] I. M. B. Bouabdallah, Lahcen Ait; Zyad, Abdelmajid; Ramdani, Abdelkrim; Zidane, Ismail; Melhaoui, Ahmed., *Natural Product Research.* 2006, 20, 1024–1030.
- [95] M. F. T. A. C. F. B. A. S. D. B. B. A. S., *Bioorganic & Medicinal Chemistry Letters.* 2002, 12, 3629–3633.
- [96] S. K. Bondock, Wesam; Fadda, Ahmed A., *European Journal of Medicinal Chemistry.* 2011, 46, 2555 - 2561
- [97] E. M. a. H. Sharshira, Nagwa Mohamed Mahrous, *molecules* 2012, 17, 4962-4971.

- [98] A. A. el-Sabbagh. O. I; Baraka. M. M; Ibrahim. S. M; Pannecouque. C; Andrei. G; Snoeck. R; Balzarini. J; Rashad, *European Journal of Medicinal Chemistry*. 2009, 44, 3746–3753.
- [99] P. R. B. C. P. T. P. H. H., *Bioorganic & Medicinal Chemistry Letters*. 2012, 22, 5129–5133.
- [100] S. Y. Hassan, *molecules*. 2013, 18, 2683-2711.
- [101] A. M. I. Vijesh, Arun M; Shetty, Prashanth; Sundershan, S; Fun, Hoong Kun, *European Journal of Medicinal Chemistry* 2013, 62, 410e415.
- [102] Y. Z. Luo, Shuai; Qiu, Ke-Ming; Liu, Zhi-Jun; Yang, Yu-Shun; Fu, Jie; Zhong, Wei-Qing; Zhu, Hai-Liang *Bioorganic & Medicinal Chemistry Letters*. 2013, 23, 1091–1095.
- [103] L.-L. Z. Xu, Chang-Ji; Sun, Liang-Peng; Miao, Jing; Piao, Hu-Ri, *European Journal of Medicinal Chemistry* 2012, 48, 174e178.
- [104] en.wikipedia.org.
- [105] M. P. Tonelli, Giuseppe; Boido, Vito; Sparatore, Fabio; Marongiu, Fabio; Marongiu, Esther; La Colla, Paolo and Loddo, Roberta., *CHEMISTRY & BIODIVERSITY*. 2008, 5, 2386 - 2401
- [106] M. S. Tonelli, Matteo; Tasso, Bruno; Novelli, Federica; Boido, Vito; Sparatore, Fabio; Paglietti, Giuseppe; Pricl, Sabrina; Giliberti, Gabriele; Blois, Sylvain; Ibba, Cristina; Sanna, Giuseppina; Loddo, Roberta; La Colla, Paolo., *Bioorganic & Medicinal Chemistry*. 2010, 18, 2937-2953.
- [107] G. C. Navarrete-Vázquez, R; Cedillo, R; Hernández-Campos, A; Yépez, L; Hernández-Luis, F; Valdez, Juan; Morales, RauÂ l; CorteÂ s, Rafael; HernaÂ ndez, Manuel and Castillo, Rafael., *Bioorganic & Medicinal Chemistry Letters*. 2001, 11, 187-190.
- [108] V. K. Klimešová, J; Waisser, K; Kaustová, J., *Il Farmaco*. 2002, 57, 259-265.
- [109] M. G. Ozarda, *New Biotechnology*. 2009, 25, S9.
- [110] Z. Y. Ates-Alagoz, Sulhiye; Buyukbingol, Erdem., *Pharmacology*. 2007, 53, 110–113.
- [111] D. W. Ismail. M. A; Brun. R; Wenzler. T; Tanious. F. A; Wilson. W. D; Boykin, *Bioorganic & Medicinal Chemistry*. 2004, 12, 5405–5413.
- [112] K. M.-H. R. J.-S. H. Jung-Mi., *Bioorganic & medicinal chemistry letters*. 2013, 23, 1639–1642.
- [113] en.wikipedia.org.

- [114] O. C. Rosati, Massimo; Marcotullio, Maria Carla; Macchiarulo, Antonio; Perfumi, Marina; Mattioli, Laura; Rismondo, Francesco and Cravotto, Giancarlo., *Bioorganic & Medicinal Chemistry Letters*. 2007, *15*, 3463–3473.
- [115] A. P. Gerpe, Oscar E; Arán, Vicente J; Azqueta, Amaia; de Ceráin, Adela López; Monge, Antonio; Rojas, Mari´a Antonieta; Gloria, Yaluff; Aguirre, Gabriela; Boiani, Lucí´a; Cerecetto, Hugo; Gonza´lez, Mercedes; Olea-Azarand, Claudio; Rigol, Carolina; Maya, Juan D and Morello, Antonio *Bioorganic & Medicinal Chemistry* 2006, *14*, 3467–3480.
- [116] M. S. Gopalakrishnan, P; Thanusu, J; Kanagarajan, V., *Journal of Enzyme Inhibition and Medicinal Chemistry*. 2008, *23*, 974–979.
- [117] C.-r. W. Zhao, Rui-qi; Li, Gang; Xue, Xiao-xia; Sun, Chang-jun; Qu, Xian-jun and Li, Wen-bao, *Bioorganic & Medicinal Chemistry Letters* 2013, *23*, 1989–1992.
- [118] M. C. R. Vega, Miriam; Montero-Torres, Alina; Fonseca-Berzal, Cristina; Escario, José Antonio; Gómez-Barrio, Alicia; Gálvez, Jorge; Marrero-Ponce, Yovani; Arán, Vicente J *European Journal of Medicinal Chemistry* 2012, *57*, 214e227.

Appendix

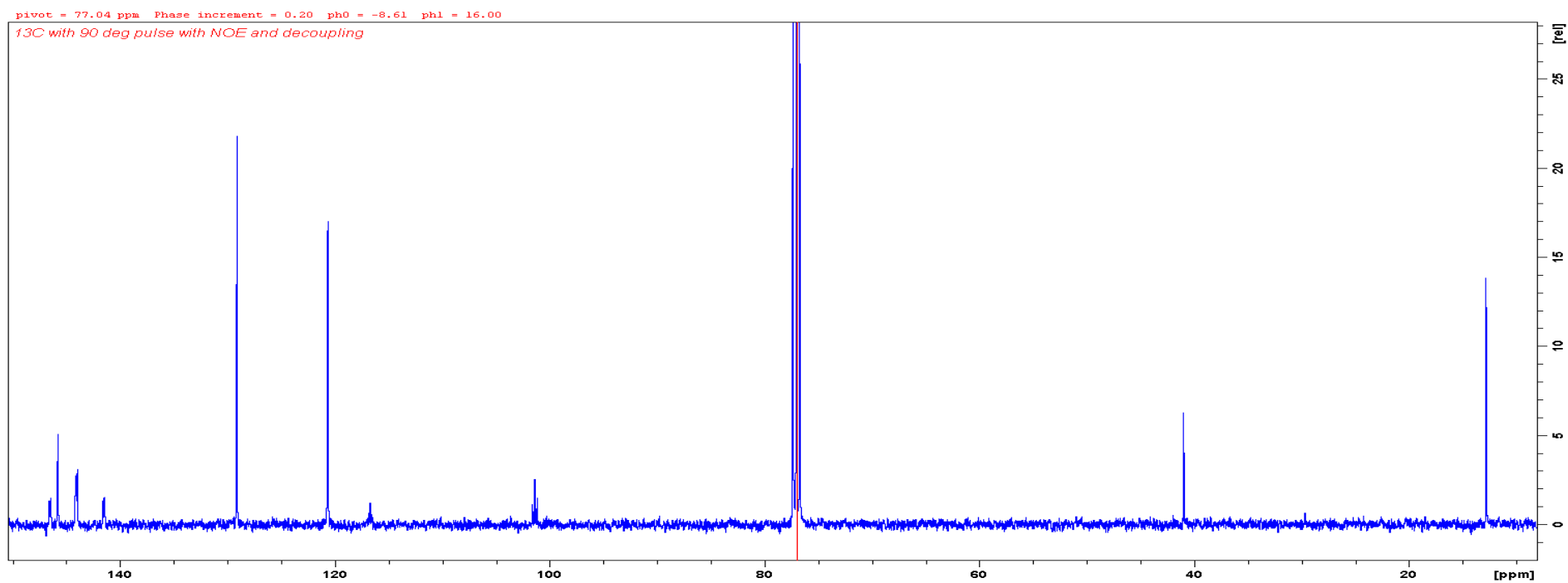


Figure 64: The ^{13}C NMR spectrum of 1-(4-bromo-2,3,5,6-tetrafluorobenzyl)-2-methylimidazole (**12**).

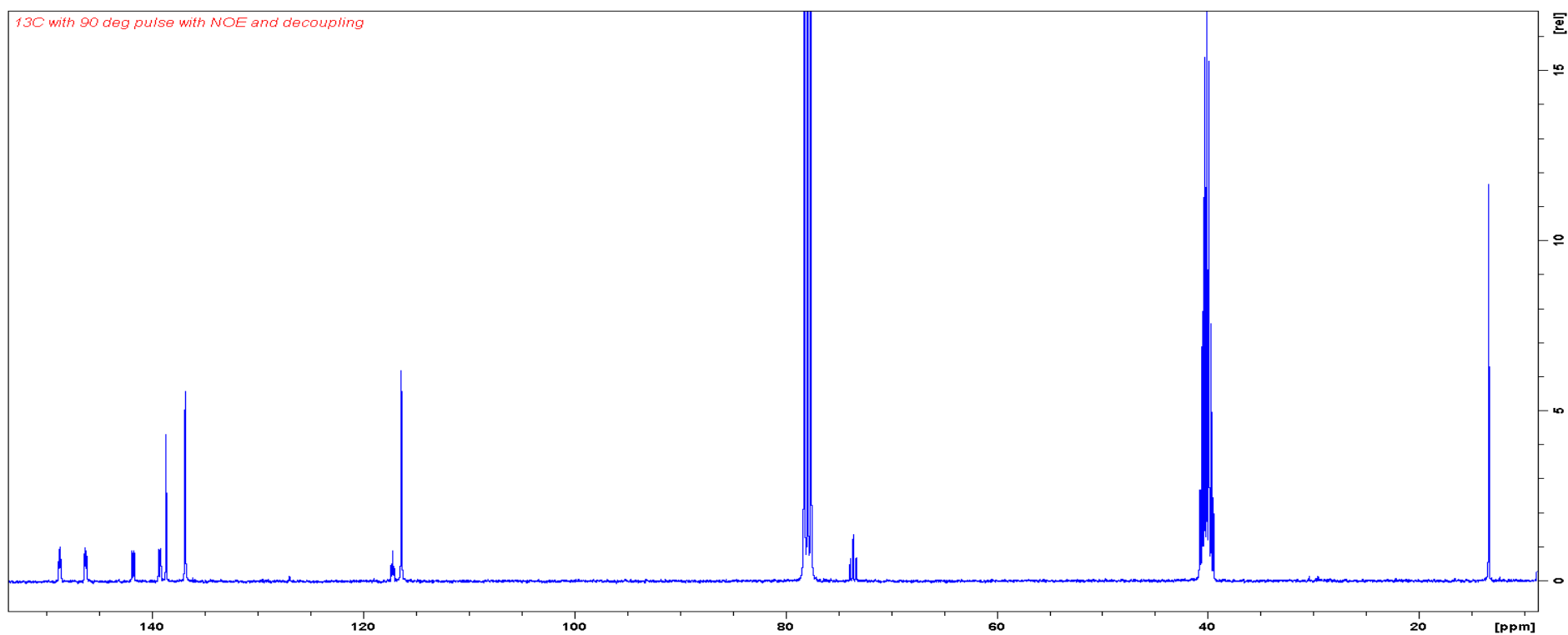


Figure 65: The ¹³C NMR spectrum of 1-(4-iodo-2,3,5,6-tetrafluorobenzyl)-4-methylimidazole (**18**).

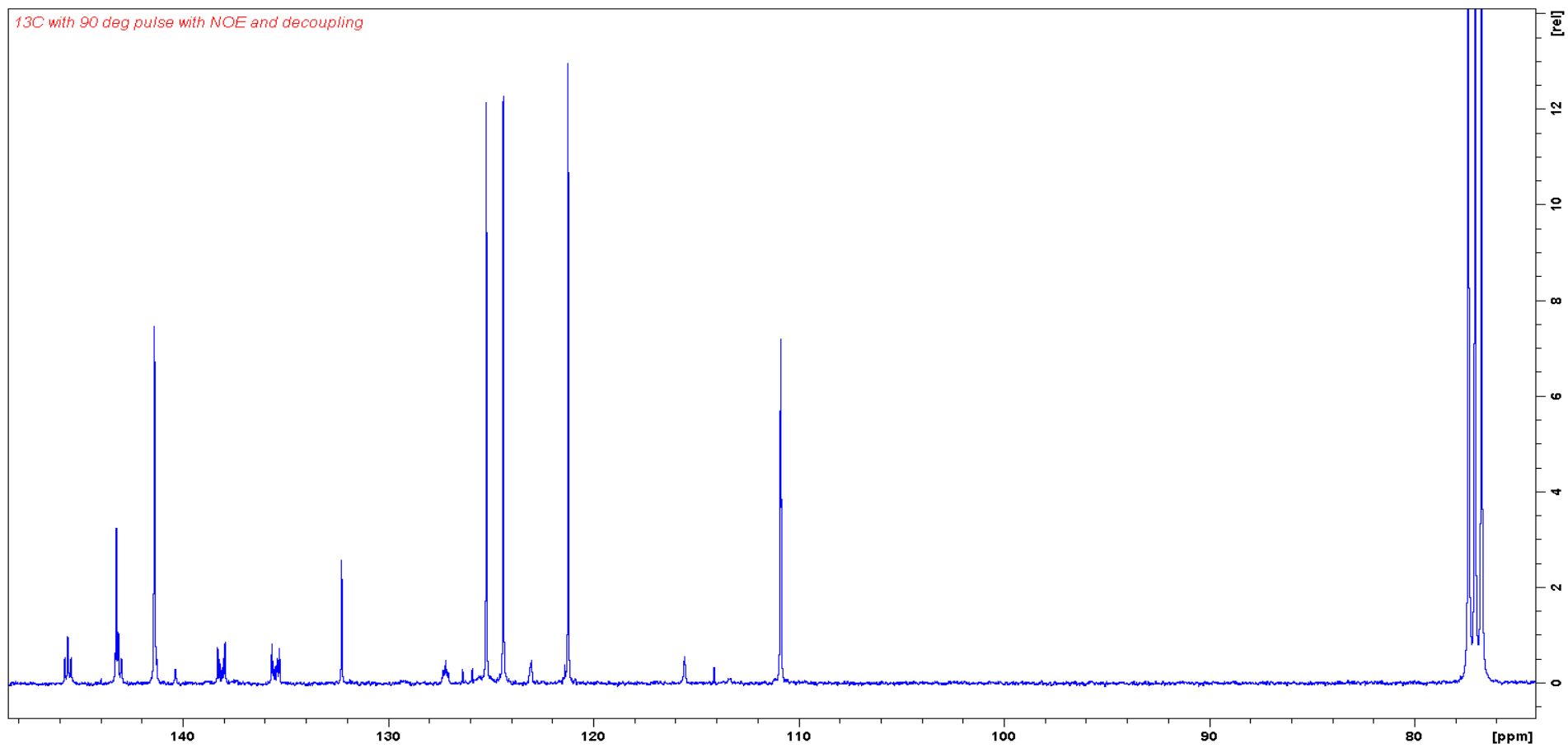


Figure 66: The ¹³C NMR spectrum of 1-(2,3,5,6-tetrafluoropyridyl)benzimidazole (**38**).

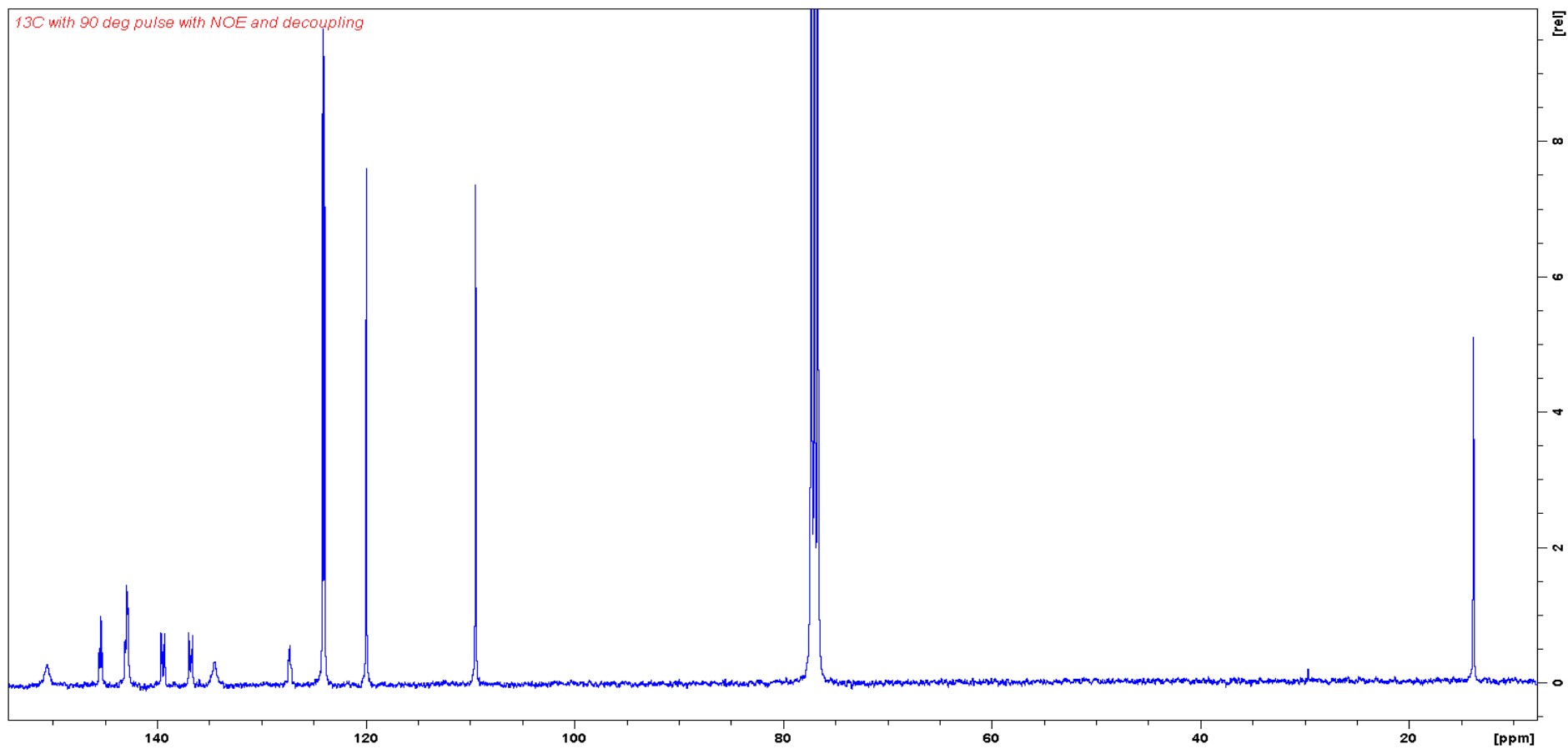


Figure 67: The ¹³C NMR spectrum of 1-(2,3,5,6-tetrafluoropyridyl)-2-methylbenzimidazole (**42**).